# ภาคผนวก

Elsevier Editorial System(tm) for Clinical Neurophysiology
Manuscript Draft

Manuscript Number: CLINPH-D-11-4957

Title: Scale-Invariant Behavior of Epileptic EEG

Article Type: Full Length Article

Section/Category: Epilepsy

Keywords: epilepsy; seizure; electroencephalography; scale-invariance; fractals; wavelet analysis

Corresponding Author: Dr. Suparerk Janjarasjitt, Ph.D.

Corresponding Author's Institution: Ubon Ratchathani University

First Author: Suparerk Janjarasjitt, Ph.D.

Order of Authors: Suparerk Janjarasjitt, Ph.D.; Kenneth A Loparo, Ph.D.

Suggested Reviewers:

Opposed Reviewers:

Objective: To investigate the scale-invariant dynamic behavior of the electrophysiology of the brain in subjects with epilepsy for different brain regions during ictal and interictal periods.
Methods: Intercranial EEG (ECoG) recordings of subjects with epilepsy obtained during ictal and interictal periods for different brain regions are examined using computational methods based on the wavelet-based representation for 1/f processes. The spectral exponent of the ECoG signals that characterizes the scale-invariant behavior is determined.
Results: The spectral exponent of the ECoG signals obtained during seizure activity (ictal periods) is significantly higher than that obtained during non-seizure activity (interictal periods). In addition, during interictal period, the spectral exponent of the ECoG signals obtained within the epileptogenic zone tends to be slightly higher than that obtained outside the epileptogenic zone.
Conclusions: The dynamics of the brain of subjects with epilepsy associated with different pathological brain states (ictal and interictal) or different brain regions exhibit different scale-invariant behaviors. The behavior of the brain dynamics during ictal periods tends to be more scale-invariant than during interictal periods. Accordingly, the ECoG signal obtained during seizure activity tends to have smoother temporal patterns than during non-seizure periods.
Significance: There is evidence that some biological systems including the brain exhibit scale-invariant or self-similar behavior, a hallmark of a complex system. Scale-invariant behavior reflects the tendency of a complex system to develop organized complexity with both temporal and spatial long-range correlation structure.

- Fractal properties of different biological systems can be significantly different in their nature, origin and appearance, where scale-invariant or scale-free behavior is a tendency of a complex system to develop long-range correlations in time and space.
- In this study, the scale-invariant dynamic behavior of the electrophysiology of the brain in subjects with epilepsy is investigated using the wavelet-based fractal analysis.
- The behavior of the brain dynamics during seizure activity tends to be more scale-invariant or have smoother temporal patterns than during non-seizure periods.

# Scale-Invariant Behavior of Epileptic EEG

S. Janjarasjitt[a,b,*], K. A. Loparo[b]

[a]*Department of Electrical and Electronic Engineering, Ubon Ratchathani University, Warinchamrab, Ubon Ratchathani 34190 Thailand*
[b]*Department of Electrical Engineering and Computer Science, Case Western Reserve University, Cleveland, Ohio 44106 USA*

## Abstract

*Objective:* To investigate the scale-invariant dynamic behavior of the electrophysiology of the brain in subjects with epilepsy for different brain regions during ictal and interictal periods.

*Methods:* Intercranial EEG (ECoG) recordings of subjects with epilepsy obtained during ictal and interictal periods for different brain regions are examined using computational methods based on the wavelet-based representation for $1/f$ processes. The spectral exponent $\gamma$ of the ECoG signals that characterizes the scale-invariant behavior is determined.

*Results:* The spectral exponent $\gamma$ of the ECoG signals obtained during seizure activity (ictal periods) is significantly higher than that obtained during non-seizure activity (interictal periods). In addition, during interictal period, the spectral exponent $\gamma$ of the ECoG signals obtained within the epileptogenic zone tends to be slightly higher than that obtained outside the epileptogenic zone.

*Corresponding author

*Email addresses:* ensupajt@ubu.ac.th,suparerk.janjarasjitt@case.edu (S. Janjarasjitt), kenneth.loparo@case.edu (K. A. Loparo)

*Conclusions:* The dynamics of the brain of subjects with epilepsy associated with different pathological brain states (ictal and interictal) or different brain regions exhibit different scale-invariant behaviors. The behavior of the brain dynamics during ictal periods tends to be more scale-invariant than during interictal periods. Accordingly, the ECoG signal obtained during seizure activity tends to have smoother temporal patterns than during non-seizure periods.

*Significance:* There is evidence that some biological systems including the brain exhibit scale-invariant or self-similar behavior, a hallmark of a complex system. Scale-invariant behavior reflects the tendency of a complex system to develop organized complexity with both temporal and spatial long-range correlation structure.

*Keywords:* epilepsy, seizure, electroencephalography, scale-invariance, fractals, wavelet analysis

---

## 1. Introduction

Recently, concepts and computational methods derived from the contemporary study of complex systems including chaos theory, nonlinear dynamics and fractals have gained increasing interest for applications in biology and medicine because physiological signals and systems can exhibit an extraordinary range of patterns and behaviors (Goldberger, 2006). The mathematical concept of a fractal is commonly associated with irregular objects that exhibit a property called scale-invariance or self-similarity (Goldberger, 2006; Mandelbrot, 1982). Fractal forms are composed of subunits resembling the

structure of the macroscopic object (Goldberger, 2006) which in nature can emerge from statistical scaling behavior in the underlying physical phenomena (Wornell, 1995). An important class of statistical scale-invariant or self-similar random processes is the $1/f$ processes (Wornell, 1995).

There is evidence that some biological systems can exhibit scale-invariant or scale-free behavior, in the sense that they do not have a characteristic length or time scale that dominates the dynamics of the underlying process (Havlin et al., 1995; Stam and de Bruin, 2004; Linkenkaer-Hansen et al., 2001). Fractal properties of different biological systems can be significantly different in their nature, origin, and appearance (Havlin et al., 1995), where scale-invariant or scale-free behavior is a tendency of a complex system to develop long-range correlations in time and space (Bassingthwaighte et al., 1994; Barabási and Stanley, 1995; Bak, 1997).

Even though it is well accepted that the dynamics of the brain are inherently complex, the activity of the brain can exhibit intriguing temporal patterns that are important as correlates of information processing (Gong et al., 2003). For example, collective synchronized oscillations at various frequencies as measured by the EEG are believed to reflect functional states of the brain and cognitive processes (Miltner et al., 1999; Mima et al., 2001; Nikolaev et al., 2001) and exhibit characteristics of scale-invariant dynamics (Gong et al., 2003). Scale-invariant characteristics are often the result of the self-organizing or self-regulating characteristics of complex systems with nonlinearly couplings (Gong et al., 2003).

A traditional mathematical model and the empirical properties of $1/f$ processes have largely been inspired by the fractional Brownian motion frame-

work (Wornell, 1995, 1993; Wornell and Oppenheim, 1992) as developed by Mandelbrot and Van Ness (Mandelbrot and Ness, 1968). In general, models of $1/f$ processes are represented using a frequency domain characterization. The dynamics of $1/f$ processes exhibit power law behavior (Watters, 1998) and can be characterized in the frequency domain by $S(\omega) \propto 1/|\omega|^{\gamma}$. In (Wornell, 1995, 1993), a wavelet-based representation for $1/f$ processes was developed. As the wavelet transform is a natural tool for characterizing self-similar or scale-invariant signals, wavelet transformations play a significant role in the study of self-similar signals and systems (Wornell, 1995). The spectral exponent $\gamma$ that specifies the distribution of power from low to high frequencies of $1/f$ processes can be characterized in terms of the slope of the log-variance of the wavelet coefficients versus scale graph.

In this study, we investigate the scale-invariant characteristics of the dynamics of the brain of subjects with epilepsy. Intercranial EEG (ECoG) recordings of subjects with epilepsy obtained from during different pathological brain states (ictal and interictal) and different brain regions are examined using computational analysis based on the wavelet-based representation for $1/f$ processes (Wornell, 1995, 1993). From the computational results, it is shown that there is a statistically significant difference between the spectral exponent $\gamma$ of the ECoG signals obtained during ictal activity and that obtained during interictal periods. This therefore suggests that the dynamics of the brain of subjects with epilepsy during ictal periods behaves significantly different from that during interictal periods. In addition, the computational results also suggests that during interictal periods the dynamics of the neuronal networks that are directly involved with the generation of

epileptic seizures behave slightly different from the dynamics of the neuronal networks that are outside the regions involved with epileptic seizures.

## 2. Methods

### *2.1. Discrete Wavelet Transform*

The discrete wavelet transform (DWT) is a representation of a signal $x(t) \in L_2$ using a countably-infinite set of wavelets that constitute an orthonormal basis (Mallat, 1998). The synthesis and analysis representations of the discrete wavelet transform of the signal $x(t)$ can be expressed as, respectively, (Mallat, 1998)

$$x(t) = \sum_m \sum_n d_{m,n} \psi_{m,n}(t) \tag{1}$$

and

$$d_{m,n} = \int_{-\infty}^{\infty} x(t) \psi_{m,n}(t) dt \tag{2}$$

where $\psi(t)$ is a given function, the mother wavelet, and $\{d_{m,n}\}$ are the wavelet coefficients. A family of wavelets $\{\psi_{m,n}(t)\}$ is obtained as normalized dilations and translations of the mother wavelet $\psi(t)$ (Daubechies, 1988; Mallat, 1989):

$$\psi_{m,n}(t) = 2^{-m/2} \psi \left(2^{-m} t - n\right) \tag{3}$$

where $m$ and $n$ are the dilation and translation indices, respectively. The mother wavelet $\psi(t)$ is localized in both time and frequency (Cohen and Kovacevic, 1996).

For larger scales $2^m$, the wavelet $\psi_{m,n}$ is a stretched version of the mother wavelet corresponding to low frequency content, while for smaller scales $2^m$,

the wavelet $\psi_{m,n}$ is a contracted version of the mother wavelet corresponding to high frequency content. From a signal processing point of view, the orthonormal wavelet transform can be interpreted as a generalized octave-band filter bank (Wornell, 1993; Wornell and Oppenheim, 1992) because the mother wavelet $\psi(t)$ is typically an impulse response of a bandpass filter. The orthonormal wavelet transform can also be interpreted in the context of multiresolution analysis (MRA) (Mallat, 1989).

### *2.2. $1/f$ Processes*

In general, models of $1/f$ processes are represented using a frequency domain characterization. The dynamics of $1/f$ processes exhibit power-law behavior (Watters, 1998) and can be characterized in the form of (Wornell, 1993)

$$S(\omega) \sim \frac{\sigma_x^2}{|\omega|^\gamma} \tag{4}$$

over several decades of frequency $\omega$, where $S(\omega)$ is the Fourier transform of the signal $x(t)$ and $\gamma$ is the spectral exponent. An increase in the spectral exponent $\gamma$ that specifies the distribution of spectral content from low to high frequencies leads to sample functions with smoother temporal patterns (Wornell, 1995, 1993).

### *2.3. Wavelet-Based Representation for $1/f$ Processes*

The wavelet-based representation for $1/f$ processes developed in (Wornell, 1993) is presented in the following theorem.

**Theorem 1.** (Wornell, 1993) *Consider any orthonormal wavelet basis with Rth-order regularity for some $R \geq 1$. Then the random process constructed*

*via the expansion*

$$x(t) = \sum_m \sum_n d_{m,n} \psi_{m,n}(t) \tag{5}$$

*where the* $d_{m,n}$ *are a collection of mutually uncorrelated, zero-mean random variables with variances*

$$\text{var}\,(d_{m,n}) = \sigma^2 2^{\gamma m} \tag{6}$$

*for some parameter* $0 < \gamma < 2R$*, has a time-averaged spectrum*

$$S_x(\omega) = \sigma^2 \sum_m 2^{\gamma m} |\Psi\,(2^m \omega)|^2 \tag{7}$$

*that is nearly* $1/f$*, i.e.,*

$$\frac{\sigma_L^2}{|\omega|^\gamma} \leq S_x(\omega) \leq \frac{\sigma_U^2}{|\omega|^\gamma} \tag{8}$$

*for some* $0 < \sigma_L^2 \leq \sigma_U^2 < \infty$*, and has octave-spaced ripple, i.e., for any integer* $k$

$$|\omega|^\gamma S_x(\omega) = |2^k \omega|^\gamma S_x\left(2^k \omega\right). \tag{9}$$

Here, $\Psi(\omega)$ denotes the Fourier transform of the mother wavelet $\psi(t)$.

Accordingly, from Theorem 1, the spectral exponent $\gamma$ of a $1/f$ process can be determined from the linear relationship between $\log_2 \text{var}\,(d_{m,n})$ and the level $m$. The spectral exponent can then be given by

$$\gamma = \frac{\Delta \log_2 \text{var}\,(d_{m,n})}{\Delta m}. \tag{10}$$

The spectral exponent $\gamma$ of a $1/f$ process is directly related to the self-similarity (Hurst) parameter $H$ (Wornell, 1995, 1993; Wornell and Oppenheim, 1992).

*2.4. Experimental Data*

The ECoG data of epilepsy patients examined in this experiment were obtained from the Department of Epileptology, University of Bonn (available online at `http://epileptologie-bonn.de/cms/front_content.php?idcat=193&lang=3&changelang=3`) and originated from the study presented in (Andrzejak et al., 2001). There are three ECoG data sets, referred to as sets $C$, $D$ and $E$, that were recorded using intercranial electrodes from five epilepsy patients. The ECoG data of set $C$ were recorded from the hippocampal formation of the opposite hemisphere of the brain from where the seizure was thought to have originated. The ECoG data of sets $D$ and $E$ were recorded from within the epileptogenic zone. Further, the data in sets $C$ and $D$ corresponds to ECoG signals during interictal (non-seizure periods) while the ECoG data in set $E$ was recorded during seizure (ictal) activity.

Each ECoG data set contains 100 epochs of a single-channel ECoG signal that were selected to be artifact free. The length of each epoch is 4097 samples (about 23.6 seconds). In addition, the epochs of the ECoG signal satisfied the weak stationarity criterion given in (Andrzejak et al., 2001). The sampling rate of the ECoG data is 173.61 Hz and a bandpass filter (passband between 0.50 Hz and 85 Hz) was used during signal acquisition. Examples of the ECoG signal for each data set are depicted in Fig. 1.

*2.5. Analytic Framework*

In the computational experiments, the discrete Meyer wavelet bases, illustrated in Fig. 2, are used to decompose the ECoG signals into 3 levels ($m = 1,\ 2$ and 3). At these three levels the $\log_2$-var of the wavelet coefficients exhibits the most linear behavior. The spectral subbands of the

discrete Meyer wavelets corresponding to levels $m = 1,\ 2$ and 3 are shown in Fig. 3. The spectral exponent $\gamma$ of the ECoG signals is determined by computing the slope of the $\log_2$-var of the wavelet coefficients as given in (Wornell, 1995, 1993).

## 3. Results

### *3.1. The* $\log_2$-var *of the Wavelet Coefficients*

The $\log_2$-var of the wavelet coefficients of the ECoG signals of the data sets $C$, $D$ and $E$ are summarized in Table 1. In addition, the $\log_2$-var of the wavelet coefficients of the ECoG signals of the data sets $C$, $D$ and $E$ at the levels $m = 1$, $m = 2$ and $m = 3$ are compared in the box plots shown in Fig. 4, Fig. 5 and Fig. 6, respectively. It is observed that the $\log_2$-var of the wavelet coefficients of the ECoG signals of all data sets tends to increase from a lower level to a higher level. At any level, the $\log_2$-var of the wavelet coefficients of the ECoG signals of the data set $E$ tends to be higher than that of the data sets $C$ and $D$.

From the two-tail, paired $t$-test of the $\log_2$-var of the wavelet coefficients of the ECoG signals between data sets $C$ and $E$ at levels $m = 1$, $m = 2$ and $m = 3$, the null hypothesis $H_0$ of all comparisons can be rejected. Likewise, the null hypothesis of the two-tail, paired $t$-test of the $\log_2$-var of the wavelet coefficients of the ECoG signals between data sets $D$ and $E$ at levels $m = 1$, $m = 2$ and $m = 3$ can be rejected. Therefore, based on the two-tail, paired $t$-test, the results suggest that there are statistically significant differences between the $\log_2$-var of the wavelet coefficients of ECogG signals of data sets $C$ and $E$ and between data sets $D$ and $E$ at any level $m$ with a $p$-value of

$p \ll 0.0001$.

On the other hand, the null hypothesis of the two-tail, paired $t$-test of the $\log_2$-var of the wavelet coefficients of the ECoG signals between data sets $C$ and $D$ cannot be rejected at any level $m$. This result therefore suggests that there are not statistically significant differences between the $\log_2$-var of the wavelet coefficients of ECoG signals between data sets $C$ and $D$ at any level $m$. The results of all two-tail, paired $t$-tests are summarized in Table 2.

### *3.2. The Spectral Exponents of Epileptic ECoG Signals*

From the $\log_2$-var of the wavelet coefficients of the ECoG signals of data sets $C$, $D$ and $E$ shown in Fig. 4, Fig. 5 and Fig. 6, the spectral exponent $\gamma$ of the ECoG signals is determined. The box plots of the spectral exponents $\gamma$ of the ECoG signals of data sets $C$, $D$ and $E$ are illustrated in Fig. 7. The mean and the standard deviation of the spectral exponents $\gamma$ of the ECoG signals for data sets $C$, $D$ and $E$ are summarized in Table 3. The spectral exponent $\gamma$ of the ECoG signals of data set $E$ tends to be higher than that of data sets $C$ and $D$ while the spectral exponent $\gamma$ of the ECoG signals of data set $D$ tend to be just slightly higher than that of data set $C$.

The two-tail, paired $t$-test is used to determine whether there is a statistically significant difference between the spectral exponents $\gamma$ of ECoG signals from the two data sets. The results of all two-tail, paired $t$-tests are summarized in Table 4. Based on the two-tail, paired $t$-tests, the results suggest that the spectral exponent $\gamma$ of the ECoG signals of data set $E$ is significantly different from that of data set $C$. Also, there is a statistically significant difference between the spectral exponents $\gamma$ of the ECoG signals of data sets $E$ and $D$. However, there is not a statistically significant difference

between the spectral exponents $\gamma$ of the ECoG signals of data sets $C$ and $D$ with a $p$-value of 0.0006.

## 4. Discussion

In this study, we investigate the scale-invariant characteristics of the dynamics of the brain as quantified using ECoG data from subjects with epilepsy associated with different pathological brain states (ictal and interictal) and different regions of the brain. The scale-invariant characteristics of the dynamics of the brain of subjects with epilepsy are examined in terms of fractal properties using a wavelet-based representation for $1/f$ processes (Wornell, 1995, 1993). From the computational results, we observe that ECoG signals associated with different ictal and interictal brain activity or different brain regions exhibit different scale-invariant characteristics.

The spectral exponent $\gamma$ of ECoG signals obtained during seizure activity tends to be higher than that of ECoG signals obtained during non-seizure activity even though the ECoG signals are acquired from different brain regions, i.e., within the epileptogenic zone and outside the epileptogenic zone. Therefore, the ECoG signal obtained during seizure activity tends to have smoother sample path patterns than ECoG signals acquired during non-seizure periods. This further suggests that ECoG signals acquired during seizure activity tends to be more self-similar than the ECoG signals obtained during non-seizure periods. Further, there are statistically significant differences between the scale-invariant characteristics or temporal patterns of ECoG signals obtained during seizure activity and that obtained during non-seizure periods.

In addition, during non-seizure activity the ECoG signals acquired from within the epileptogenic zone tends to exhibit different scale-invariant characteristics from ECoG signals acquired from outside the epileptogenic zone. During non-seizure activity, the spectral exponent $\gamma$ obtained from within the epileptogenic zone tends to be slightly higher than that obtained from outside the epileptogenic zone. This therefore suggests that the dynamics of the brain activity as quantified by the ECoG signals obtained from within the epileptogenic zone during non-seizure activity are slightly more self-similar than ECoG signal obtained from outside the epileptogenic zone.

The computational results suggests that the dynamics of neuronal networks of subjects with epilepsy during ictal and interictal periods have distinguishing self-similar characteristics. During ictal activity thedynamics of the brain tends to be more scale-invariant (self-similar) than that during interictal periods. Accordingly, the neuronal networks during seizure activity generate ECoG signals with a smoother temporal patterns than those generated by neuronal networks during interictal periods. During non-seizure periods, the dynamics of neuronal networks that are involved with the generation of epileptic seizures (within the epileptogenic zone) also behave differently from the neuronal networks that are outside the regions involved with epileptic seizure activity. An ECoG signal acquired from within the epileptogenic zone during an interictal period has scale-invariant behavior that is slightly similar to the scale-invariant behavior of ECoG signals acquired during seizure activity.

## Acknowledgments

This work is supported by a TRF-CHE Research Grant for New Scholar, jointly funded by the Thailand Research Fund (TRF) and the Commission on Higher Education (CHE), the Ministry of Education, Thailand, under Contract No. MRG5280189.

## Conflict of Interest

None.

## References

Andrzejak, R. G., Lehnertz, K., Mormann, F., Rieke, C., David, P., Elger, C. E., 2001. Indications of nonlinear deterministic and finit-dimensional structures in time series of brain electrical activity: Dependence on recording region and brain state. Phys. Rev. E 64, (061907)1–8.

Bak, P., 1997. How nature works. Oxford UP, Oxford.

Barabási, A. L., Stanley, H. E., 1995. Fractal concepts in surface growth. Cambridge UP, Cambridge, UK.

Bassingthwaighte, J. B., Liebovitch, L. S., West, B. J., 1994. Fractal physiology. Oxford UP, New York.

Cohen, A., Kovacevic, J., 1996. Wavelets: the mathematical background. Proceedings of the IEEE 84, 514–522.

Daubechies, I., 1988. Orthonormal bases of compactly supported wavelets. Commun. Pure Appl. Math. XLI, 909–996.

Goldberger, A. L., 2006. Complex systems. Proc. Am. Thorac. Soc. 3, 467–472.

Gong, P., Nikolaev, A. R., van Leeuwen, C., 2003. Scale-invariant fluctuations of the dynamical synchronization in human brain electrical activity. Neurosci. Lett. 336, 33–36.

Havlin, S., Buldyrev, S. V., Goldberger, A. L., Mantegna, R. N., Ossadnik, S. M., Peng, C.-K., Simons, M., Stanley, H., 1995. Fractals in biology and medicine. Chaos, Solitons & Fractals 6, 171–201.

Linkenkaer-Hansen, K., Nikouline, V. V., Palva, J. M., Ilmoniemi, R. J., 2001. Long-range temporal correlations and scaling behavior in human brain oscillations. J. of Neurosci. 21, 1370–1377.

Mallat, S., 1998. A wavelet tour of signal processing. Academic Press, San Diego.

Mallat, S. G., 1989. A theory for multiresolution signal decomposition: the wavelet representation. IEEE Trans. Pattern Analysis and Machine Intelligence 11, 674–693.

Mandelbrot, B. B., 1982. The fractal geometry of nature. WH Freeman, San Francisco.

Mandelbrot, B. B., Ness, H. W. V., 1968. Fractional brownian motions, fractional noises and applications. SIAM Rev. 10, 422–436.

Miltner, W. H. R., Braun, C., Arnold, M., Witte, H., Taub, E., 1999. Coher-

ence of gamma-band eeg activity as a basis for associate learning. Nature 397, 434–436.

Mima, T., Oluwatimilehin, T., Hiraoka, T., Hallett, M., 2001. Transient interhemispheric neuronal synchrony correlates with object recognition. J. of Neurosci. 21, 3942–3948.

Nikolaev, A. R., Ivanitsky, G. A., Ivanitsky, A. M., Posner, M. I., Abdullaev, Y. G., 2001. Correlation of brain thythms between frontal and left temporal (wernicke's) cortical areas during verbal thinking. Neurosci. Lett. 298, 107–110.

Stam, C. J., de Bruin, E. A., 2004. Scale-free dynamics of global functional connectivity in the human brain. Human Brain Mapping 22, 97–109.

Watters, P. A., 1998. Fractal structure in the electroencephalogram. Complexity International 5.

Wornell, G. W., 1993. Wavelet-based representations for the $1/f$ family of fractal processes. Proceedings of the IEEE 81, 1428–1450.

Wornell, G. W., 1995. Signal processing with fractals: A wavelet-based approach. Prentice Hall, New Jersey.

Wornell, G. W., Oppenheim, A. V., 1992. Estimation of fractal signals from noisy measurements using wavelets. IEEE Trans. on Signal Processing 40, 611–623.

Table 1: The $\log_2$-var of the wavelet coefficients of the EEG signals

| Data Set | Level | Mean | S.D. |
|---|---|---|---|
| $C$ | $m = 1$ | 2.9911 | 1.3968 |
| $C$ | $m = 2$ | 6.2340 | 1.6298 |
| $C$ | $m = 3$ | 9.5324 | 1.5395 |
| $D$ | $m = 1$ | 2.9810 | 1.4276 |
| $D$ | $m = 2$ | 6.5519 | 1.7542 |
| $D$ | $m = 3$ | 10.0206 | 1.7979 |
| $E$ | $m = 1$ | 6.2813 | 2.0866 |
| $E$ | $m = 2$ | 12.4262 | 1.9566 |
| $E$ | $m = 3$ | 16.7179 | 2.0089 |

Table 2: Results of two-tail, paired $t$-test of the $\log_2$-var of the wavelet coefficients between the EEG data sets

| Data Sets | Level | Hypothesis | $p$-value |
|---|---|---|---|
| $C$ vs $D$ | $m = 1$ | $H_0$ not rejected | 0.9596 |
| $C$ vs $E$ | $m = 1$ | $H_0$ rejected | $\ll 0.0001$ |
| $D$ vs $E$ | $m = 1$ | $H_0$ rejected | $\ll 0.0001$ |
| $C$ vs $D$ | $m = 2$ | $H_0$ not rejected | 0.1858 |
| $C$ vs $E$ | $m = 2$ | $H_0$ rejected | $\ll 0.0001$ |
| $D$ vs $E$ | $m = 2$ | $H_0$ rejected | $\ll 0.0001$ |
| $C$ vs $D$ | $m = 3$ | $H_0$ not rejected | 0.0405 |
| $C$ vs $E$ | $m = 3$ | $H_0$ rejected | $\ll 0.0001$ |
| $D$ vs $E$ | $m = 3$ | $H_0$ rejected | $\ll 0.0001$ |

Table 3: The spectral exponents $\gamma$ of the wavelet coefficients of the EEG signals

| Data Set | Mean | S.D. |
|---|---|---|
| $C$ | 3.2706 | 0.4239 |
| $D$ | 3.5198 | 0.5806 |
| $E$ | 5.2183 | 0.5423 |

Table 4: Results of two-tail, paired $t$-test of the spectral exponents $\gamma$ of the wavelet coefficients between the EEG data sets

| Data Sets | Hypothesis | $p$-value |
|---|---|---|
| $C$ vs $D$ | $H_0$ not rejected | 0.0006 |
| $C$ vs $E$ | $H_0$ rejected | $\ll 0.0001$ |
| $D$ vs $E$ | $H_0$ rejected | $\ll 0.0001$ |

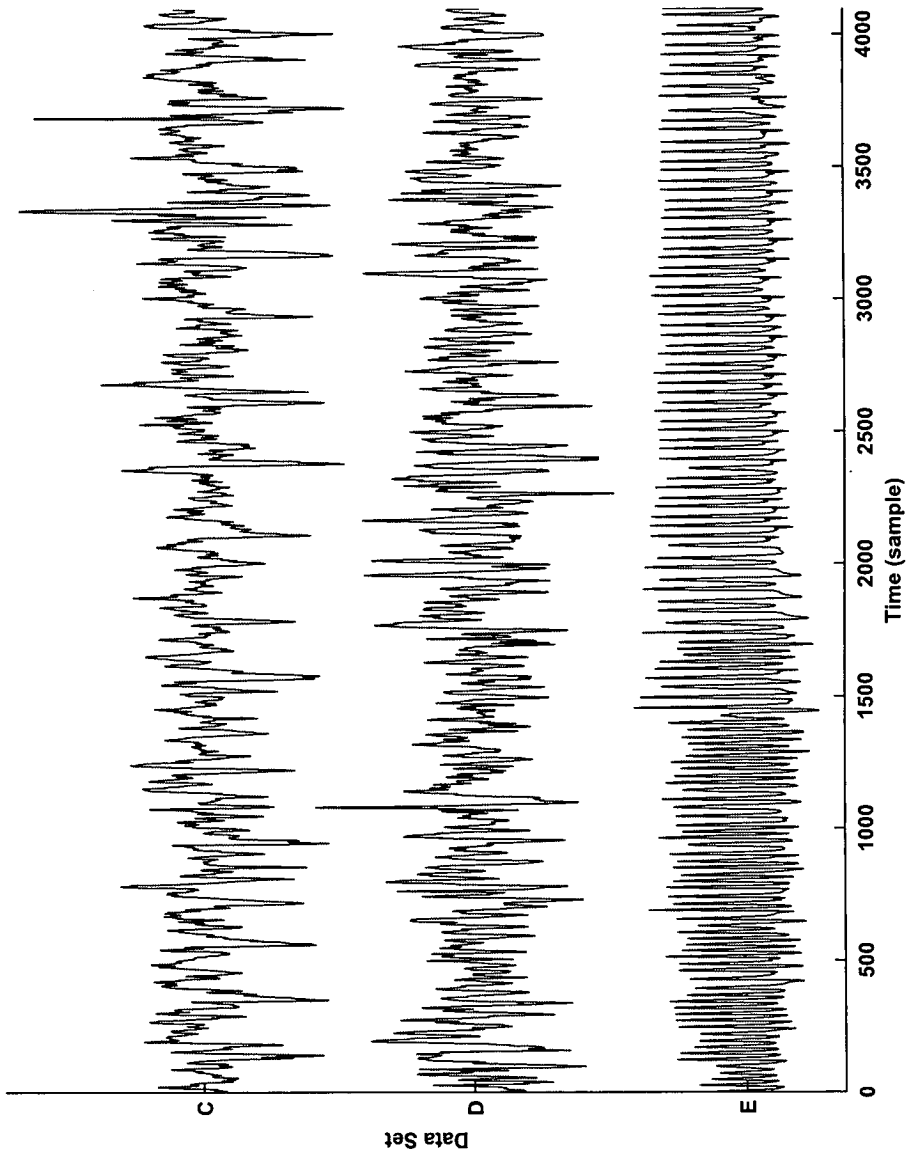


Figure 1: Examples of EEG signals of the data sets $C$, $D$ and $E$.

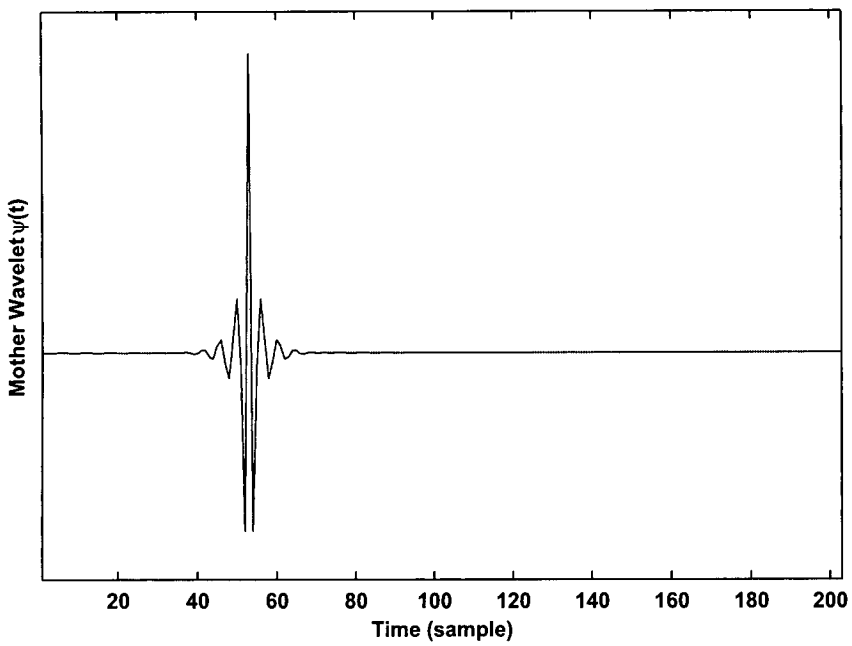


Figure 2: The mother wavelet of the discrete Meyer basis.

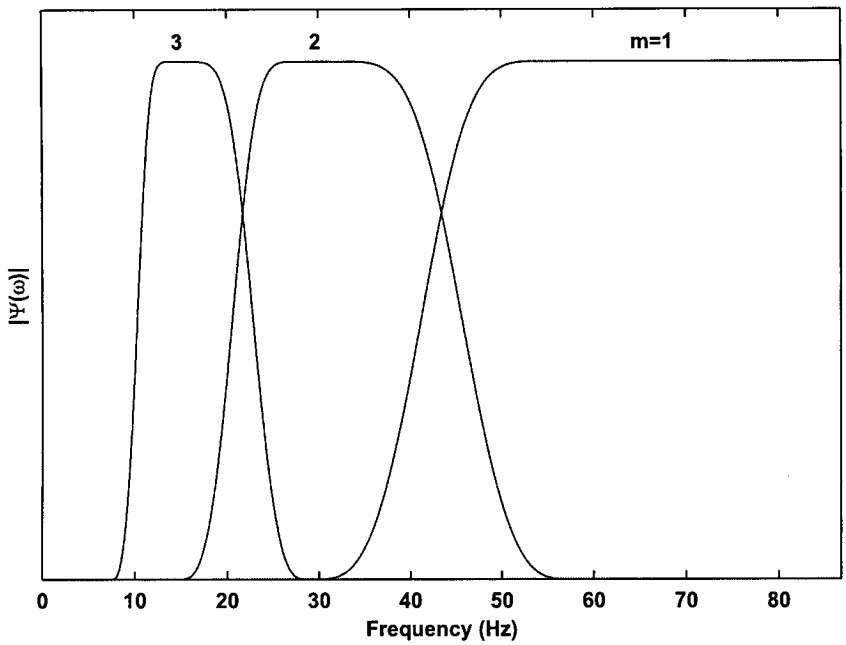


Figure 3: The corresponding spectral subbands of the discrete Meyer wavelets at the levels $m = 1,\ 2$ and 3.

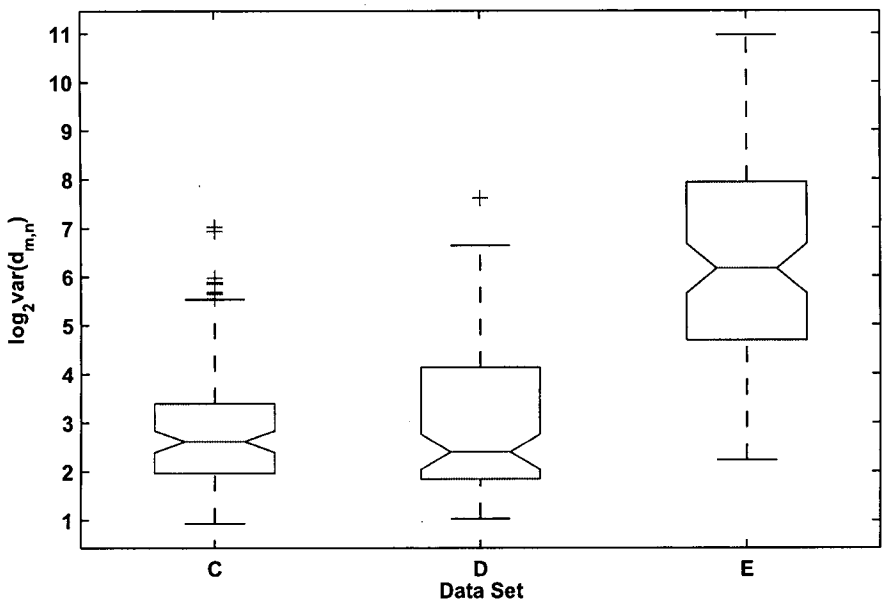


Figure 4: The $\log_2$-var of the wavelet coefficients of the EEG signals corresponding to the level $m = 1$.

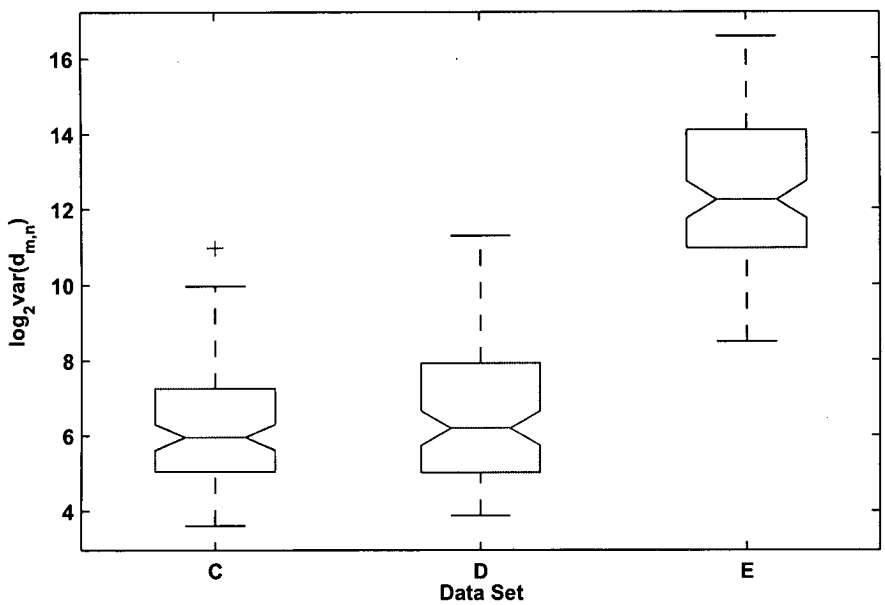


Figure 5: The $\log_2$-var of the wavelet coefficients of the EEG signals corresponding to the level $m = 2$.

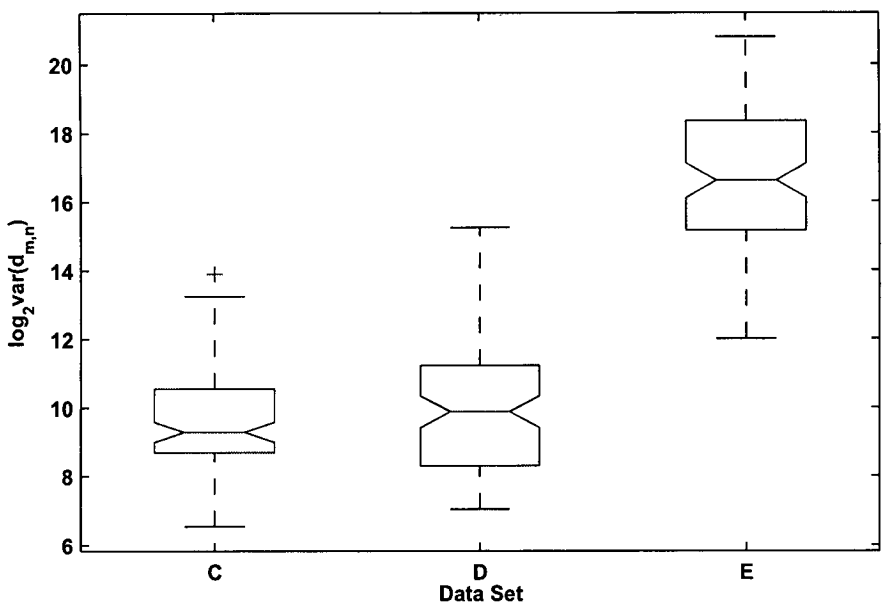


Figure 6: The $\log_2$-var of the wavelet coefficients of the EEG signals corresponding to the level $m = 3$.

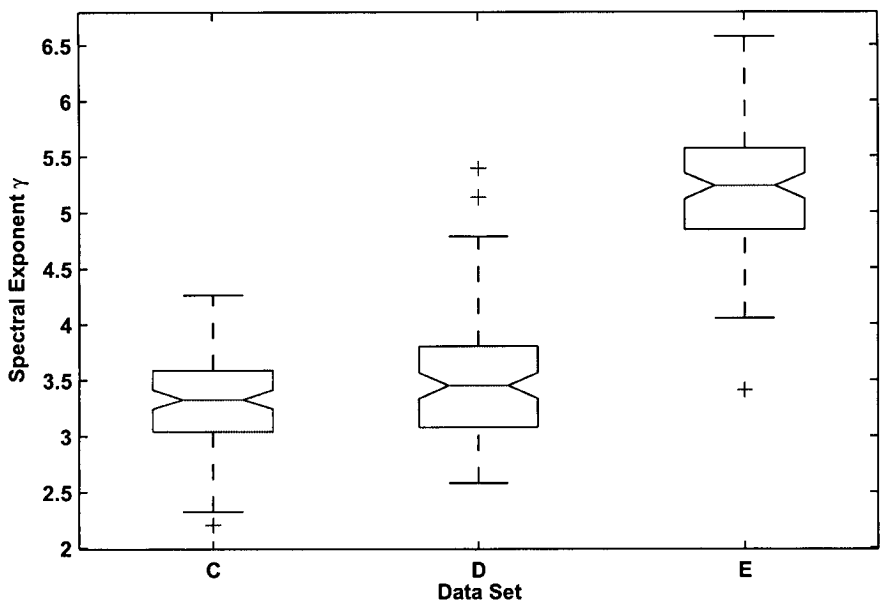


Figure 7: The spectral exponents of the ECoG signals of data sets $C$, $D$ and $E$.

# Examination of Scale-Invariant Behaviors of Epileptic ECoG Signals for Seizure Localization: A Preliminary Study

S. Janjarasjitt[a,b,*], K. A. Loparo[b]

[a]*Department of Electrical and Electronic Engineering, Ubon Ratchathani University, Warinchamrab, Ubon Ratchathani 34190 Thailand*
[b]*Department of Electrical Engineering and Computer Science, Case Western Reserve University, Cleveland, Ohio 44106 USA*

## ıbstract

*)bjective:* To investigate the scale-invariant behaviors of the brain for evidence of epileptic seizure localization.
*Aethods:* ECoG data of a subject diagnosed with right mesial temporal lobe epilepsy (MTLE) obtained from various egions of the brain and associated with different pathological states are analyzed using wavelet-based fractal analysis o compute the spectral exponent $\gamma$, a computational measure used for quantifying the scale-invariant behavior of the rain.
*'esults:* The brain of a subject with mesial temporal lobe epilepsy (MTLE) associated with different states exhibits ifferent scale-invariant behaviors. The spectral exponent of the ECoG data substantially increases during an epileptic eizure event. Furthermore, this characteristic can be observed only in regions of the brain that are involved with the eneration of epileptiform activity (epileptogenic zone).
*'onclusions:* The computational results suggest that there are significant differences between the scale-invariant beavior of ECoG data during an ictal phase and that during both pre-ictal and post-ictal phases. The scale-invariant ehavior of the ECoG data obtained from inside the epileptogenic zone is significantly different from that obtained from utside the epileptogenic zone. In addition, the interaction effect between the regions of the brain and the phases is not atistically significant.
*'ignificance:* The computational results provide preliminary evidence that the epileptogenic zone of mesial temporal obe epilepsy may be localized both temporally and spatially by examining the scale-invariant characteristics.

*'eywords:* epilepsy, seizure, localization, epileptogenic zone, fractals, scale-invariant

## . Introduction

Epilepsy is a common neurological disorder in which lusters of nerve cells or neurons in the brain sometimes ignal abnormally [1]. Around 50 milllion people world-ide are affected by epilepsy [2]. Epilepsy is characterized y recurrent seizures that are physical reactions to sudden, sually brief, excessive electrical discharges in clusters of erve cells [2]. The normal pattern of neuronal activity iat is disturbed, in epilepsy, can cause strange sensa-ons, emotions, and behaviors, or sometimes convulsions .e. violent and involuntary contractions of the muscles), iuscle spasms, and loss of consciousness [1]. There are iany possible causes for seizures ranging from illness to rain damage to abnormal brain development [1].

Seizures are divided into two major categories: focal eizures and generalized seizures [1]. Focal seizures, also alled partial seizures, occur in just one part of the brain while generalized seizures are a result of abnormal neuronal activity on both hemispheres of the brain [1]. At the present time, there is no cure for epilepsy [1]. Currently available treatments can control seizures at least some of the time [1], and prescription antiepileptic drugs are the most common treatment approach [1]. Recent studies in developed and developing countries have shown that up to 70% of newly diagnosed children and adults with epilepsy can be successfully treated with antiepileptic drugs [2]. Epilepsy surgery is an alternative treatment for patients who respond poorly to antiepileptic drugs [1, 2]. The most common type of surgery for epilepsy is removal of a seizure focus or small area of the brain where seizures originate [1].

There are a number of different tests that have been developed for diagnosing epilepsy. The most common diagnostic test for epilepsy is the investigation of EEG (electroencephalogram) [1]. EEG signals display the electrical activity of the brain, usually recorded by electrodes placed on the scalp. Scalp EEG is however very sensitive to signal attenuation and artifacts, and also has poor spatial resolution. Intracranial EEG or electrocorticogram (ECoG) is an invasive approach to provide improved mea-

*Corresponding author
*Email addresses:*
ısupajt@ubu.ac.th,suparerk.janjarasjitt@case.edu (S. anjarasjitt), kenneth.loparo@case.edu (K. A. Loparo)

irement of electrical activity of the brain by placing elec-odes on the cortex. Abnormalities in the brain's electri-il activity can be detected in the EEG and ECoG sig-als. Another useful and significant diagnosis technique : epilepsy is through the use of brain scans. The most ommonly used brain scans include CT (computed tomog-aphy), PET (positron emission tomography), and MRI nagnetic resonance imaging) [1].

Recently, concepts and computational methods derived om the contemporary study of complex systems including aos theory, nonlinear dynamics and fractals have gained creasing interest for applications in biology and medicine ecause physiological signals and systems can exhibit an traordinary range of patterns and behaviors [3]. The athematical concept of a fractal is commonly associated ith irregular objects that exhibit a property called scale-variance or self-similarity [3, 4]. Fractal forms are com-osed of subunits resembling the structure of the macro-opic object [3] that can emerge in nature from statisti-il scaling behavior in the underlying physical phenomena ]. An important class of statistical scale-invariant or self-milar random processes is the family of $1/f$ processes [5].

There is evidence that some biological systems can ex-ibit scale-invariant or scale-free behavior, in the sense at they do not have a characteristic length or time scale at dominates the dynamics of the underlying process , 7, 8]. Fractal properties of different biological systems an be significantly different in their nature, origin, and ppearance [6], where scale-invariant or scale-free behav-r is a tendency of a complex system to develop long-range rrelations in time and space [9, 10, 11]. Even though it is ell accepted that the dynamics of the brain are inherently mplex, the activity of the brain can exhibit intriguing mporal patterns that are important correlates of the un-erlying dynamics of information encoding and processing .2].

A traditional mathematical model and the empirical roperties of $1/f$ processes have largely been inspired by e fractional Brownian motion framework [5, 13, 14] as eveloped by Mandelbrot and Van Ness [15]. In general, odels of $1/f$ processes are represented using a frequency omain characterization. The dynamics of $1/f$ processes chibit power law behavior [16] and can be characterized the frequency domain by $S(\omega) \propto 1/|\omega|^{\gamma}$. In [5, 13], wavelet-based representation for $1/f$ processes was de-eloped. As the wavelet transform is a natural tool for me-frequency analysis, it is well suited for quantifying lf-similar or scale-invariant characteristics of signals and lay a significant role in the study of self-similar signals nd systems [5]. The spectral exponent $\gamma$ that specifies e distribution of power from low to high frequencies of $/f$ processes can be computed in terms of the slope of the g-variance of the wavelet coefficients versus scale graph.

In this study we investigate the scale-invariant behav-rs of the brain for an evidence of epileptic seizure lo-alization. ECoG data of a subject diagnosed with right esial temporal lobe epilepsy (MTLE) obtained from various regions of the brain and associated with different pathological states of the brain are used to compute the spectral exponent $\gamma$ a computational measure for quantifying scale-invariant behavior of the brain. The computational results show that there is a substantial and sudden increase in the spectral exponent $\gamma$ during an epileptic seizure event. In addition, this substantial and sudden increase in the spectral exponent $\gamma$ is a key signature of an epileptic seizure that is only observed in regions of the brain that are involved with the development of epileptic seizure (epileptogenic zone). Therefore, this provides preliminary evidence that epileptic seizures can be localized temporally and spatially by quantifying the scale-invariant behavior of the brain.

## 2. Background

### *2.1. Discrete Wavelet Transform*

The discrete wavelet transform (DWT) is a representation of a signal $x(t) \in L_2$ using a countably-infinite set of wavelets that constitute an orthonormal basis [17]. The synthesis and analysis representations of the discrete wavelet transform of the signal $x(t)$ can be expressed, respectively, as [17]

$$x(t) = \sum_m \sum_n d_{m,n} \psi_{m,n}(t) \tag{1}$$

and

$$d_{m,n} = \int_{-\infty}^{\infty} x(t) \psi_{m,n}(t) dt \tag{2}$$

where $\psi(t)$ is a given function, the mother wavelet, and $\{d_{m,n}\}$ are the wavelet coefficients. A family of wavelets $\{\psi_{m,n}(t)\}$ is obtained as normalized dilations and translations of the mother wavelet $\psi(t)$ [18, 19]:

$$\psi_{m,n}(t) = 2^{-m/2} \psi\left(2^{-m}t - n\right) \tag{3}$$

where $m$ and $n$ are the dilation and translation indices, respectively. The mother wavelet $\psi(t)$ is localized in both time and frequency [20].

For large scale $2^m$, the wavelet $\psi_{m,n}$ is a stretched version of the mother wavelet corresponding to the low frequency content, while for small scale $2^m$, the wavelet $\psi_{m,n}$ is a contracted version of the mother wavelet corresponding to the high frequency content. From a signal processing perspective, the orthonormal wavelet transform can be interpreted as a generalized octave-band filter bank [13, 14] because the mother wavelet $\psi(t)$ is typically the impulse response of a bandpass filter. The orthonormal wavelet transform can also be interpreted in the context of multiresolution analysis (MRA) [19].

### *2.2. $1/f$ Processes*

In general, models of $1/f$ processes are represented using a frequency domain characterization. The dynamics of

$1/f$ processes exhibit power-law behavior [16] and can be characterized in the form of [13]

$$S(\omega) \sim \frac{\sigma_x^2}{|\omega|^\gamma} \tag{4}$$

over several decades of frequency $\omega$, where $S(\omega)$ is the Fourier transform of the signal $x(t)$ and $\gamma$ is a spectral exponent. An increase in the spectral exponent $\gamma$ specifying the distribution of spectral content from low to high frequencies leads to sample functions with smoother temporal patterns [5, 13, 14].

### 2.3. Wavelet-Based Representation for $1/f$ Processes

The wavelet-based representation for $1/f$ processes developed in [13] is presented in the following theorem.

**Theorem 1.** [13] *Consider any orthonormal wavelet basis with Rth-order regularity for some $R \geq 1$. Then the random process constructed via the expansion*

$$x(t) = \sum_m \sum_n d_{m,n} \psi_{m,n}(t) \tag{5}$$

*where the $d_{m,n}$ are a collection of mutually uncorrelated, zero-mean random variables with variances*

$$\text{var}\,(d_{m,n}) = \sigma^2 2^{\gamma m} \tag{6}$$

*for some parameter $0 < \gamma < 2R$, has a time-averaged spectrum*

$$S_x(\omega) = \sigma^2 \sum_m 2^{\gamma m} |\Psi\,(2^m \omega)|^2 \tag{7}$$

*that is nearly $1/f$, i.e.,*

$$\frac{\sigma_L^2}{|\omega|^\gamma} \leq S_x(\omega) \leq \frac{\sigma_U^2}{|\omega|^\gamma} \tag{8}$$

*for some $0 < \sigma_L^2 \leq \sigma_U^2 < \infty$, and has octave-spaced ripple, i.e., for any integer $k$*

$$|\omega|^\gamma S_x(\omega) = |2^k \omega|^\gamma S_x\left(2^k \omega\right). \tag{9}$$

*Here, $\Psi(\omega)$ denotes the Fourier transform of the mother wavelet $\psi(t)$.*

Accordingly, from Theorem 1, the spectral exponent of a $1/f$ process can be determined from the linear relationship between $\log_2 \text{var}\,(d_{m,n})$ and the level $m$. The spectral exponent can then be given by

$$\gamma = \frac{\Delta \log_2 \text{var}\,(d_{m,n})}{\Delta m}. \tag{10}$$

and is related to the self-similarity (Hurst) parameter $H$ [5, 13, 14].

## 3. Methods

### 3.1. Data and Subject

Long-term multi-channel ECoG data of an epilepsy patient studied at University Hospitals of Cleveland, Case Medical Center in Cleveland, Ohio, USA are examined. With the consent of the patient, the long-term ECoG data were recorded for a few days using a Nihon-Kohden EEG system (band-pass (0.10–300 Hz) filter, 1,000 Hz sampling rate) prior to surgery. The patient was diagnosed with right mesial temporal lobe epilepsy (MTLE).

A 12-hour section of the long-term ECoG data recorded between 1:55 p.m. and 1:55 a.m is examined in this study. This section of long-term ECoG data contains 4 epileptic seizure events and consists of 11 channels of differential ECoG signals as follow: 3 channels of right posterior basal temporal lobe (referred to as RPT1, RPT2 and RPT3), 3 channels of right anterior basal temporal lobe (referred to as RAT1, RAT2 and RAT3), and 5 channels of right mesial temporal lobe (referred to as RMT1, RMT2, RMT3, RMT4 and RMT5). The first, second, third, and fourth epileptic seizure events occur between 02:42:48 and 02:44:03, 03:54:36 and 03:56:25, 05:02:24 and 05:03:45, and 06:41:36 and 06:43:14 of the section, respectively.

Segments of the ECoG signals around the first, second, third and last epileptic seizure events are shown in Fig. 1, Fig. 2, Fig. 3 and Fig. 4, respectively. Evidently, there are only a number of channels recording from the right mesial temporal lobe region, i.e., RMT3, RMT4 and RMT5, that are directly affected by the epileptic seizures.

### 3.2. Analytic Framework

In the computational experiment, the ECoG data are partitioned into epochs of 8,000 samples (8 seconds) each with a sliding window of 2,000 samples (2 seconds). The epochs of ECoG data are decomposed into 6 levels using the 5th order Coiflet mother wavelet that provides the highest number of vanishing moments for both $\phi$ and $\psi$ for a given support. Wavelet coefficients of all levels, i.e., $m = 1, 2, \ldots, 6$, are used to estimate the spectral exponent $\gamma$ using a linear least-squares regression technique.

In addition, a weighted moving average filter is applied to smooth the spectral exponents of the epochs of ECoG data to reveal their main characteristics. The smoothed spectral exponent is given by

$$\tilde{\gamma}(n) = \sum_{k=n-N}^{n+N} w(k - (n - N))\gamma(k) \tag{11}$$

where $\gamma(k)$ denotes the spectral exponent of the $k$th epoch of an ECoG signal and $N = 59$. The window function $w(n)$ used for the weighted moving average filter is a Hamming window given by

$$w(n) = \frac{1}{63.8}\left(0.54 - 0.46 \cos\left(2\pi \frac{n}{2N}\right)\right) \tag{12}$$

for $n = 0, 1, \ldots, 2N$.

Furthermore, in the computational experiment, the states the brain are divided into three phases as follow: pre-tal, ictal and post-ictal phases. The pre-ical phase in is study is defined as a five-minute period before an ileptic seizure onset while the post-ictal phase is defined a five-minute period after an epileptic seizure event. Re-ark: the times of epileptic seizure onsets are identified visual changes in the ECoG signals by trained clinical ersonnel. To test whether spectral exponents of ECoG ata obtained from different regions of the brain and as-ociated with different phases have a common mean, a vo-way analysis of variance (ANOVA) is used.

## Results

*1. Localization of Epileptogenic Zone*

The spectral exponents $\gamma$ of the first 4-hour section, ie second 4-hour section and the last 4-hour section of ie ECoG data are shown, respectively, in Fig. 5, Fig. 6 id Fig. 7. Likewise, the smoothed spectral exponents $\bar{\gamma}$ of ie first 4-hour section, the second 4-hour section and the st 4-hour section of the ECoG data are shown in Fig. 8, ig. 9 and Fig. 10, respectively. The spectral exponents (the smoothed spectral exponents $\bar{\gamma}$) of the ECoG data ury corresponding to various states of the brain. Further, ie different channels of the ECoG data exhibit different aracteristics of the spectral exponents $\gamma$ (the smoothed ectral exponents $\bar{\gamma}$) even in the same state of the brain.

In addition, the smoothed spectral exponents $\bar{\gamma}$ of the CoG data around the first, second, third and fourth epilep-c seizure events are illustrated in Fig. 11, Fig. 12, Fig. 13, id Fig. 14, respectively. There are distinguishable changes the spectral exponents $\gamma$ (the smoothed spectral expo-ents $\bar{\gamma}$) corresponding to the epileptic seizure events in ie ECoG channels RMT3, RMT4 and RMT5. It can e observed that the smoothed spectral exponents $\bar{\gamma}$ sub-atially increase at an epileptic seizure onset and then ecrease right after an epileptic seizure in the ECoG chan-els that are recording from the epileptogenic zone where ie seizure originates.

The ECoG channels which are in the epileptogenic zone, ., RMT3, RMT4 and RMT5, are further investigated. he smoothed spectral exponents $\bar{\gamma}$ of the first 4-hour sec-on, the second 4-hour section and the last 4-hour section the ECoG channels RMT3, RMT4 and RMT5 are illus-ated in Fig. 15, Fig. 16, and Fig. 17, respectively. The rresponding smoothed spectral exponents $\bar{\gamma}$ (plotted in ack) are compared to the ECoG channel RMT4 (plot-d in gray) around the first, second, third and fourth ileptic seizure events in Fig. 18, Fig. 19, Fig. 20 and g. 21, respectively. The dashed lines indicate the epilep-c seizure onset. Clearly, the spectral exponents $\gamma$ signifi-ntly change corresponding to the epileptic seizure events.

*2. Comparison of Spectral Exponents*

The mean, standard deviation (S.D.) and median of e smoothed spectral exponents $\bar{\gamma}$ of every ECoG channels corresponding to pre-ictal, ictal and post-ictal phases, are summarized in Table 1. Box plots shown in Fig. 22, Fig. 23 and Fig. 24 compare the smoothed spectral exponents $\bar{\gamma}$ of all ECoG channels corresponding to pre-ictal, ictal and post-ictal phases, respectively. Obviously, there are differences in the smoothed spectral exponents $\bar{\gamma}$ between either different channels or different states of the brain.

The mean, standard deviation (S.D.) and median of the smoothed spectral exponents $\bar{\gamma}$ of different regions of the brain, i.e., RPT, RAT and RMT, corresponding to various states of the brain are summarized in Table 2. In addition, the smoothed spectral exponents $\bar{\gamma}$ of different regions of the brain corresponding to various states of the brain are compared in a box plot shown in Fig. 25. The smoothed spectral exponent $\bar{\gamma}$ of the ECoG channels obtained from the right mesial temporal lobe region during the ictal phase tends to be higher than that during the pre-ictal and post-ictal phases. Furthermore, during the ictal phase the smoothed spectral exponent $\bar{\gamma}$ of the ECoG channels obtained from the right mesial temporal lobe region tends to be higher than that obtained from the right posterior basal temporal lobe and right anterior basal temporal lobe regions. Apparently, there are conspicuous characteristics of the spectral exponents of the ECoG channels obtained from the right mesial temporal lobe region during the ictal phase.

A two-way analysis of variance (ANOVA) is used with regions of the brain and phases as the two factors. For the regions of the brain there are three levels (RPT, RAT and RMT) and for the phases there are three levels (pre-ictal, ictal and post-ictal). Table 4 and Table 5 summarize the mean square, $F$-statistic and $p$-value of the two-way ANOVA of the spectral exponents $\gamma$ and the smoothed spectral exponents $\bar{\gamma}$, respectively. From the two-way ANOVA, the results indicate that the individual factors, i.e., regions of the brain and phases, have the most significant influence on the spectral exponent (and also the smoothed spectral exponent). In addition, there is an evidence that the interaction effect between the regions of the brain and the phases is not significant.

## 5. Conclusions

In this study, we examine the scale-invariant behaviors of the brain of a subject diagnosed with right mesial temporal lobe epilepsy (MTLE) using wavelet-based fractal analysis. ECoG data recorded from various regions of the brain (right posterior basal temporal lobe (RPT), right anterior basal temporal lobe (RAT) and right mesial temporal lobe (RMT)) and associated with different pathological states of the brain (pre-ictal, ictal and post-ictal phases) are analyzed. The spectral exponent $\gamma$ that specifies a distribution of spectral content from low to high frequencies is used as a computational measure for quantifying scale-invariant behavior. An increase in the spectral exponent $\gamma$

ads to sample functions with smoother temporal patterns nd less complexity.

From the computational results, the spectral exponent (and the smoothed spectral exponent $\bar{\gamma}$) of the ECoG ata vary corresponding to the pathological states of the rain. There is a substantial increase in the spectral expoent $\gamma$ during an epileptic seizure event. The spectral exponent $\gamma$ of the ECoG data during an ictal phase is signifiantly higher than that during both pre-ictal and post-ictal hases. In addition, the ECoG data that is recorded from ifferent regions of the brian also exhibit different characeristics of the spectral exponent $\gamma$. The distinguishable haracteristics of the spectral exponent $\gamma$ during an epilepc seizure event can be observed only in the channels that re involved with the generation of an epileptic seizure vent or inside the epileptogenic zone. This therefore sugests that ECoG data recorded from within the epileptoenic zone during an epileptic seizure event have smoother mporal patterns and are less complex than ECoG data ecorded from outside the epileptogenic zone and ECoG ata that are recorded in the absence of epileptic seizures.

Clearly the underlying process of the brain behaves difrently corresponding to different states of the brain. The ıcrease of the spectral exponent $\gamma$ of the ECoG data durıg an epileptic seizure event suggests that the underlying rocess of the brain during an epileptic seizure event beomes more self-similar. Since such self-similar or scaleıvariant characteristics can be observed only in the chanels inside the epileptogenic zone, the underlying neuronal etworks inside the epileptogenic zone are not strongly oupled with the underlying neuronal networks outside ıe epileptogenic zone during the seizure. From statistical ests, it is shown that both the pathological state of the rain and the region of the brain individually have an inuence on the scale-invariant behavior. Furthermore, the ıteraction effect between the state of the brain and the egion of the brain does not have a significant influence on ıe scale-invariant behavior.

## . Discussion

The goal of presurgical epilepsy evaluation is to idenfy and delineate the cortical area that is primarily reonsible for the generation of the epileptic seizures (the pileptogenic zone) [21]. From the computational results, is shown that all epileptic seizure events can be visullized from the characteristics of the spectral exponent used as a computational measure for quantifying the ale-invariant behavior. This therefore provides preliminary evidence that the onset of an epileptic seizure can be lentified by temporally localizing changes in the spectral xponent. Furthermore, the epileptogenic zone can also e identified by analyzing these changes in the spectral xponent..


## Acknowledgments

This work is supported by a TRF-CHE Research Grant for New Scholar, jointly funded by the Thailand Research Fund (TRF) and the Commission on Higher Education (CHE), the Ministry of Education, Thailand, under Contract No. MRG5280189.


## References


[1] National Institute of Neurological Disorders and Stroke (NINDS). Seizure and Epilepsy: Hope through Research [online, cited 2010].

[2] Wolrd Health Organization (WHO). Epilepsy [online, cited 2010].

[3] A. L. Goldberger, Complex systems, Proc. Am. Thorac. Soc. 3 (2006) 467–472.

[4] B. B. Mandelbrot, The fractal geometry of nature, WH Freeman, San Francisco, 1982.

[5] G. W. Wornell, Signal processing with fractals: A wavelet-based approach, Prentice Hall, New Jersey, 1995.

[6] S. Havlin, S. V. Buldyrev, A. L. Goldberger, R. N. Mantegna, S. M. Ossadnik, C. k. Peng, M. Simons, H. Stanley, Fractals in biology and medicine, Chaos, Solitons & Fractals 6 (1995) 171–201.

[7] C. J. Stam, E. A. de Bruin, Scale-free dynamics of global functional connectivity in the human brain, Human Brain Mapping 22 (2004) 97–109.

[8] K. Linkenkaer-Hansen, V. V. Nikouline, J. M. Palva, R. J. Ilmoniemi, Long-range temporal correlations and scaling behavior in human brain oscillations, J. of Neurosci. 21 (2001) 1370–1377.

[9] J. B. Bassingthwaighte, L. S. Liebovitch, B. J. West, Fractal physiology, Oxford UP, New York, 1994.

[10] A. L. Barabási, H. E. Stanley, Fractal concepts in surface growth, Cambridge UP, Cambridge, UK, 1995.

[11] P. Bak, How nature works, Oxford UP, Oxford, 1997.

[12] P. Gong, A. R. Nikolaev, C. van Leeuwen, Scale-invariant fluctuations of the dynamical synchronization in human brain electrical activity, Neurosci. Lett. 336 (2003) 33–36.

[13] G. W. Wornell, Wavelet-based representations for the $1/f$ family of fractal processes, Proceedings of the IEEE 81 (1993) 1428–1450.

[14] G. W. Wornell, A. V. Oppenheim, Estimation of fractal signals from noisy measurements using wavelets, IEEE Trans. on Signal Processing 40 (1992) 611–623.

[15] B. B. Mandelbrot, H. W. V. Ness, Fractional brownian motions, fractional noises and applications, SIAM Rev. 10 (1968) 422–436.

[16] P. A. Watters, Fractal structure in the electroencephalogram, Complexity International 5.

[17] S. Mallat, A wavelet tour of signal processing, Academic Press, San Diego, 1998.

[18] I. Daubechies, Orthonormal bases of compactly supported wavelets, Commun. Pure Appl. Math. XLI (1988) 909–996.

[19] S. G. Mallat, A theory for multiresolution signal decomposition: the wavelet representation, IEEE Trans. Pattern Analysis and Machine Intelligence 11 (1989) 674–693.

[20] A. Cohen, J. Kovacevic, Wavelets: the mathematical background, Proceedings of the IEEE 84 (1996) 514–522.

[21] N. Foldvary-Schaefer, K. Unnwongse, Localizing and lateralizing features of auras and seizures, Epilepsy & Behavior-doi:10.1016/j.yebeh.2010.08.034.

Table 1: Statistical values of smoothed spectral exponents of ECoG channels corresponding to various brain states

| Phase | Channel | Mean | S.D. | Median |
|---|---|---|---|---|
| Pre-ictal | RPT1 | 3.3249 | 0.0684 | 3.3245 |
| Pre-ictal | RPT2 | 3.2034 | 0.0609 | 3.2235 |
| Pre-ictal | RPT3 | 3.1211 | 0.0540 | 3.1347 |
| Pre-ictal | RAT1 | 3.0245 | 0.0442 | 3.0344 |
| Pre-ictal | RAT2 | 3.1094 | 0.0637 | 3.1113 |
| Pre-ictal | RAT3 | 3.2465 | 0.0871 | 3.2254 |
| Pre-ictal | RMT1 | 3.0391 | 0.0638 | 3.0097 |
| Pre-ictal | RMT2 | 3.1416 | 0.0607 | 3.1114 |
| Pre-ictal | RMT3 | 3.2257 | 0.0639 | 3.2039 |
| Pre-ictal | RMT4 | 3.1129 | 0.1053 | 3.1217 |
| Pre-ictal | RMT5 | 3.1386 | 0.1113 | 3.1382 |
| Ictal | RPT1 | 3.2734 | 0.0707 | 3.3125 |
| Ictal | RPT2 | 3.1431 | 0.1049 | 3.1849 |
| Ictal | RPT3 | 3.0399 | 0.1009 | 3.0811 |
| Ictal | RAT1 | 3.0938 | 0.0595 | 3.1134 |
| Ictal | RAT2 | 3.0569 | 0.0727 | 3.0815 |
| Ictal | RAT3 | 3.1509 | 0.0774 | 3.1423 |
| Ictal | RMT1 | 3.0962 | 0.0559 | 3.0911 |
| Ictal | RMT2 | 3.1960 | 0.0608 | 3.1809 |
| Ictal | RMT3 | 3.4323 | 0.0908 | 3.4478 |
| Ictal | RMT4 | 3.4595 | 0.0662 | 3.4763 |
| Ictal | RMT5 | 3.4674 | 0.0725 | 3.4793 |
| Post-ictal | RPT1 | 3.2561 | 0.0642 | 3.2544 |
| Post-ictal | RPT2 | 3.1676 | 0.0728 | 3.1835 |
| Post-ictal | RPT3 | 3.0689 | 0.0540 | 3.0829 |
| Post-ictal | RAT1 | 2.9665 | 0.0820 | 2.9383 |
| Post-ictal | RAT2 | 2.9706 | 0.0594 | 2.9874 |
| Post-ictal | RAT3 | 3.0684 | 0.0706 | 3.0617 |
| Post-ictal | RMT1 | 3.1849 | 0.0729 | 3.1980 |
| Post-ictal | RMT2 | 3.2780 | 0.0782 | 3.2976 |
| Post-ictal | RMT3 | 3.3802 | 0.0778 | 3.3853 |
| Post-ictal | RMT4 | 3.2868 | 0.1591 | 3.2292 |
| Post-ictal | RMT5 | 3.1902 | 0.1944 | 3.1226 |

Table 2: Statistical values of smoothed spectral exponents of different regions of the brain corresponding to various brain states

| Phase | Region | Mean | S.D. | Median |
|---|---|---|---|---|
| Pre-ictal | RPT | 3.2164 | 0.1038 | 3.2082 |
| Pre-ictal | RAT | 3.1268 | 0.1135 | 3.1128 |
| Pre-ictal | RMT | 3.1316 | 0.1031 | 3.1327 |
| Ictal | RPT | 3.1521 | 0.1336 | 3.1688 |
| Ictal | RAT | 3.1005 | 0.0801 | 3.0989 |
| Ictal | RMT | 3.3303 | 0.1694 | 3.3526 |
| Post-ictal | RPT | 3.1642 | 0.0998 | 3.1655 |
| Post-ictal | RAT | 3.0018 | 0.0853 | 3.0068 |
| Post-ictal | RMT | 3.2640 | 0.1459 | 3.2626 |

Table 3: Statistical values of spectral exponents of different regions of the brain corresponding to various brain states

| Phase | Region | Mean | S.D. | Median |
|---|---|---|---|---|
| Pre-ictal | RPT | 3.2197 | 0.131 | 3.2152 |
| Pre-ictal | RAT | 3.1277 | 0.1411 | 3.1033 |
| Pre-ictal | RMT | 3.1191 | 0.1494 | 3.1148 |
| Ictal | RPT | 3.1343 | 0.3585 | 3.1841 |
| Ictal | RAT | 3.1311 | 0.2464 | 3.1465 |
| Ictal | RMT | 3.4242 | 0.365 | 3.3143 |
| Post-ictal | RPT | 3.1673 | 0.1318 | 3.1588 |
| Post-ictal | RAT | 2.9927 | 0.1247 | 2.9837 |
| Post-ictal | RMT | 3.2314 | 0.2042 | 3.2245 |

Table 4: Results of the two-factor analysis of variance of the spectral exponents

| Factor | Mean square | $F$ | $p$ |
|---|---|---|---|
| Phase | 13.1201 | 273.2794 | 0.000 |
| Region | 25.5121 | 531.3938 | 0.000 |
| Phase & Region | 14.6949 | 306.0813 | 0.000 |

Table 5: Results of the two-factor analysis of variance of the smoothed spectral exponents

| Factor | Mean square | $F$ | $p$ |
|---|---|---|---|
| Phase | 13.8645 | 288.8364 | 0.000 |
| Region | 25.0303 | 521.4504 | 0.000 |
| Phase & Region | 14.3601 | 299.1608 | 0.000 |

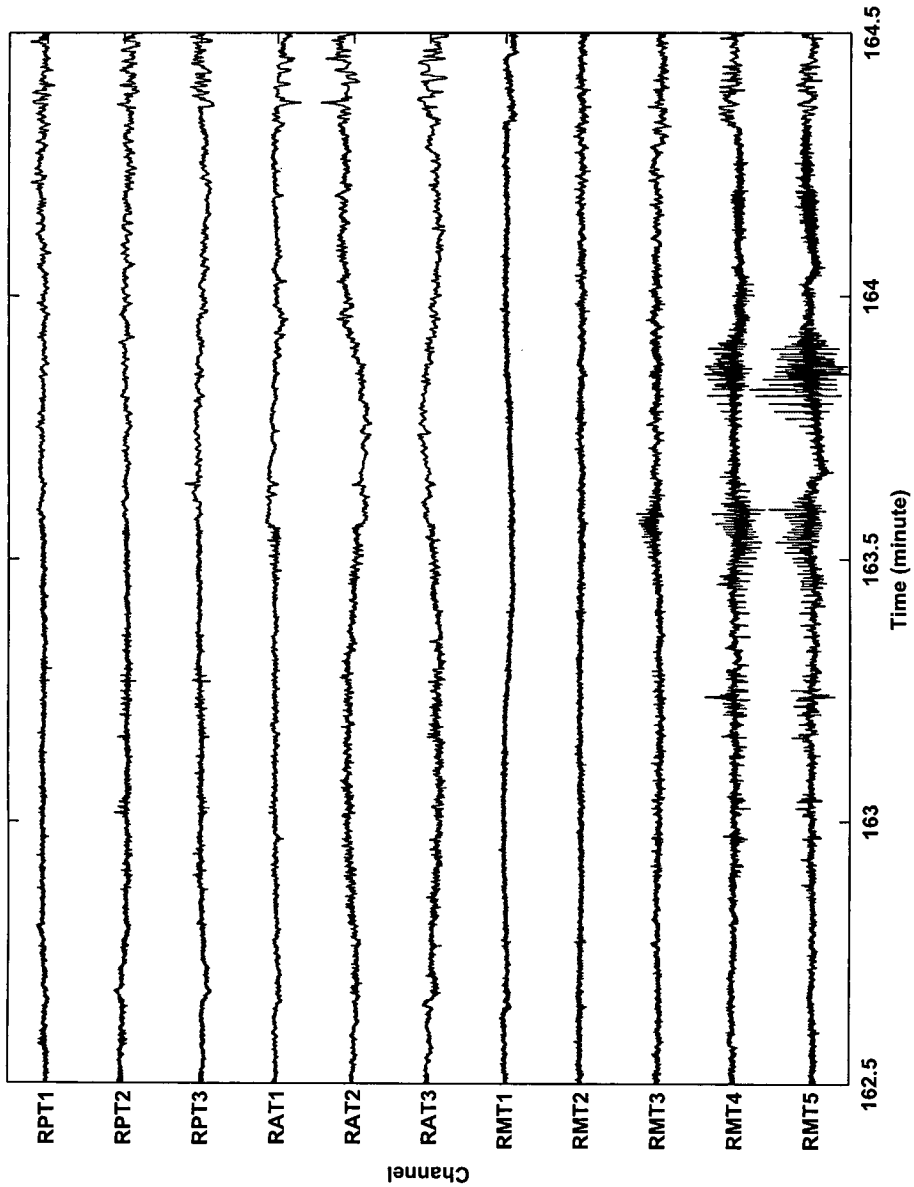


Figure 1: A segment of the ECoG signal around the first epileptic seizure event.

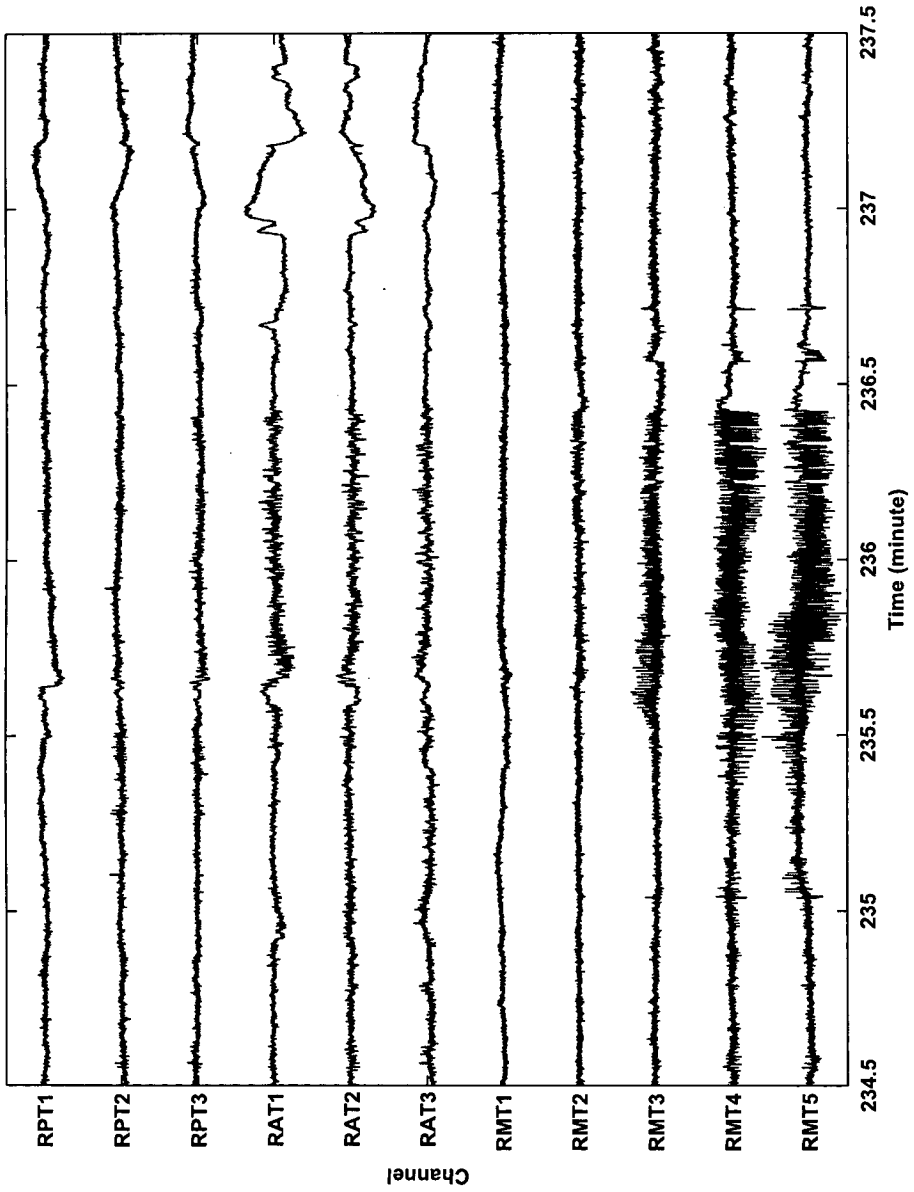


Figure 2: A segment of the ECoG signal around the second epileptic seizure event.

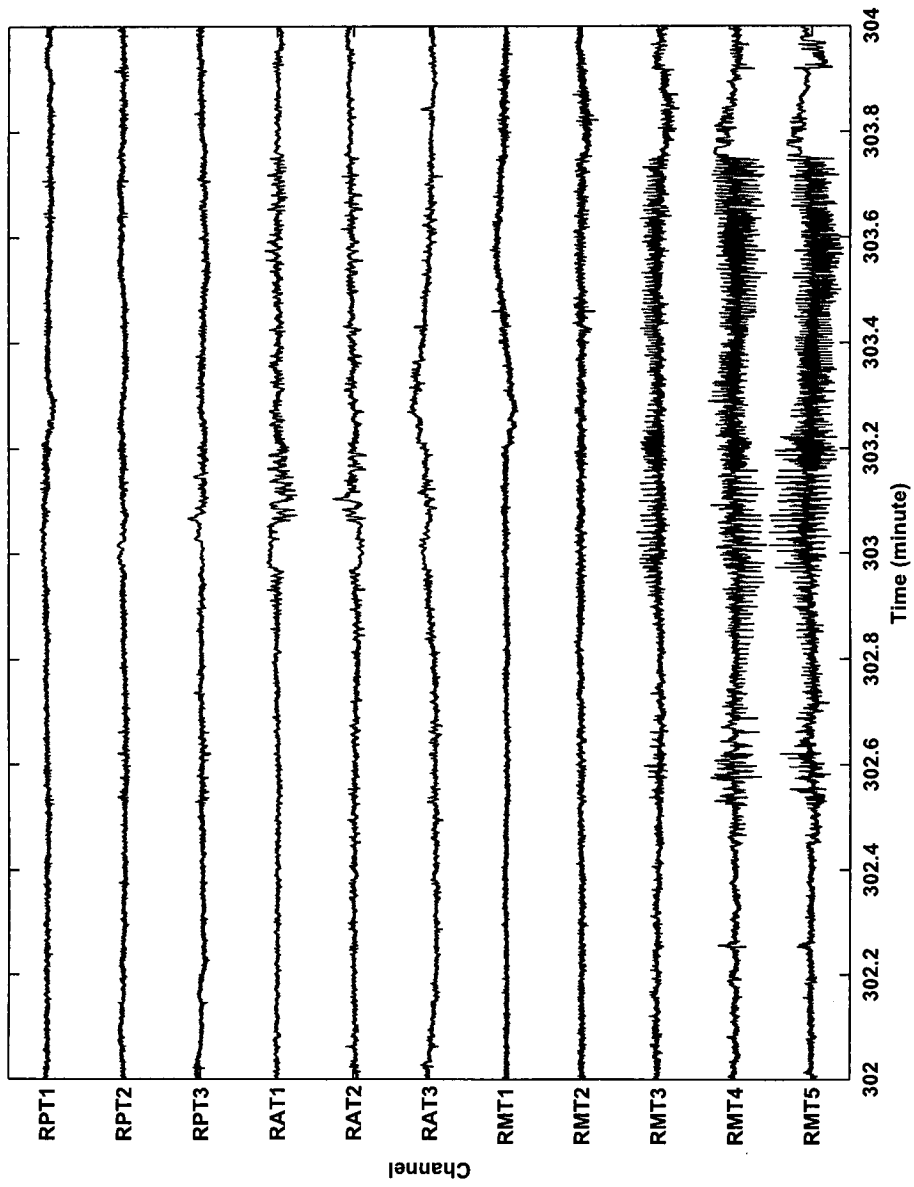


Figure 3: A segment of the ECoG signal around the third epileptic seizure event.

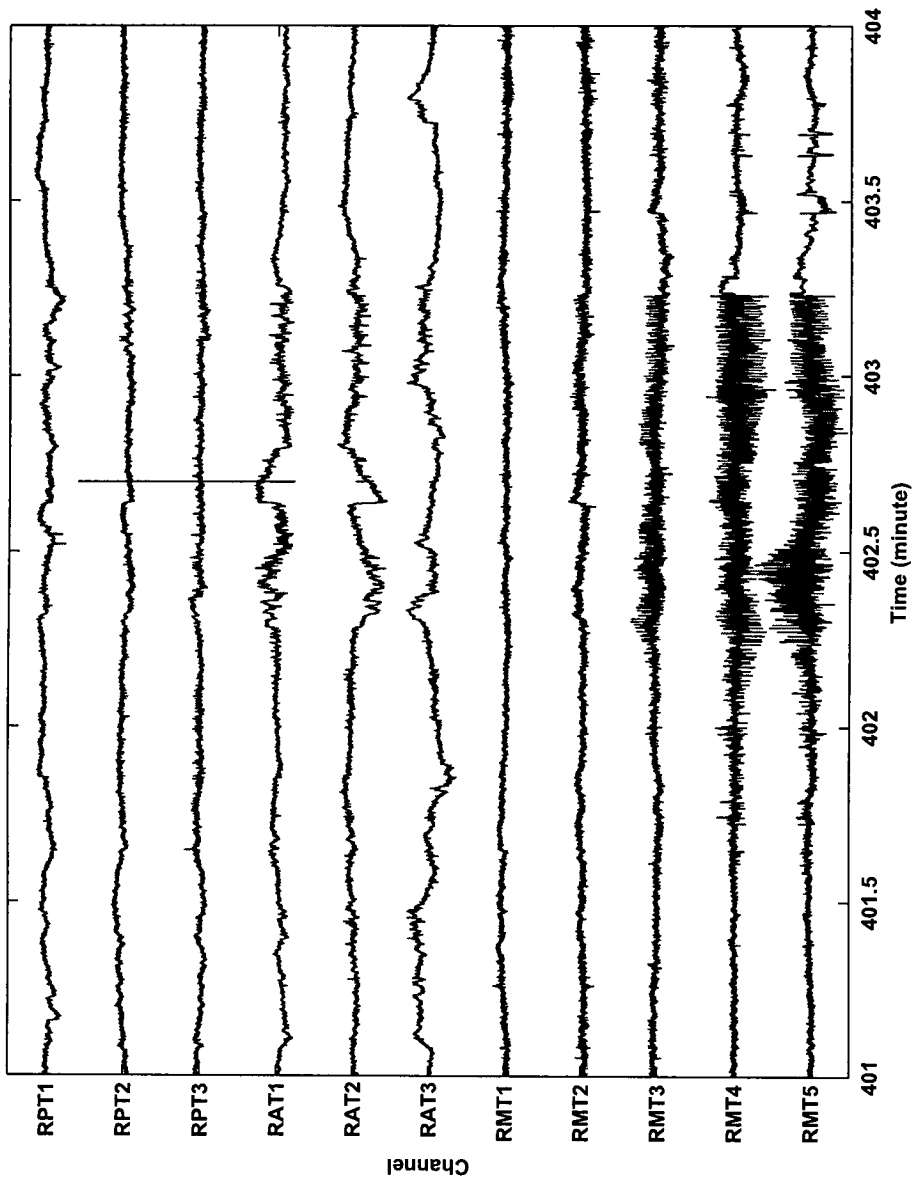


Figure 4: A segment of the ECoG signal around the last epileptic seizure event.

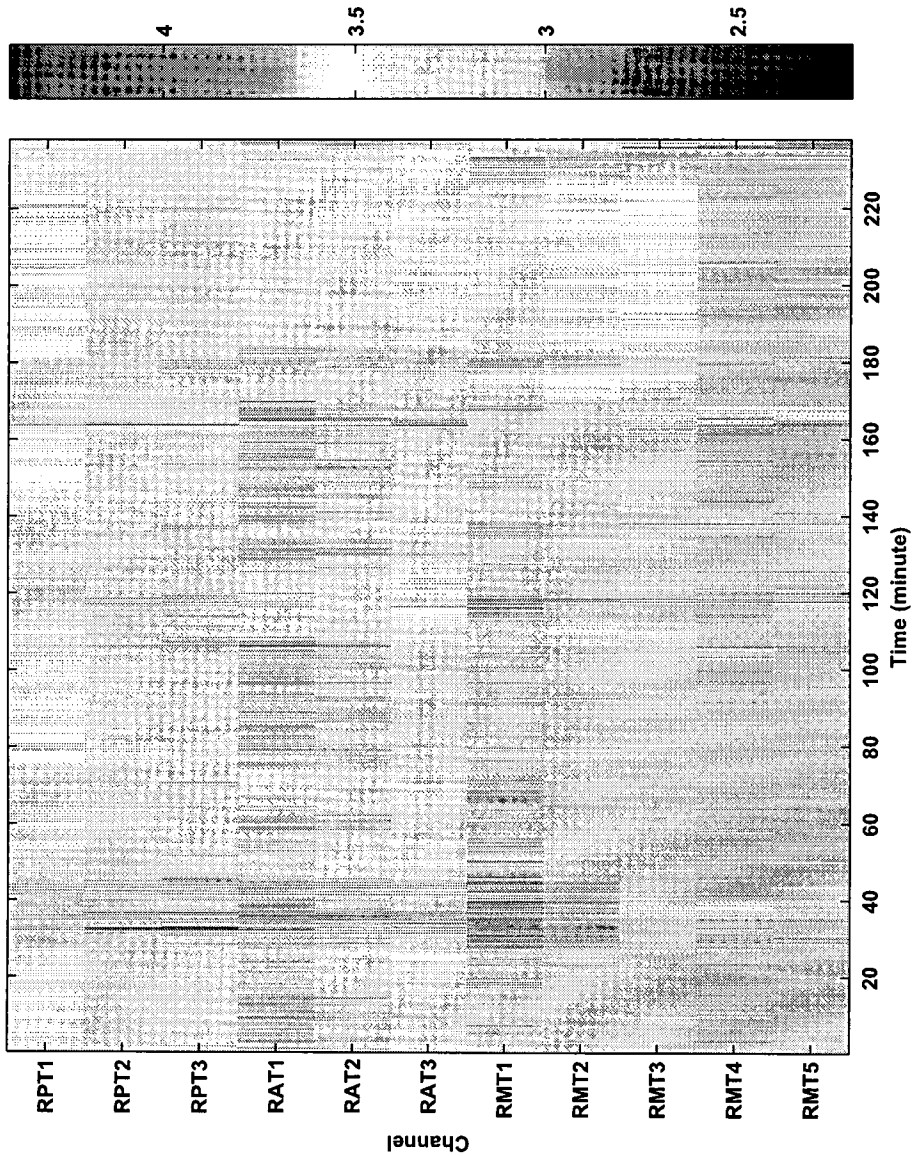


Figure 5: The spectral exponent of the first 4-hour section of the ECoG.

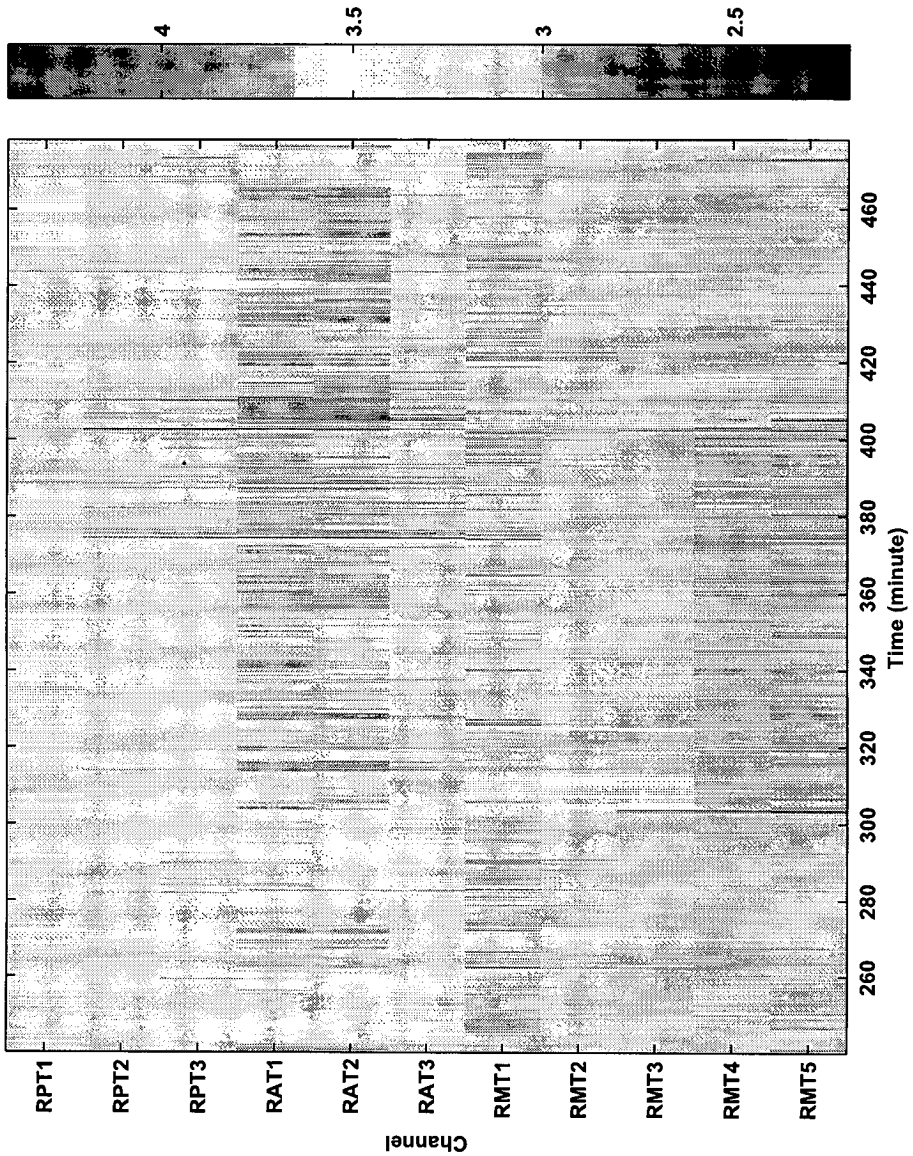


Figure 6: The spectral exponent of the second 4-hour section of the ECoG.

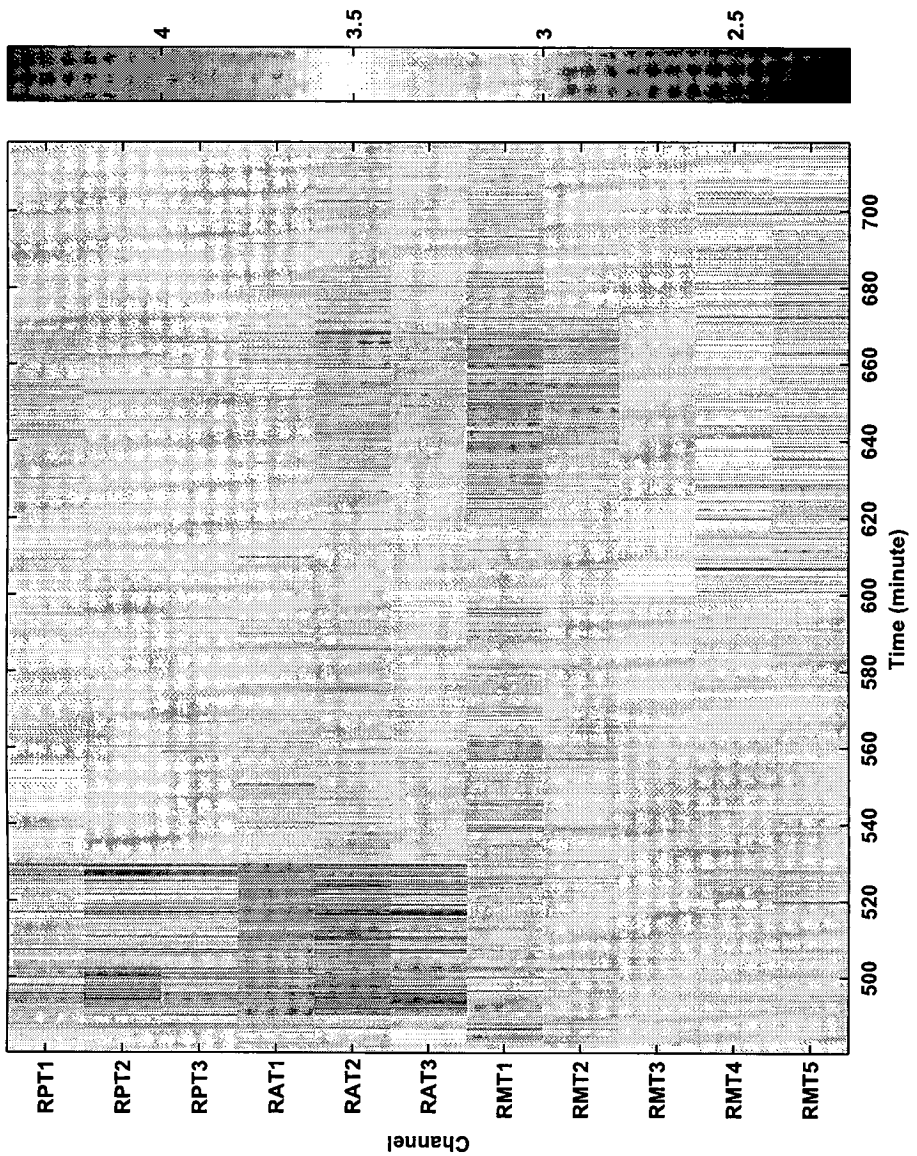


Figure 7: The spectral exponent of the last 4-hour section of the ECoG.

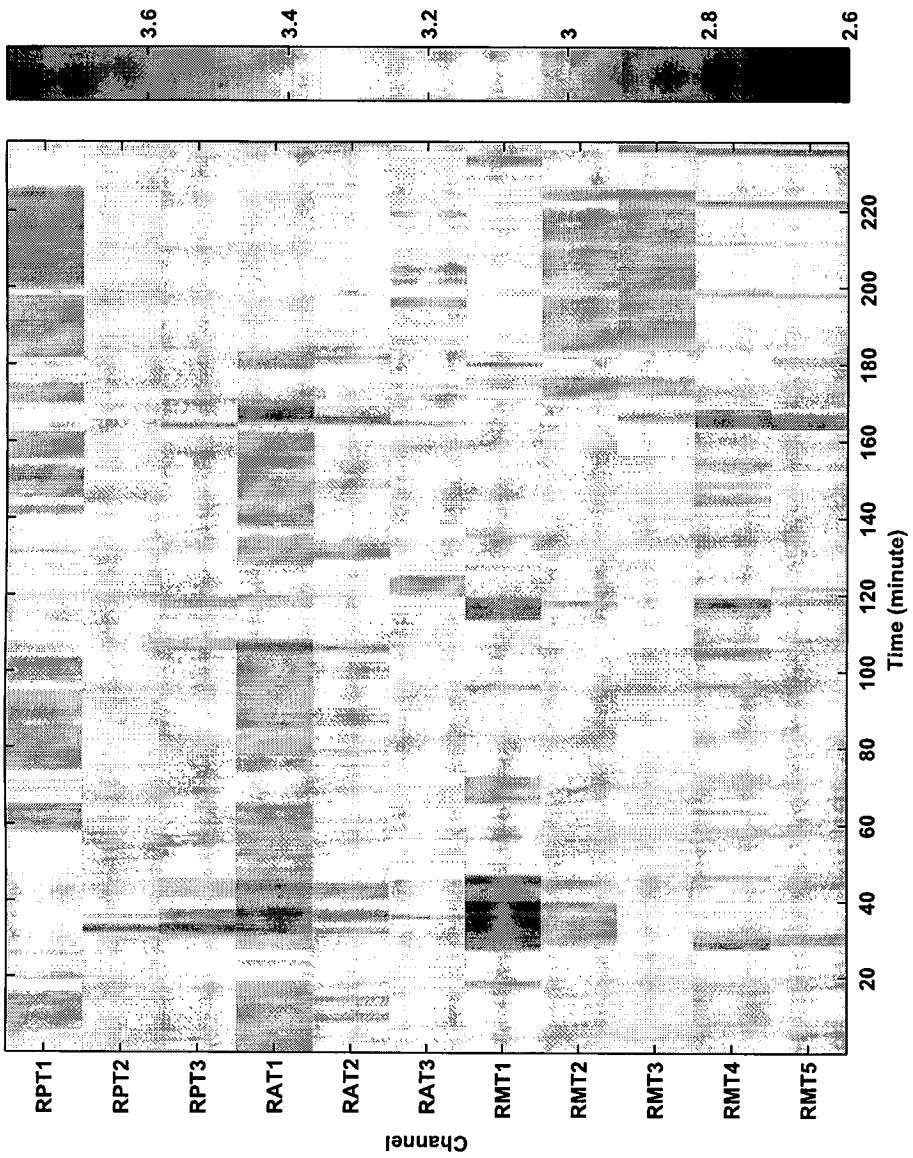


Figure 8: The smoothed spectral exponent of the first 4-hour section of the ECoG.

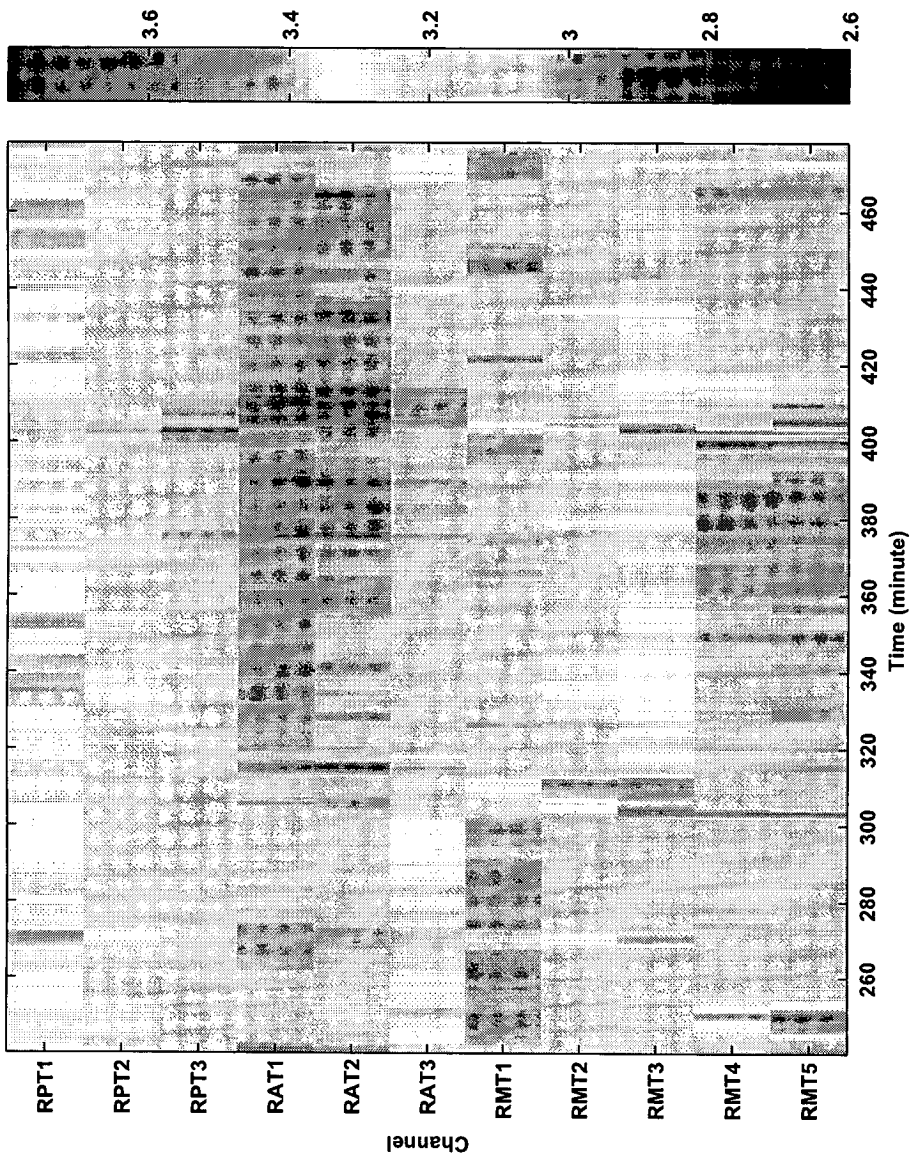


Figure 9: The smoothed spectral exponent of the second 4-hour section of the ECoG.

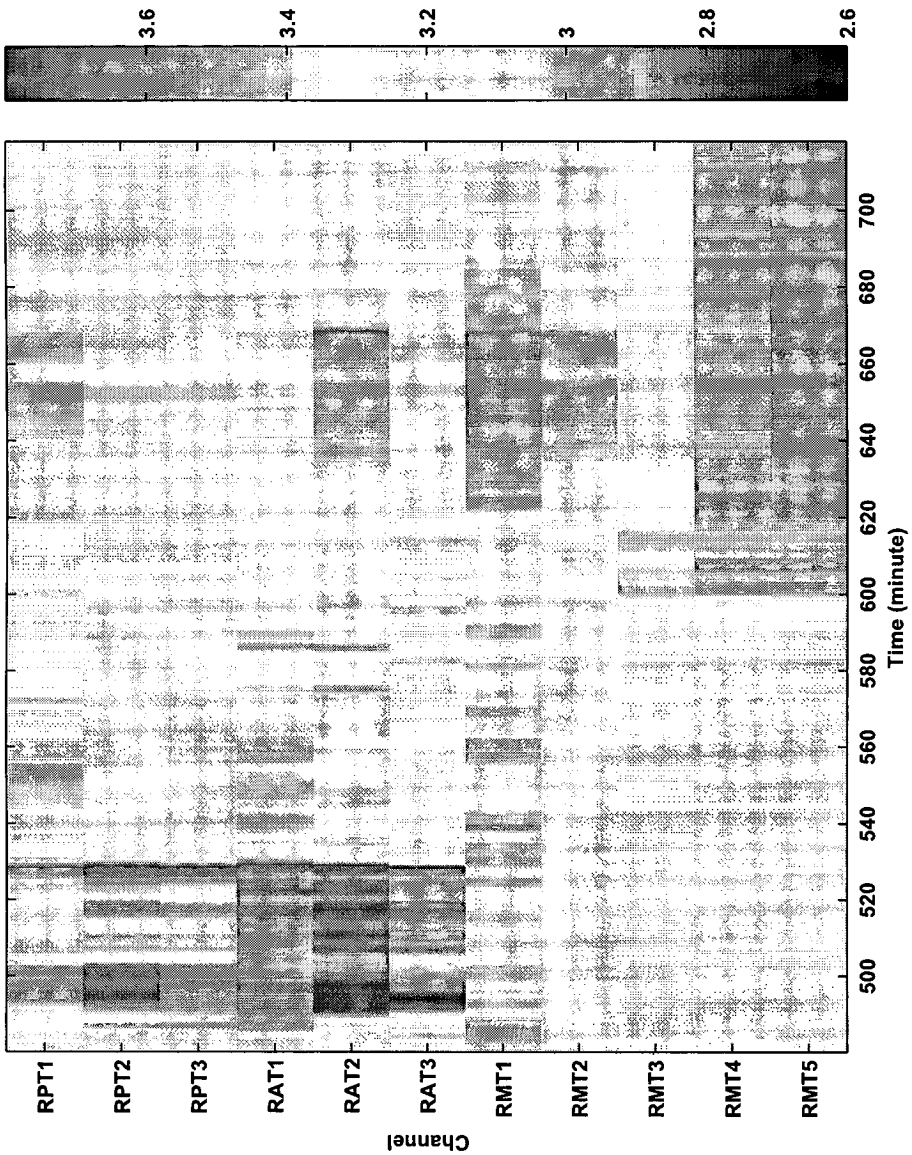


Figure 10: The smoothed spectral exponent of the last 4-hour section of the ECoG.

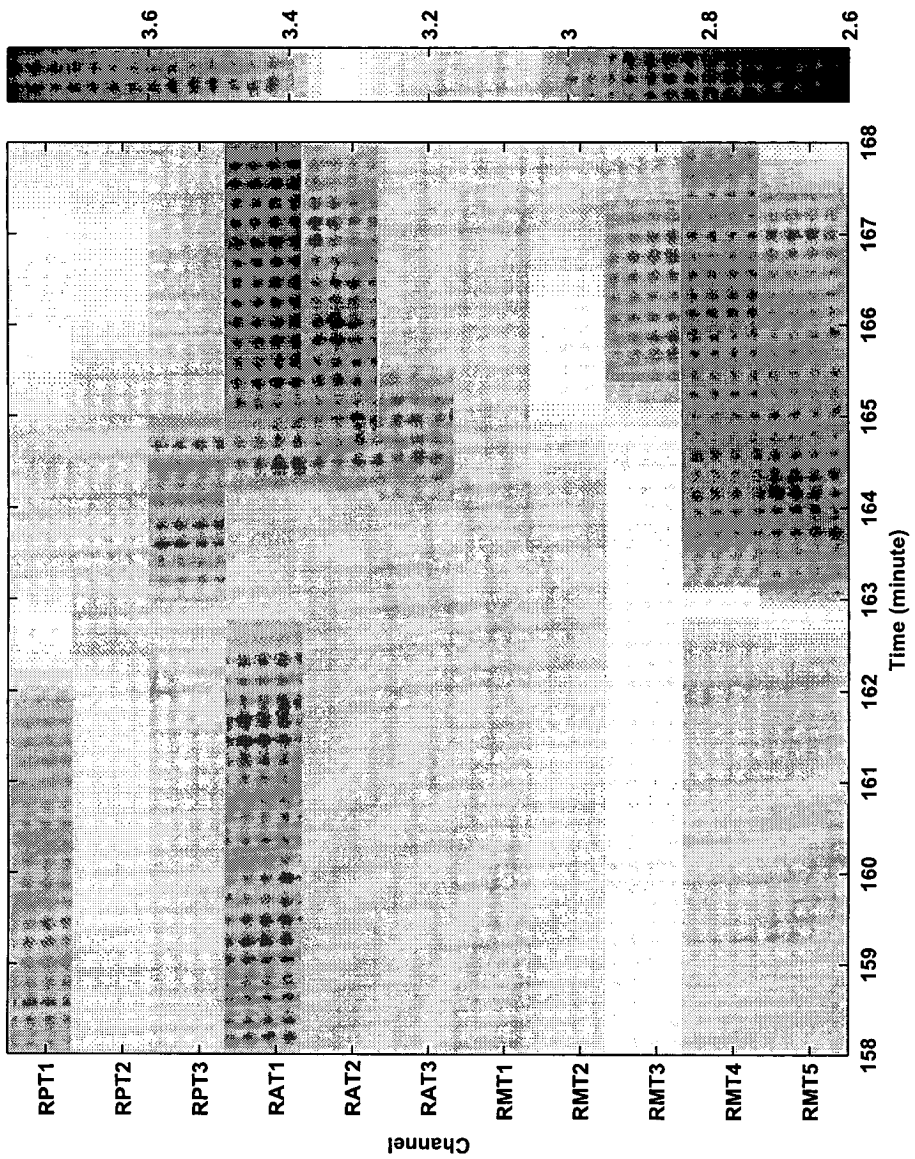


Figure 11: The smoothed spectral exponent of the ECoG around the first epileptic seizure event.

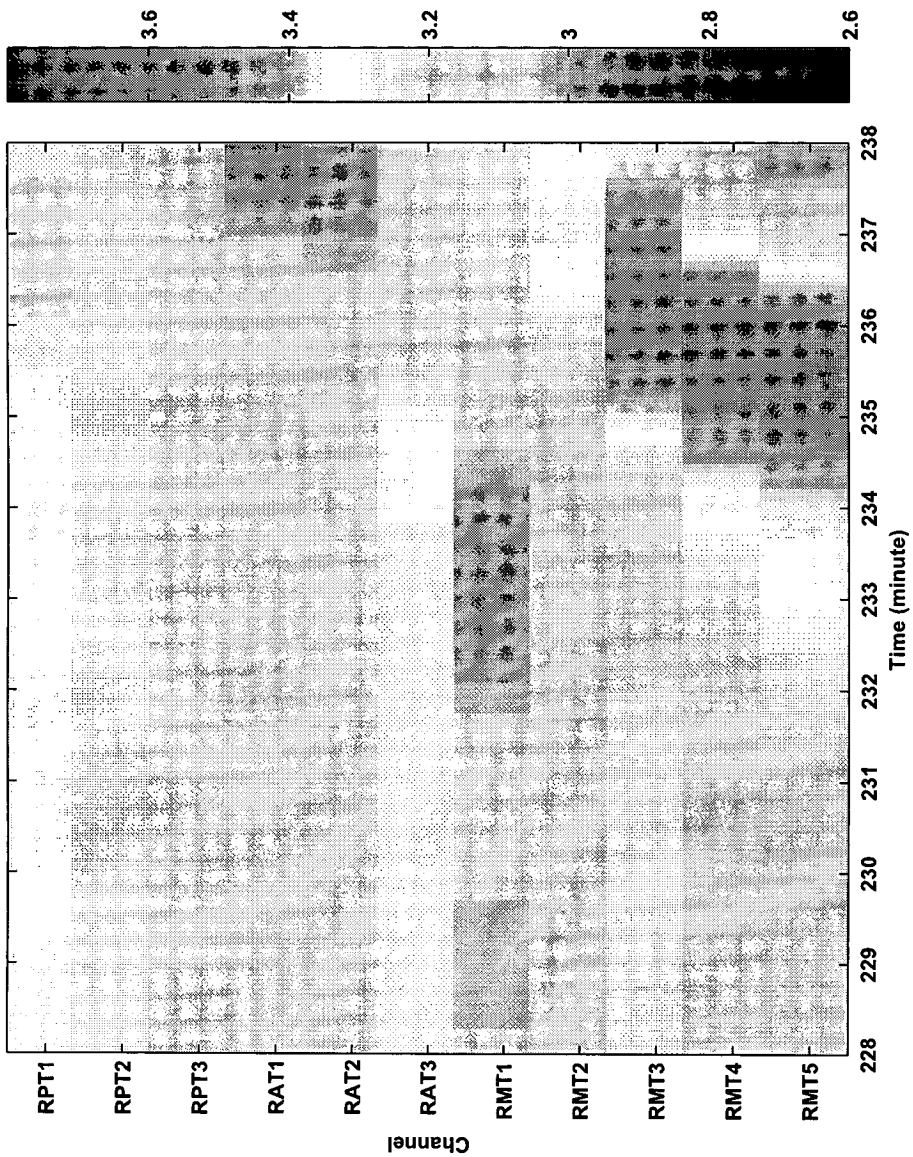


Figure 12: The smoothed spectral exponent of the ECoG around the second epileptic seizure event.

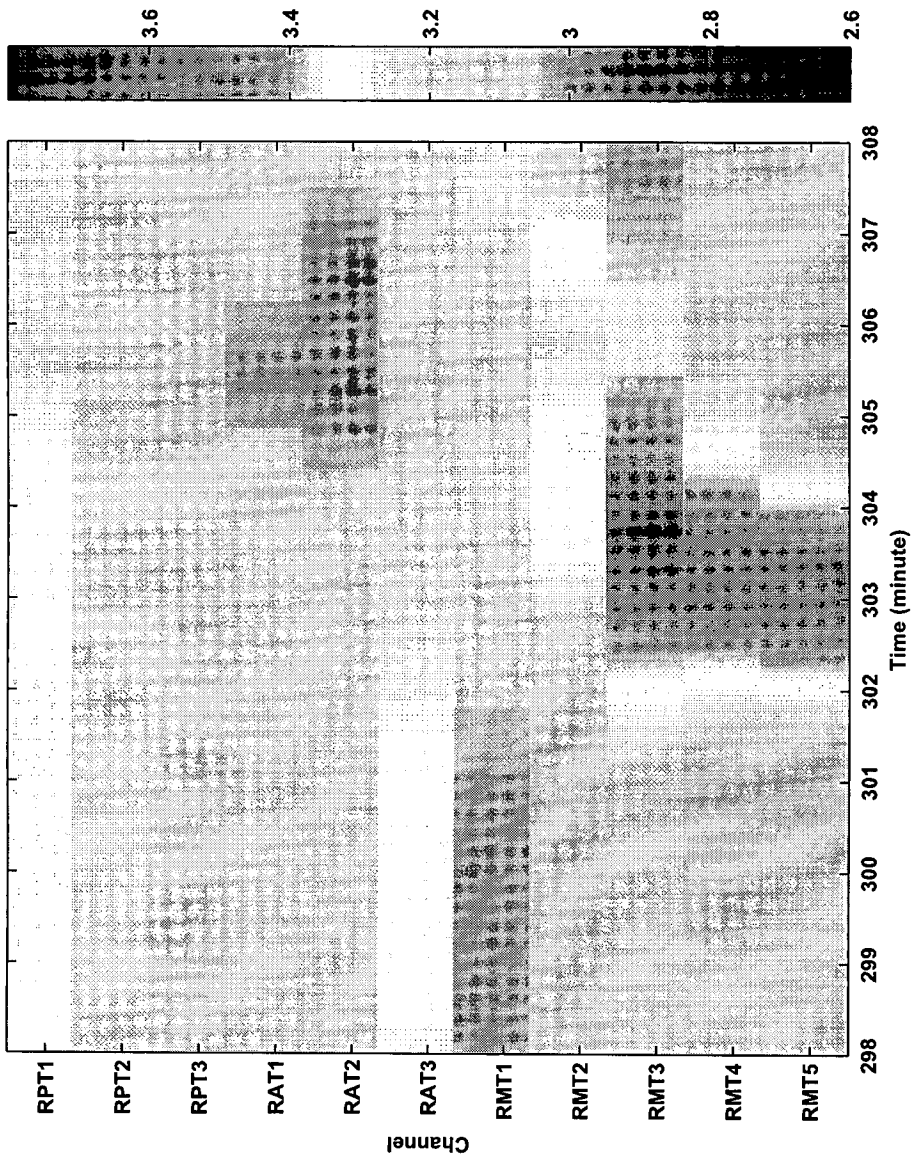


Figure 13: The smoothed spectral exponent of the ECoG around the third epileptic seizure event.

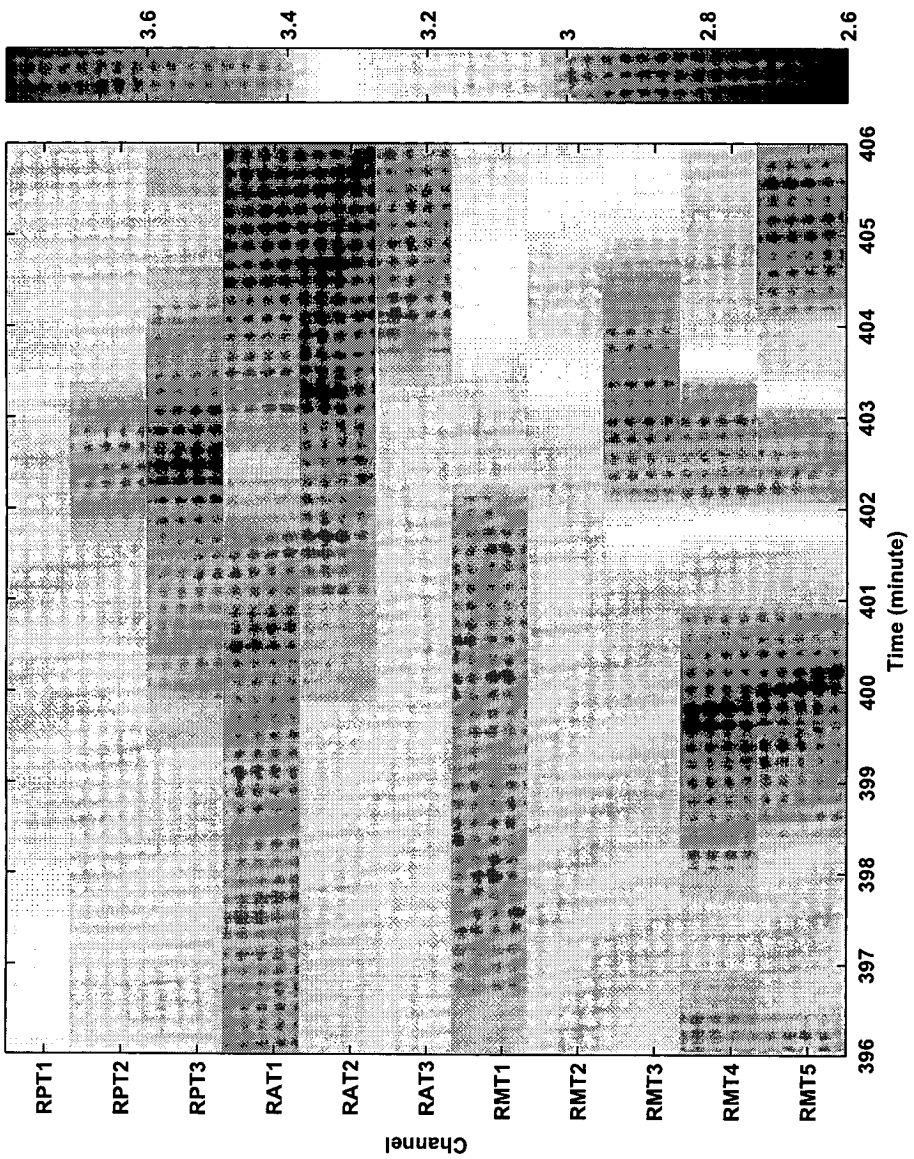


Figure 14: The smoothed spectral exponent of the ECoG around the last epileptic seizure event.

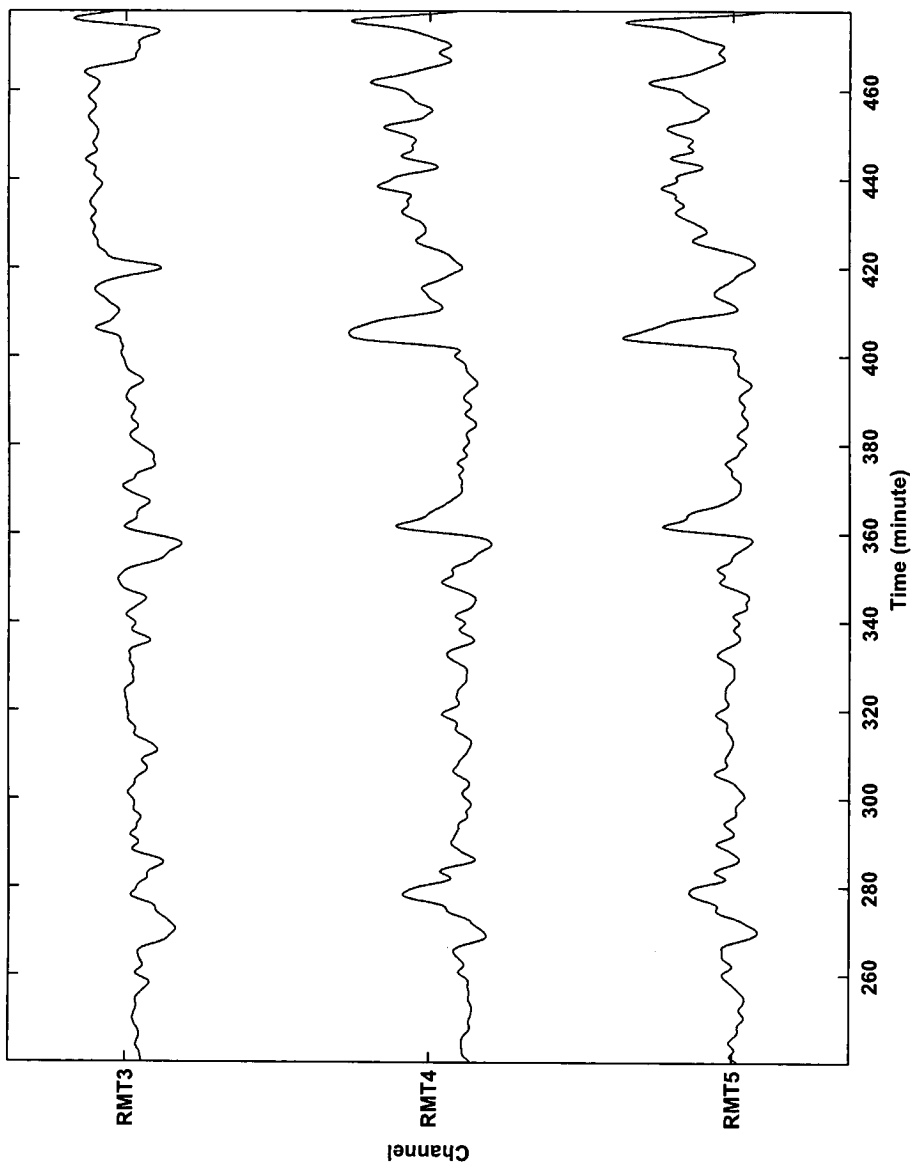


Figure 15: The smoothed spectral exponent of the first 4-hour section of the RMT3, RMT4 and RMT5 channels.

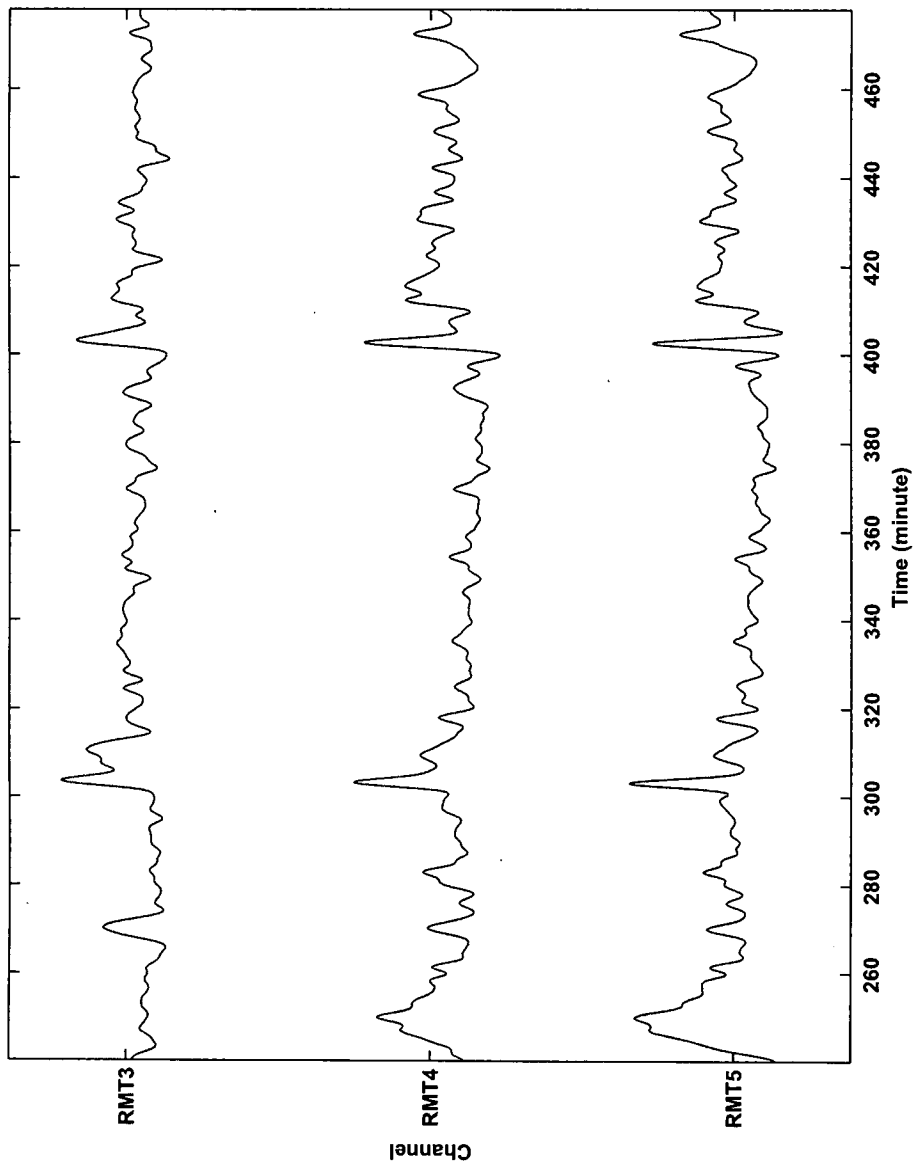


Figure 16: The smoothed spectral exponent of the second 4-hour section of the RMT3, RMT4 and RMT5 channels.

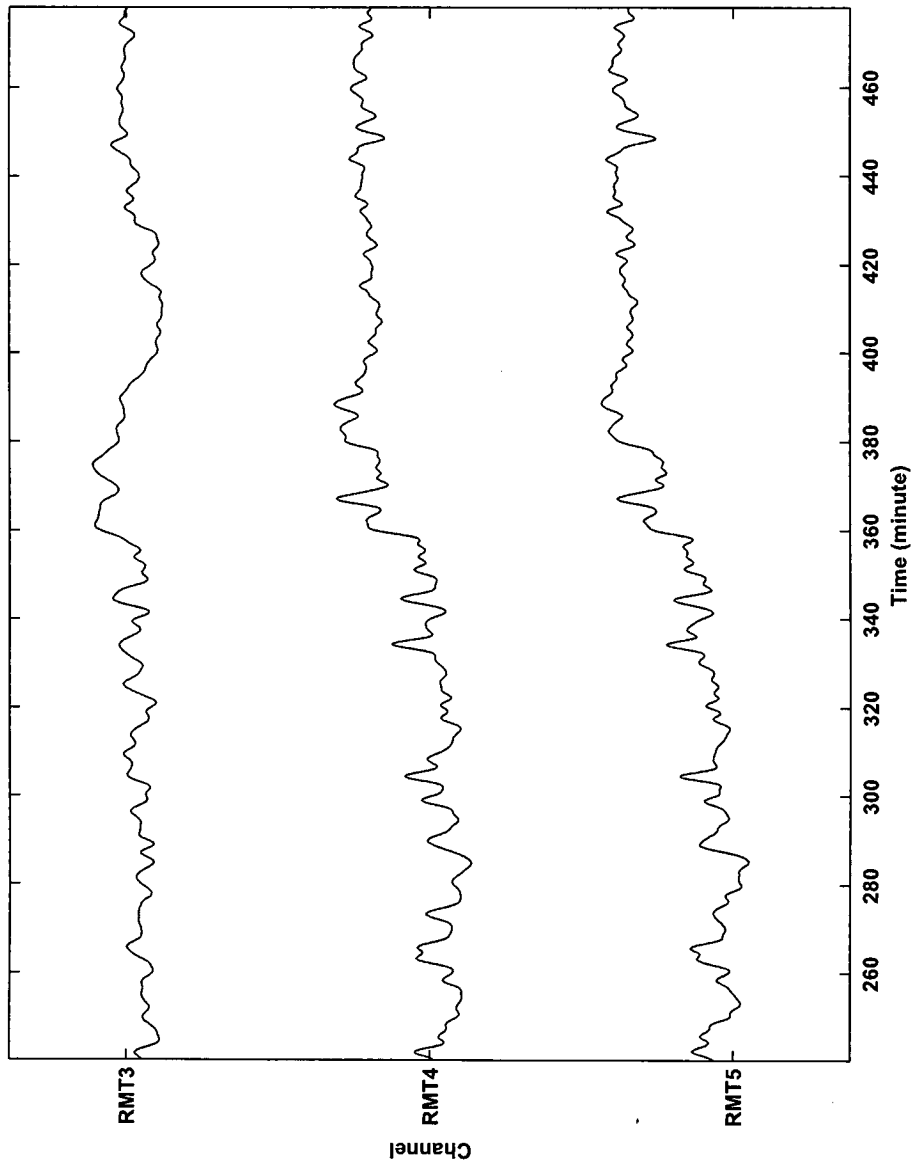


Figure 17: The smoothed spectral exponent of the last 4-hour section of the RMT3, RMT4 and RMT5 channels.

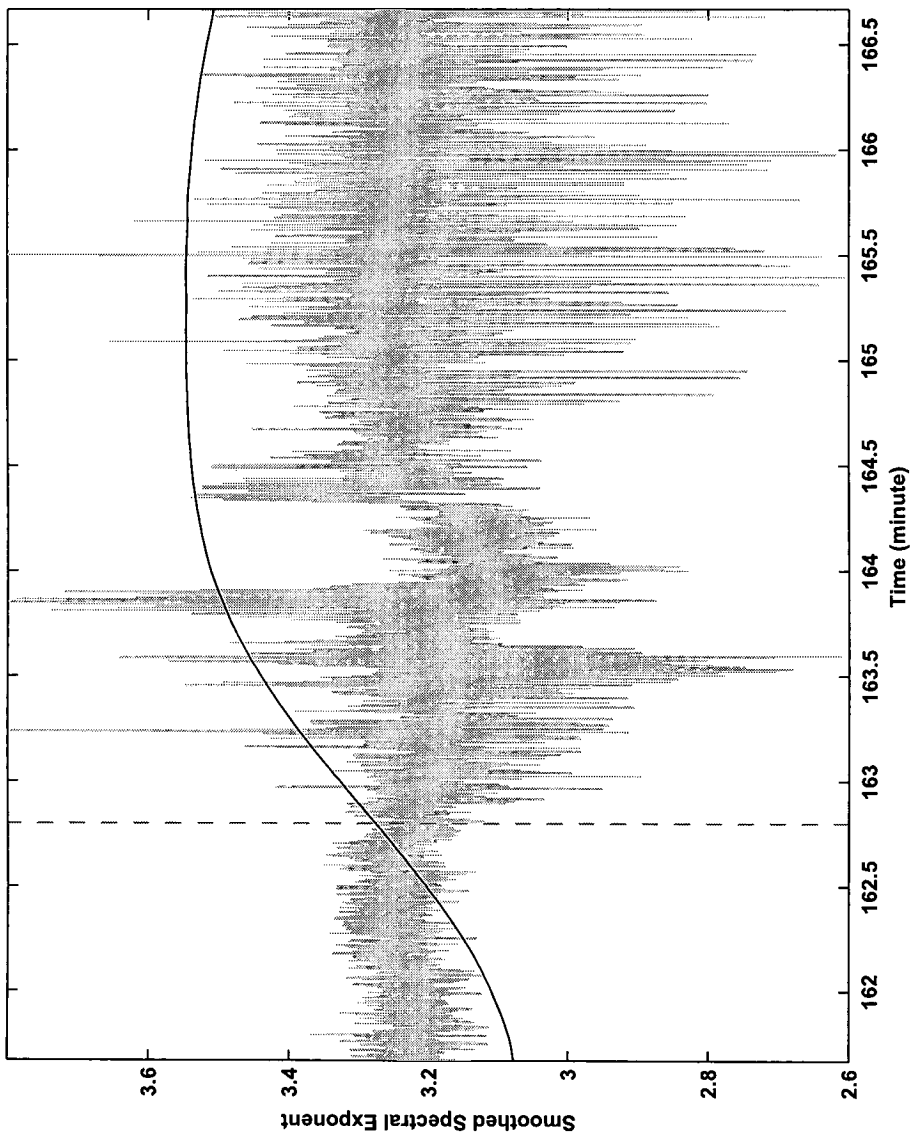


Figure 18: The corresponding smoothed spectral exponent compared to the RMT4 channel around the first epileptic seizure event.

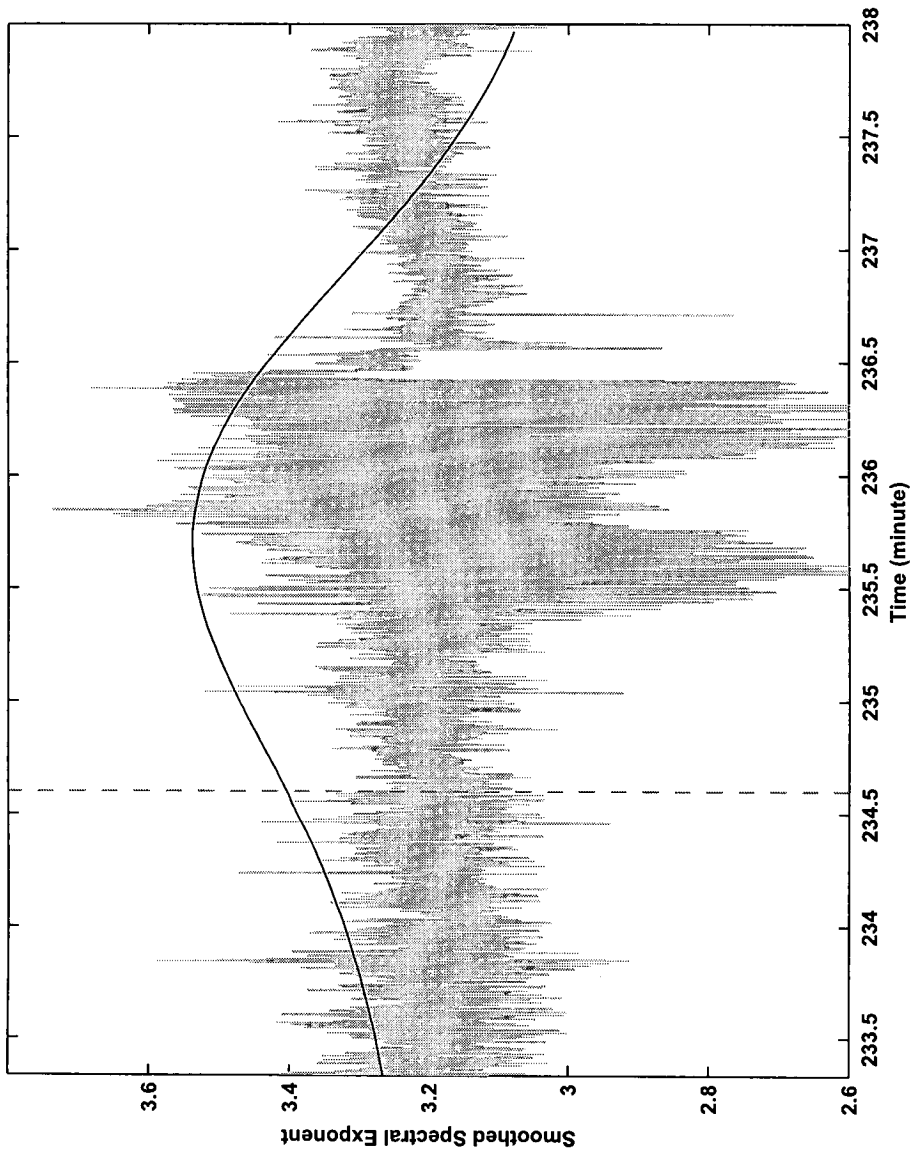


Figure 19: The corresponding smoothed spectral exponent compared to the RMT4 channel around the second epileptic seizure event.

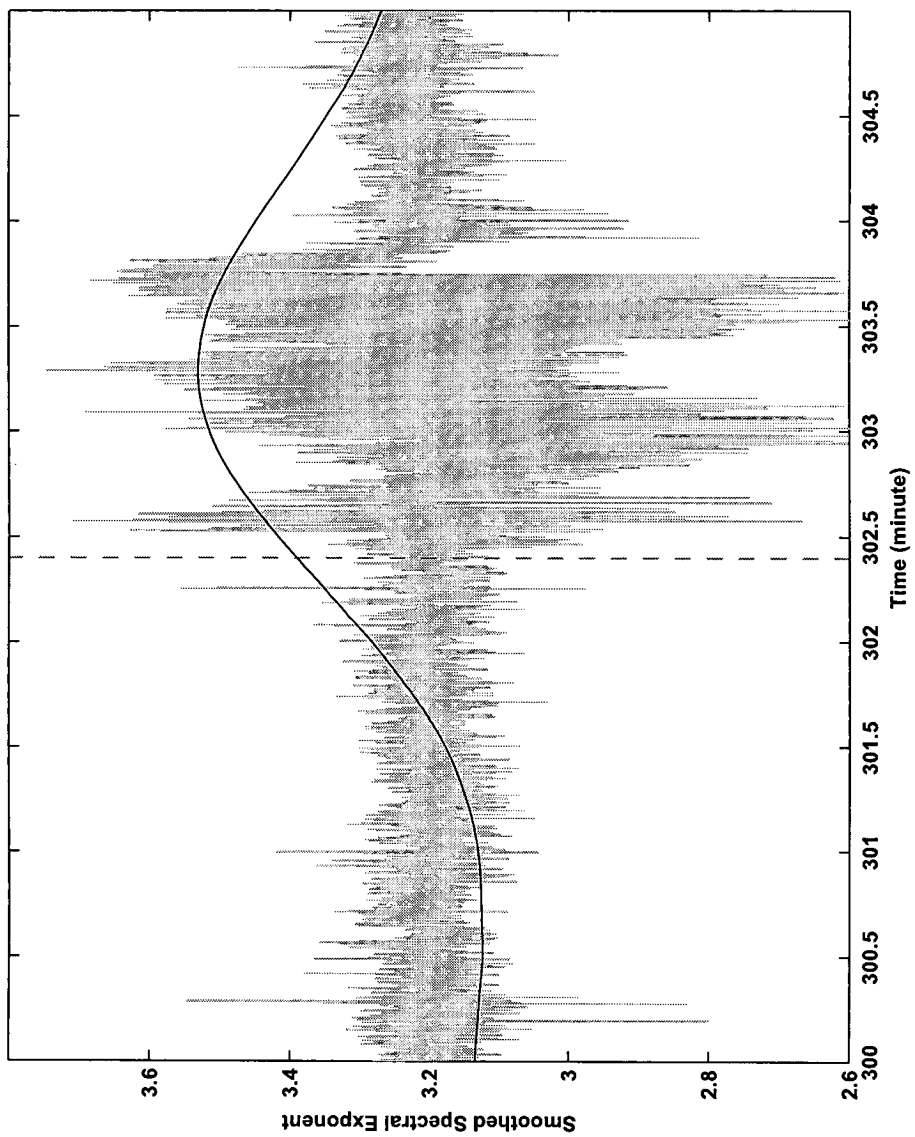


Figure 20: The corresponding smoothed spectral exponent compared to the RMT4 channel around the third epileptic seizure event.

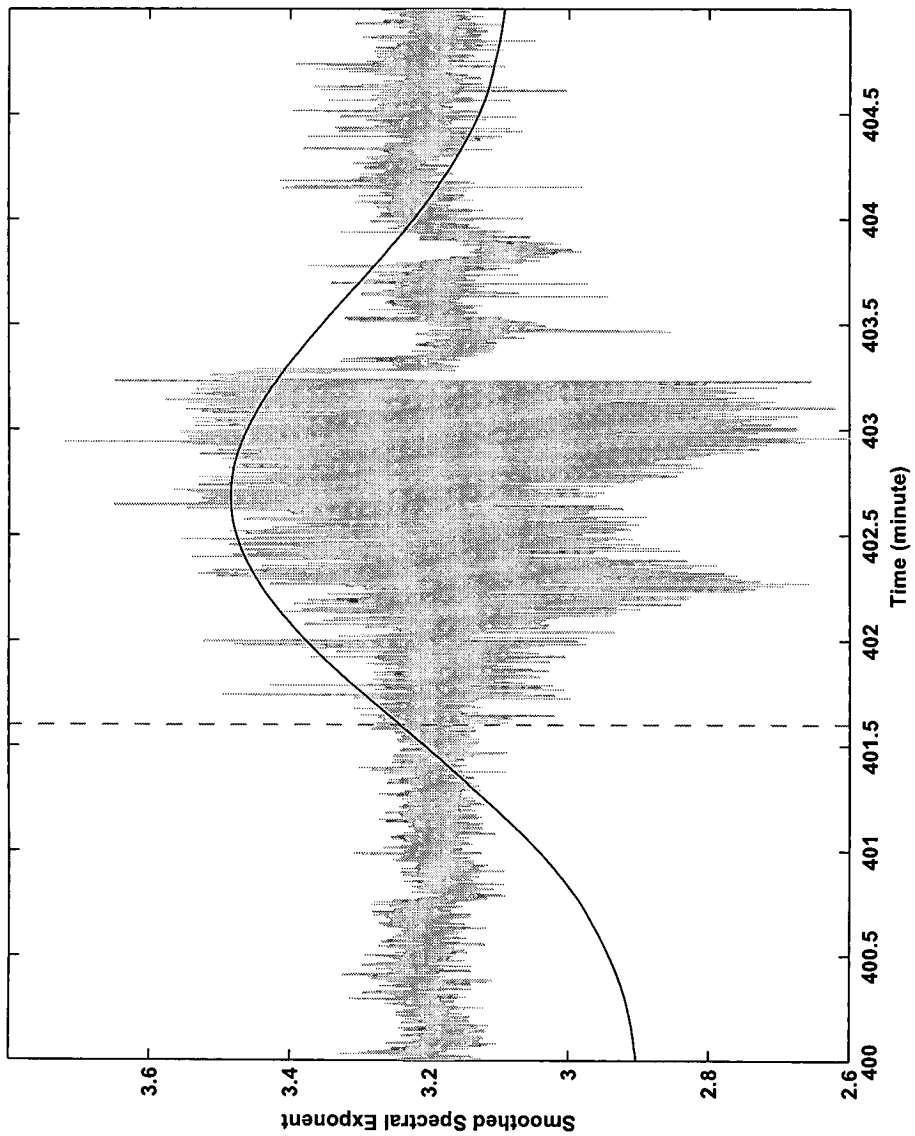


Figure 21: The corresponding smoothed spectral exponent compared to the RMT4 channel around the last epileptic seizure event.

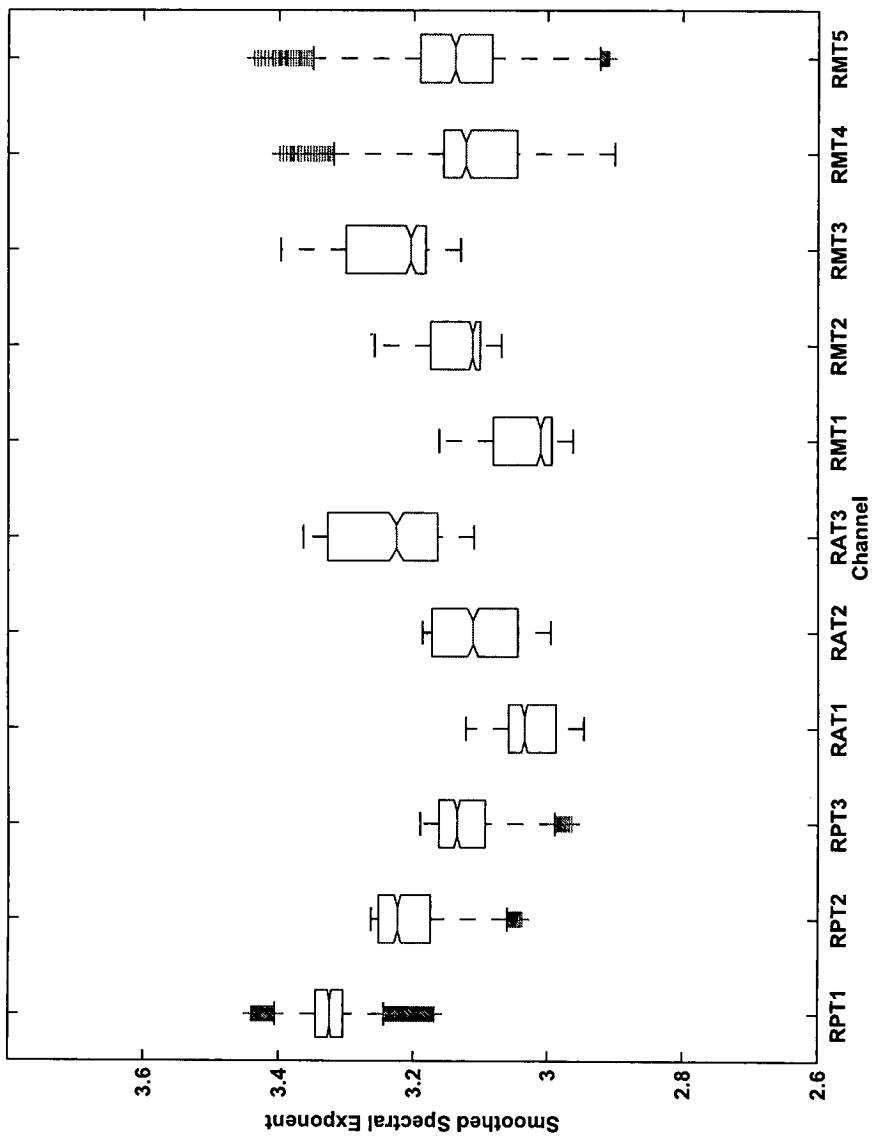


Figure 22: Comparison of the smoothed spectral exponents of individual channels during the pre-ictal phase.

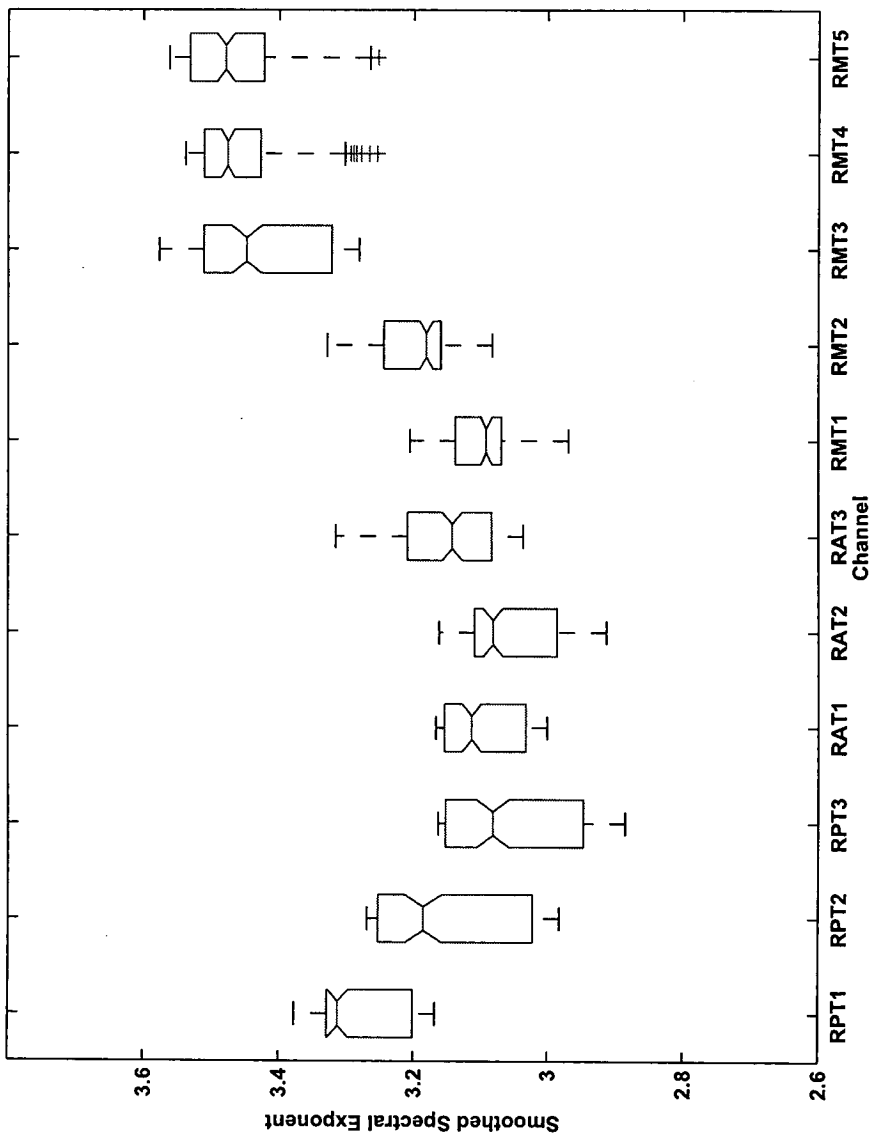


Figure 23: Comparison of the smoothed spectral exponents of individual channels during the ictal phase.

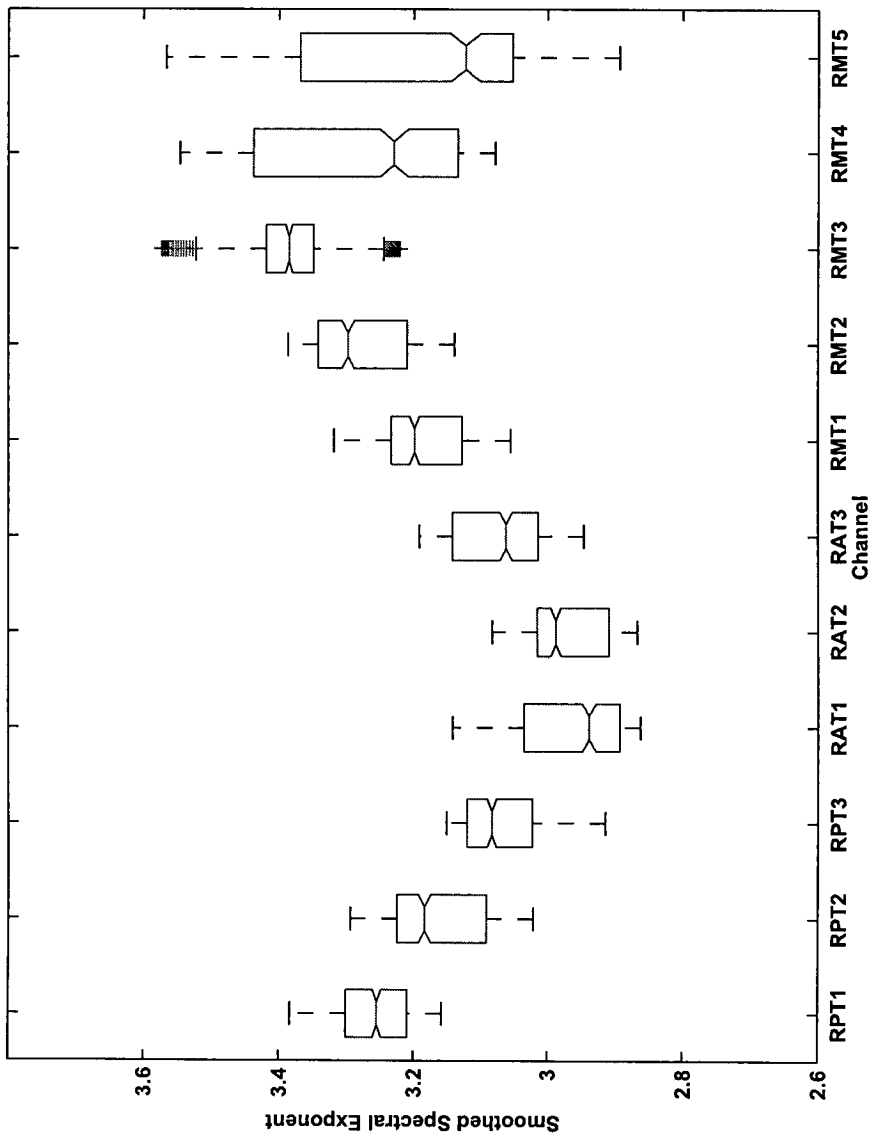


Figure 24: Comparison of the smoothed spectral exponents of individual channels during the post-ictal phase.

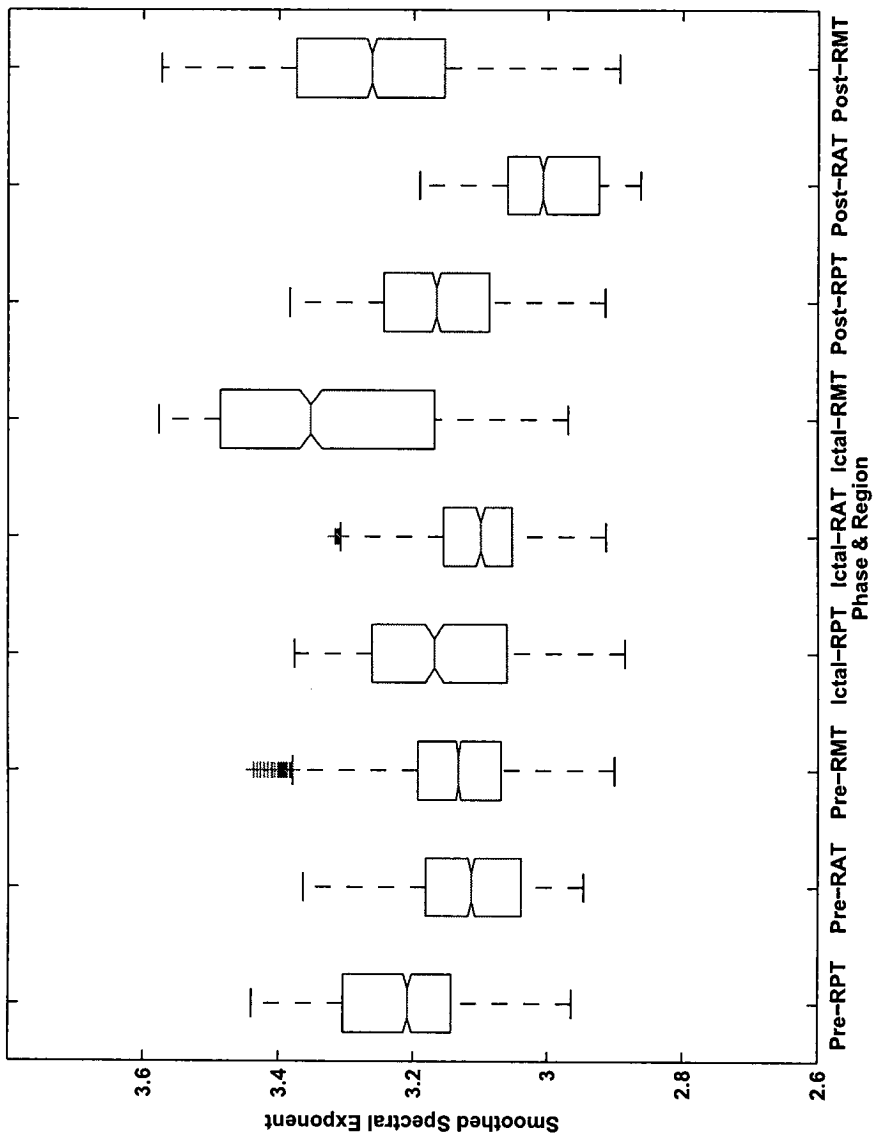


gure 25: Comparison of the smoothed spectral exponents of each regions of the brain associated with different pathological states of the ain.

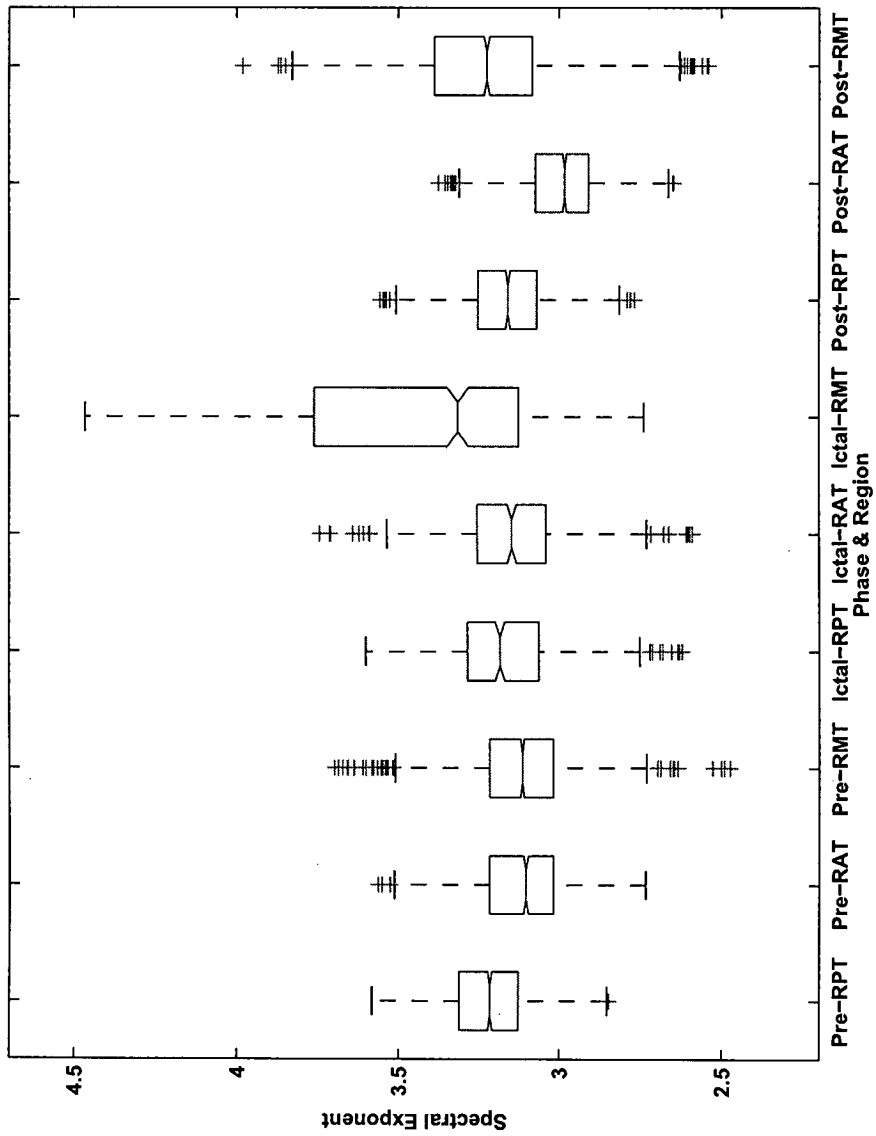


Figure 26: Comparison of the spectral exponents of each regions of the brain associated with different pathological states of the brain.

# Comparison of Complexity Measures Using Two Complex System Analysis Methods Applied to the Epileptic ECoG

S. Janjarasjitt[a,b,*], K. A. Loparo[b]

[a]*Department of Electrical and Electronic Engineering, Ubon Ratchathani University, Warinchamrab, Ubon Ratchathani 34190 Thailand*
[b]*Department of Electrical Engineering and Computer Science, Case Western Reserve University, Cleveland, Ohio 44106 USA*

## Abstract

Complex system analysis has been widely applied to examine the characteristics of EEG in health and disease, as well as the dynamics of the brain. In this study, two complexity measures, correlation dimension and spectral exponent, are applied to ECoG data of subjects with epilepsy obtained during different states (seizure and non-seizure) and from different brain regions are examined. From the computational results, it is observed that the spectral exponent obtained from wavelet-based fractal analysis provides complementary information to the correlation dimension, derived from nonlinear dynamical systems analysis. ECoG data obtained during seizure activity have smoother temporal patterns and are less complex than that during non-seizure activity. In addition, there are significant differences between these two ECoG complexity measures when applied to ECoG data of subjects with epilepsy obtained from different brain regions.

*Keywords:* epilepsy, seizure, complexity, nonlinear dynamics, correlation dimension, fractals, wavelet analysis

## 1. Introduction

Epilepsy is a common neurological disorder in which clusters of nerve cells or neurons in the brain sometimes signal abnormally [1]. Epilepsy is characterized by recurrent seizures that are physical reactions to sudden, usually brief, excessive electrical discharges in clusters of nerve cells, and around 50 milllion people worldwide are affected by epilepsy [2]. The normal pattern of neuronal activity that is disturbed in epilepsy, can cause strange sensations, emotions, and behaviors, or sometimes convulsions (i.e. violent and involuntary contractions of the muscles), muscle spasms, and loss of consciousness [1]. There are many possible causes for seizures ranging from illness to brain damage to abnormal brain development [1].

Seizures are divided into two major categories: focal seizures and generalized seizures [1]. Focal seizures, also called partial seizures, occur in just one part of the brain while generalized seizures are a result of abnormal neuronal activity on both hemispheres [1]. At the present time, epilepsy cannot be cured [1], and available treatments can control seizures at least some of the time [1]. Although antiepileptic drugs are the most common approach to treating epilepsy [1], surgery may be required for patients who respond poorly to antiepileptic drugs [1, 2]. The most common type of epilepsy surgery involves removal of the seizure focus, small area of the brain where seizures originate [1].

There are a number of different tests that have been developed for diagnosing epilepsy. The most common diagnostic test for epilepsy is the investigation of EEG (electroencephalogram) [1]. EEG signals, usually recorded using electrodes placed on the scalp, display the electrical activity of the brain. Scalp EEG is however very sensitive to signal attenuation and artifacts, and also has poor spatial resolution. Intracranial EEG or electrocorticogram (ECoG) is an alternative approach to measure the electrical activity of the brain by placing electrodes on the cortex. Abnormalities in the electrical activity of the brain can be detected in using both EEG and ECoG recordings.

Recently, concepts and computational methods derived from the contemporary study of complex systems including chaos theory, nonlinear dynamics and fractals have gained increasing interest for applications in biology and medicine because physiological signals and systems can exhibit an extraordinary range of patterns and behaviors [3]. Also many complex and interesting phenomena in nature are complex nonlinear phenomena.

Nonlinear dynamical system analysis methods have been applied to various types of EEG recordings obtained for both normal and abnormal clinical situations [4] including the resting state, sleep, coma, different states of cognition, and epilepsy. In general, nonlinear dynamical analysis methods have been used to characterize the underlying neuronal dynamics of the brain associated with different physiological states. A number of nonlinear dynamics measures have also been developed to quantify features of

*Corresponding author
*Email addresses:* ensupajt@ubu.ac.th, parerk.janjarasjitt@case.edu (S. Janjarasjitt ), nneth.loparo@case.edu (K. A. Loparo)

rain dynamics [5]. Epilepsy is one of the most important pplications for nonlinear dynamical analysis in biology nd medicine at this time [6].

The information obtained from nonlinear dynamical nalysis is primarily quantified in terms of the complexy parameter which is associated with the dimensionality the underlying system dynamics [7]. Dimensions specifing how the attractor, a geometrical object in the phase pace of the system, is spatially distributed [8], and esmating the dimension of the attractor is one approach detecting and quantifying self-organization of complex ystems [9]. The correlation dimension $D_2$ introduced by rassberger and Procaccia [10, 11] is one of the most comonly used dimensional measures [5].

The mathematical concept of a fractal is commonly ssociated with irregular objects that exhibit a property alled scale-invariance or self-similarity [3, 12]. Fractal rms are composed of subunits resembling the structure the macroscopic object [3] which in nature can emerge om statistical scaling behavior in the underlying physical henomena [13]. An important class of statistical scalenvariant or self-similar random processes is the $1/f$ prosses [13].

A traditional mathematical model and empirical propties of $1/f$ processes have largely been inspired by the actional Brownian motion framework [13, 14, 15] as deeloped by Mandelbrot and Van Ness [16]. In general, odels of $1/f$ processes are represented using a frequency omain characterization. The dynamics of $1/f$ processes chibit power law behavior [17] and can be characterized the frequency domain by $S(\omega) \propto 1/|\omega|^{\gamma}$.

There is evidence that some biological systems can exibit scale-invariant or scale-free behavior, in the sense nat they do not have a characteristic length or time scale nat dominates the dynamics of the underlying process .8, 19, 20]. Fractal properties of different biological sysems can be significantly different in their nature, origin, nd appearance [18], where scale-invariant or scale-free beavior is a tendency of a complex system to develop longnge correlations in time and space [21, 22, 23].

In [13, 14], a wavelet-based representation for $1/f$ prosses was developed. As the wavelet transform is a natul tool for time-frequency analysis is also provides a conenient computational framework for characterizing selfmilar or scale-invariant signal characteristics [13]. The pectral exponent $\gamma$ that specifies the distribution of power om low to high frequencies of $1/f$ processes can be dermined in terms of the slope of the log-variance of the avelet coefficients versus scale graph. Furthermore, an crease in the spectral exponent $\gamma$ leads to sample funcons with smoother temporal patterns [13, 14].

In this study, we investigate the complexity of ECoG ata of subjects with epilepsy using two different comlex system analysis methods; one derived from nonlinear ynamical analysis (correlation dimension) and the other om wavelet-based fractal analysis (spectral exponent). CoG data of subjects with epilepsy obtained during different pathological brain states (ictal and interictal) and different brain regions (within and outside the epileptogenic zone) are used in the analysis.

From the computational results, it is shown that there are statistically significant differences between the means of the spectral exponent and the correlation dimension of the ECoG data obtained during ictal and interictal periods and from different brain regions (within and outside the epileptogenic zone). Further, the ECoG data obtained during seizure activity tends to have smoother temporal patterns with less complexity than during non-seizure activity. Clearly, both the spectral exponent $\gamma$ and the correlation dimension $D_2$, although derived with different signal attributes in mind, provide consistent results. Therefore, wavelet-based fractal analysis can be used to quantify complex dynamics of neuronal networks with similar results as would be obtained using the correlation dimension $D_2$.

## 2. Methods

### *2.1. Experimental Data*

The ECoG data from epilepsy patients examined in this experiment were obtained from the Department of Epileptology, University of Bonn (available online at `http://epileptologie-bonn.de/cms/front_content.php?idcat=193&lang=3&changelang=3`) and originated from the study presented in [24]. There are three ECoG data sets, referred to as sets $C$, $D$ and $E$, that were recorded using intercranial electrodes from five epilepsy patients. The ECoG data of set $C$ were recorded from the hippocampal formation of the opposite hemisphere of the brain from where the seizure was thought to have originated. The ECoG data of sets $D$ and $E$ were recorded from within the epileptogenic zone. Further, the data in sets $C$ and $D$ corresponds to ECoG signals during interictal (non-seizure periods) while the ECoG data in set $E$ was recorded during seizure (ictal) activity.

Each ECoG data set contains 100 epochs of a single-channel ECoG signal that were selected to be artifact free. The length of each epoch is 4097 samples (about 23.6 seconds). In addition, the epochs of the ECoG signal satisfied the weak stationarity criterion given in [24]. The sampling rate of the ECoG data is 173.61 Hz and a bandpass filter (passband between 0.50 Hz and 85 Hz) was used during signal acquisition. Examples of the ECoG signal for each data set are depicted in Fig. 1.

### *2.2. The Wavelet-Based Fractal Analysis*

#### *2.2.1. Discrete Wavelet Transform*

The discrete wavelet transform (DWT) is a representation of a signal $x(t) \in L_2$ using a countably-infinite set of wavelets that constitute an orthonormal basis [25]. The synthesis and analysis representations of the discrete wavelet transform of the signal $x(t)$ can be expressed as, respectively, [25]

$$x(t) = \sum_m \sum_n d_{m,n} \psi_{m,n}(t) \qquad (1)$$

ıd

$$d_{m,n} = \int_{-\infty}^{\infty} x(t)\psi_{m,n}(t)dt \tag{2}$$

here $\psi(t)$ is a given (mother wavelet) function, and $\{d_{m,n}\}$ 'e the wavelet coefficients. A family of wavelets $\{\psi_{m,n}(t)\}$ obtained as normalized dilations and translations of the other wavelet $\psi(t)$ [26, 27]:

$$\psi_{m,n}(t) = 2^{-m/2}\psi\left(2^{-m}t - n\right) \tag{3}$$

here $m$ and $n$ are the dilation and translation indices, ıspectively. The mother wavelet $\psi(t)$ is localized in both me and frequency [28].

For larger scales $2^m$, the wavelet $\psi_{m,n}$ is a stretched ersion of the mother wavelet corresponding to the low equency content, while for smaller scales $2^m$, the wavelet $_{n,n}$ is a contracted version of the mother wavelet corsponding to the high frequency content. From a signal ·ocessing perspective, the orthonormal wavelet transform ın be interpreted as a generalized octave-band filter bank 4, 15] because the mother wavelet $\psi(t)$ is typically the ıpulse response of a bandpass filter. The orthonormal avelet transform can also be interpreted in the context multiresolution analysis (MRA) [27].

### 2.2. $1/f$ Processes

In general, models of $1/f$ processes are represented usg a frequency domain characterization. The dynamics of $f$ processes exhibit power-law behavior [17] and can be ıaracterized in the form of [14]

$$S(\omega) \sim \frac{\sigma_x^2}{|\omega|^\gamma} \tag{4}$$

'er several decades of frequency $\omega$, where $S(\omega)$ is the ɔurier transform of the signal $x(t)$ and $\gamma$ is the spectral :ponent. The spectral exponent $\gamma$ specifies the distribuɔn of spectral content from low to high frequencies, and ı increase in $\gamma$ leads to sample functions with smoother mporal patterns [13, 14].

### 2.3. Wavelet-Based Representation for $1/f$ Processes

The wavelet-based representation for $1/f$ processes deloped in [14] is summarized in the following theorem.

**heorem 1.** [14] *Consider any orthonormal wavelet basis with Rth-order regularity for some $R \geq 1$. Then the ndom process constructed via the expansion*

$$x(t) = \sum_m \sum_n d_{m,n}\psi_{m,n}(t) \tag{5}$$

*ıere the $d_{m,n}$ are a collection of mutually uncorrelated, ro-mean random variables with variances*

$$\text{var}\,(d_{m,n}) = \sigma^2 2^{\gamma m} \tag{6}$$

*r some parameter $0 < \gamma < 2R$, has a time-averaged ectrum*

$$S_x(\omega) = \sigma^2 \sum_m 2^{\gamma m}|\Psi\left(2^m\omega\right)|^2 \tag{7}$$

*that is nearly $1/f$, i.e.,*

$$\frac{\sigma_L^2}{|\omega|^\gamma} \leq S_x(\omega) \leq \frac{\sigma_U^2}{|\omega|^\gamma} \tag{8}$$

*for some $0 < \sigma_L^2 \leq \sigma_U^2 < \infty$, and has octave-spaced ripple, i.e., for any integer $k$*

$$|\omega|^\gamma S_x(\omega) = |2^k\omega|^\gamma S_x\left(2^k\omega\right). \tag{9}$$

*Here, $\Psi(\omega)$ denotes the Fourier transform of the mother wavelet $\psi(t)$.*

Accordingly, from Theorem 1, the spectral exponent $\gamma$ of a $1/f$ process can be determined from the linear relationship between $\log_2 \text{var}\,(d_{m,n})$ and the level $m$. The spectral exponent can then be given by

$$\gamma = \frac{\Delta \log_2 \text{var}\,(d_{m,n})}{\Delta m}. \tag{10}$$

and is directly related to the self-similarity (Hurst) parameter $H$ [13, 14, 15].

### 2.3. Nonlinear Dynamical Analysis

In practice, when we analyze a nonlinear dynamical system, what we have to begin with are not the dynamics of the system (a set of differential equations, for example); but rather a set of observations that may or may not be include all the actual variables of the system. We therefore do not have a complete description of the underlying dynamics of the system, including measurements of system state. Nonlinear dynamical systems analysis refers to methods that can be used to obtain a more complete description of the underlying dynamics of the system from measurable observations [5].

The process of nonlinear dynamical analysis consists of two steps: i) reconstruction of the dynamics of the system; and ii) characterization of the reconstructed attractor.

#### 2.3.1. Attractor Reconstruction

The main problem in applying nonlinear dynamical systems analysis is that only partial measurements of variables of the system are available. The true state of the system of the system is not known, and the method of time-delay embedding allows us to obtain a more comprehensive description of the dynamics and the states of the system by unfolding the observed time series into a higher dimensional state space, called the embedding space.

Let $\{x[n]\}$ be a one-dimensional (observed) measurement of the dynamical system. Note that the dynamical system of interest in this study is the neuronal network, and the set of observations available for the analysis are EEG of ECoG recordings. The $m$-dimensional embedding vector of the time series $x$ is given by [9]

$$\mathbf{x}_n = \begin{bmatrix} x[n] & x[n+\tau] & \dots & x[n+(m-1)\tau] \end{bmatrix}^{\mathrm{T}} \tag{11}$$

here $m$ and $\tau$ are embedding parameters denoting the nbedding dimension and the time-delay, respectively. A quence of embedding vectors $\{\mathbf{x}_n\}$ is used to reconstruct e attractor. It is known that the reconstructed attractor is the same dynamical properties as the actual attractor 9].

The choice of embedding dimension $m$ and time-delay $\tau$ is an effect on the accuracy of estimating the correlation mension. The most important parameter for time-delay nbedding is neither the embedding dimension $m$ nor the me-delay $\tau$ individually, but their combined influence in nbedding window [30]. There are a number of methods r determining the appropriate time-delay $\tau$ such as auto-rrelation [30], mutual information [31], average displace-ent [32], etc. A sufficient embedding dimension $m$ can e determined using the false nearest neighbor technique 3], for example.

### 3.2. Correlation Integral and Dimension

The correlation dimension $D_2$ computed using the Grassberger-rocaccia algorithm is the easiest dimension to compute 4], although the computational time required can be pro-bitive. The calculation of the correlation dimension is ased upon the correlation integral. The correlation inte-al $C(r)$ computed from the reconstructed attractor $\{\mathbf{x}_n\}$ defined by [10, 11]

$$C(r) = \lim_{N\to\infty} \frac{2}{N_c} \sum_{i=0}^{N-1} \sum_{j=i+1}^{N-1} \Theta\left(r - \|\mathbf{x}_i - \mathbf{x}_j\|\right) \qquad (12)$$

here $N$ denotes the length of the reconstructed attractor, $_c = N(N-1)$ and the Heaviside function $\Theta(n) = 1$ if $\geq 0$; 0 otherwise. The correlation integral is thus a easure of the probability that pairwise distances of points the attractor in the state space are less than or equal to specific distance $r$. A revised algorithm was introduced Theiler [9] to correct for autocorrelation effects in the ne series by adding a new parameter called the Theiler ndow $w$.

According to Grassberger and Procaccia [10, 11], the rrelation integral $C(r)$ behaves as a power of $\nu$ for small stances $r$, that is,

$$C(r) \propto r^{\nu}. \qquad (13)$$

d the exponent $\nu$ is defined as the correlation dimension . The correlation dimension can be estimated from the al slope of the log-log plot, i.e.,

$$\nu = \lim_{r\to 0} \frac{\log(C(r))}{\log(r)}. \qquad (14)$$

d quantifies the active degrees of freedom or the com-exity of the dynamical system on the attractor.

### 4. Analytic Framework

In the computational experiments, for the wavelet-based ctal analysis, the discrete Meyer wavelet bases are used to decompose the ECoG signal into 3 levels ($m$ = 1, 2 and 3). At these three levels the $\log_2$-var of the wavelet coefficients exhibits the most linear behavior. The spectral exponent $\gamma$ of the ECoG signal is determined by computing the slope of the $\log_2$-var of the wavelet coefficients as given in [13, 14] using a linear least-squares regression technique. In addition, the attractor of the ECoG signal is reconstructed using the embedding dimension $m = 7$ and the time-delay $\tau = 1$. The correlation dimension $D_2$ of the ECoG signal is also estimated using a linear least-squares regression technique. In fact, different sets of the embedding parameters, i.e., embedding dimension $m$ and time-delay $\tau$, are also used, and the same conclusion can be obtained.

The one-way analysis of variance (ANOVA) is performed to determine whether the complexity measures of the ECoG data obtained during different pathological brain states and for different brain regions have a common mean. Furthermore, multiple comparison tests are performed to determine whether there are any statistically significant differences among means of specific pairs of the complexity measures of the ECoG data.

## 3. Results

### 3.1. Characteristics of the Spectral Exponent

The spectral exponents $\gamma$ of the ECoG data sets $C$, $D$ and $E$ are compared in the box plots shown in Fig. 2. In addition, the mean, the median, and the standard deviation of the spectral exponents $\gamma$ of the ECoG data sets $C$, $D$ and $E$ are summarized in Table 1. The spectral exponent $\gamma$ of the ECoG data set $E$ tends to be higher than that of the data sets $C$ and $D$ while the spectral exponent $\gamma$ of the ECoG data set $D$ tends to be just slightly higher than that of the data set $C$.

From the ANOVA of the spectral exponents $\gamma$ of the ECoG data, the mean square, $F$-statistic and $p$-value are 112.3435, 415.6471 and 0, respectively. The ANOVA test result implies that the means of the spectral exponents $\gamma$ of the ECoG data sets $C$, $D$ and $E$ are statistically significantly different. In addition, from the multiple comparison tests, it is shown that the spectral exponent $\gamma$ of the ECoG data set $E$ are statistically significantly different from that of both data sets $C$ and $D$ with $p \ll 0.0001$. There is however no statistically significant difference between the spectral exponents $\gamma$ of the ECoG data sets $C$ and $D$.

### 3.2. Characteristics of the Correlation Dimension

The box plots of the correlation dimensions $D_2$ of the ECoG data sets $C$, $D$ and $E$ are illustrated in Fig. 2. Table 2 summarizes the mean, the median, and the standard deviation of the correlation dimensions $D_2$. The correlation dimension $D_2$ of the ECoG data set $E$ tends to be lower than that of the data set $C$. The correlation dimension $D_2$ of the ECoG data set $D$ tends to be higher than

ıat of the data set $E$ but slightly lower than that of the ıta set $C$.

From the ANOVA of the correlation dimensions $D_2$ the ECoG data, the mean square, $F$-statistic and $p$-ılue are 55.1015, 81.7871 and 0, respectively. Again, the NOVA test result suggests that the means of the correlation dimensions $D_2$ of the ECoG data sets $C$, $D$ and $E$ ·e also statistically significantly different. Further, from ıe multiple comparison tests, it is shown that the correlaon dimension $D_2$ of the ECoG data set $E$ is statistically gnificantly different from that of both data sets $C$ and ' with $p \ll 0.0001$. On the other hand, the correlation mension $D_2$ of the ECoG data set $D$ is not significantly fferent from that of the data set $C$.

## Discussion

From the computational results, we observe that the CoG data associated with different pathological brain ates (ictal and interictal) and different brain regions (within ıd outside the epileptogenic zone) exhibit different char-:teristics in terms of the complexity measures used in ıis study. The correlation dimension $D_2$ of the ECoG ıta collected during seizure activity is significantly lower ıan that of the ECoG collected during non-seizure activ-y even though the ECoG data are acquired from different gions of the brain, i.e., within the epileptogenic zone and ıtside the epileptogenic zone. This thus suggests that the CoG collected during seizure activity is less complex than at during non-seizure activity, independent of region.

The spectral exponent $\gamma$ of the ECoG collected dur-g seizure activity tends to be higher than that of the CoG collected during non-seizure activity even though e ECoG data were acquired from different regions of the ·ain. Therefore, the ECoG collected during seizure ac-vity tends to have smoother temporal patterns than the CoG acquired during non-seizure periods. Further, there e statistically significant differences between the tempo-l patterns of ECoG data collected during seizure activity ɔm that collected during non-seizure periods and the re-ɔn of the brain does not seem to influence this conclusion.

In addition, during non-seizure activity the ECoG ac-ıired from within the epileptogenic zone also tends to hibit different scale-invariant characteristics from the CoG acquired from outside the epileptogenic zone. Dur-g non-seizure activity, the spectral exponent $\gamma$ obtained ɔm within the epileptogenic zone tends to be slightly gher than that obtained from outside the epileptogenic ne. This therefore suggests that the ECoG obtained ɔm within the epileptogenic zone during non-seizure ac-ity tends to have slightly smoother temporal patterns an that obtained from outside the epileptogenic zone.

The computational results also suggests that the dy-mics of neuronal networks of subjects with epilepsy dur-g ictal and interictal periods have distinguishing charac-ristics. The statistical test results imply that the means both complexity measures ($\gamma$ and $D_2$) of the ECoG data associated with different pathological brain states and different brain regions are significantly different, implying that the dynamics of the neuronal networks within and outside the epileptogenic zone, during seizure and non-seizure periods, have different dynamical characteristics.

Even though the two complexity measures studied in this work are based on different concepts, and quantify different characteristics of the epileptic ECoG signal, both complexity measures (spectral exponent $\gamma$ and correlation dimension $D_2$) provide similar interpretations. Therefore, the wavelet-based fractal analysis can be used to quantify the dynamics of neuronal networks providing consistent information to the more commonly used complexity measure ($D_2$).

## Acknowledgments

This work is supported by a TRF-CHE Research Grant for New Scholar, jointly funded by the Thailand Research Fund (TRF) and the Commission on Higher Education (CHE), the Ministry of Education, Thailand, under Contract No. MRG5280189.

## References

[1] N. I. of Neurological Disorders, S. (NINDS), Seizures and epilepsy: Hope through research, available: http://www.ninds.nih.gov/disorders/epilepsy/detail_epilepsy.htm,.

[2] Wolrd Health Organization (WHO), Epilepsy, available: http://www.who.int/mediacentre/factsheets/fs999/en/.

[3] A. L. Goldberger, Complex systems, Proc. Am. Thorac. Soc. 3 (2006) 467–472.

[4] C. J. Stam, W. S. Pritchard, Dynamics underlying rhythmic and non-rhythmic variants of abnormal, waking delta activity, Int. J. Psychophysiol. 34 (1999) 5–20.

[5] C. J. Stam, Nonlinear dynamical analysis of eeg and meg: review of an emerging field, Clinical Neurophysiology 116 (2005) 2266–2301.

[6] C. E. Elger, G. Widman, R. Andrzejak, M. Dumpelman, J. Arnhold, P. Grassberger, K. Lehnertz, Value of nonlinear time series analysis of the eeg in neocortical epilepsies, in: P. D. Williamson, A. M. Siegel, D. W. Roberts, V. M. Thadani, M. S. Gazzaniga (Eds.), Advances in Neurology, Lippincott Williams & Wilkins, Philadelphia, 2000.

[7] W. S. Tirsch, P. Stude, H. Scherb, M. Keidel, Temporal order of nonlinear dynamics in human brain, Brain Research Reviews 45 (2004) 79–95.

[8] H. D. I. Abarbanel, R. Brown, J. J. Sidorowich, L. S. Tsimring, The analysis of observed chaotic data in physical systems, Reviews of Modern Physics 65 (1993) 1331–1392.

[9] J. Theiler, Estimating fractal dimension, J. Opt. Soc. Am. A 7 (1990) 1055–1073.

[10] P. Grassberger, I. Procaccia, Measuring the strangeness of strange attractors, Physica D 9 (1983) 189–208.

[11] P. Grassberger, I. Procaccia, Estimation of the kolmogorov entropy from a chaotic signal, Phys. Rev. A 28 (1983) 2591–2593.

[12] B. B. Mandelbrot, The fractal geometry of nature, WH Freeman, San Francisco, 1982.

[13] G. W. Wornell, Signal processing with fractals: A wavelet-based approach, Prentice Hall, New Jersey, 1995.

[14] G. W. Wornell, Wavelet-based representations for the $1/f$ family of fractal processes, Proceedings of the IEEE 81 (1993) 1428–1450.

5] G. W. Wornell, A. V. Oppenheim, Estimation of fractal signals from noisy measurements using wavelets, IEEE Trans. on Signal Processing 40 (1992) 611–623.

5] B. B. Mandelbrot, H. W. V. Ness, Fractional brownian motions, fractional noises and applications, SIAM Rev. 10 (1968) 422–436.

7] P. A. Watters, Fractal structure in the electroencephalogram, Complexity International 5.

3] S. Havlin, S. V. Buldyrev, A. L. Goldberger, R. N. Mantegna, S. M. Ossadnik, C.-K. Peng, M. Simons, H. Stanley, Fractals in biology and medicine, Chaos, Solitons & Fractals 6 (1995) 171–201.

9] C. J. Stam, E. A. de Bruin, Scale-free dynamics of global functional connectivity in the human brain, Human Brain Mapping 22 (2004) 97–109.

0] K. Linkenkaer-Hansen, V. V. Nikouline, J. M. Palva, R. J. Ilmoniemi, Long-range temporal correlations and scaling behavior in human brain oscillations, J. of Neurosci. 21 (2001) 1370–1377.

.] J. B. Bassingthwaighte, L. S. Liebovitch, B. J. West, Fractal physiology, Oxford UP, New York, 1994.

2] A. L. Barabási, H. E. Stanley, Fractal concepts in surface growth, Cambridge UP, Cambridge, UK, 1995.

8] P. Bak, How nature works, Oxford UP, Oxford, 1997.

4] R. G. Andrzejak, K. Lehnertz, F. Mormann, C. Rieke, P. David, C. E. Elger, Indications of nonlinear deterministic and finit-dimensional structures in time series of brain electrical activity: Dependence on recording region and brain state, Phys. Rev. E 64 (2001) (061907)1–8.

5] S. Mallat, A wavelet tour of signal processing, Academic Press, San Diego, 1998.

5] I. Daubechies, Orthonormal bases of compactly supported wavelets, Commun. Pure Appl. Math. XLI (1988) 909–996.

7] S. G. Mallat, A theory for multiresolution signal decomposition: the wavelet representation, IEEE Trans. Pattern Analysis and Machine Intelligence 11 (1989) 674–693.

5] A. Cohen, J. Kovacevic, Wavelets: the mathematical background, Proceedings of the IEEE 84 (1996) 514–522.

0] F. Takens, Detecting strange attractors in turbulence, in: D. A. Rand, L.-S. Young (Eds.), Dynamical Systems and Turbulence, Springer-Verlag, Berlin, 1981.

0] A. M. Albano, J. Muench, C. Schwartz, A. I. Mees, P. E. Rapp, Singular-value decomposition and the grassberger-procaccia algorithm, Phys. Rev. A 38 (1988) 3017–3026.

.] H. S. A.M. Fraser, Independent coordinates for strange attractors from mutual information, Phys. Rev. A 33 (1986) 1134–1140.

2] M. T. Rosenstein, J. J. Collins, C. J. de Lucca, Reconstruction expansion as a geometry-based framework for choosing proper delay times, Physica D 73 (1994) 82.

5] M. B. Kennel, R. Brown, H. D. I. Abarbanel, Determining embedding dimen- sion for phase-space reconstruction using a geometrical construction, Phys. Rev. A 45 (1992) 3403–3411.

:] W. S. Pritchard, D. W. Duke, Measuring chaos in the brain: a tutorial review of eeg dimension estimation, Brain Cogn. 27 (1995) 353–397.

Table 1: The statistical values of the spectral exponents $\gamma$ of the ECoG data

| Data Set | Mean | Median | S.D. |
|---|---|---|---|
| ? | 3.2706 | 3.3272 | 0.4239 |
| D | 3.5198 | 3.4503 | 0.5806 |
| E | 5.2183 | 5.2338 | 0.5423 |

Table 2: The statistical values of the correlation dimensions $D_2$ of the ECoG data

| Data Set | Mean | Median | S.D. |
|---|---|---|---|
| C | 4.2172 | 4.1803 | 0.7529 |
| D | 3.8239 | 3.8452 | 1.0815 |
| E | 2.7807 | 2.8117 | 0.5334 |

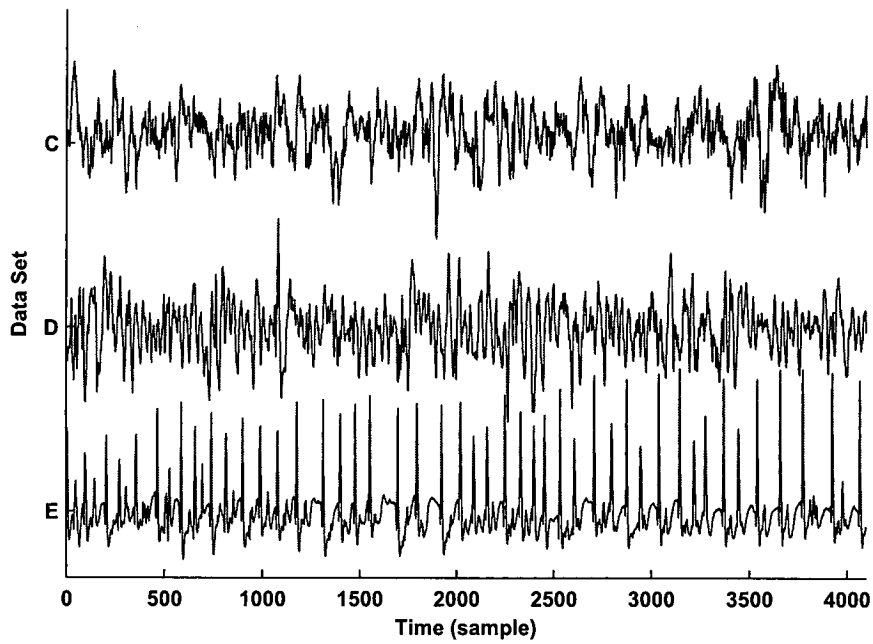


Figure 1: Examples of ECoG signals of the data sets $C$, $D$ and $E$.

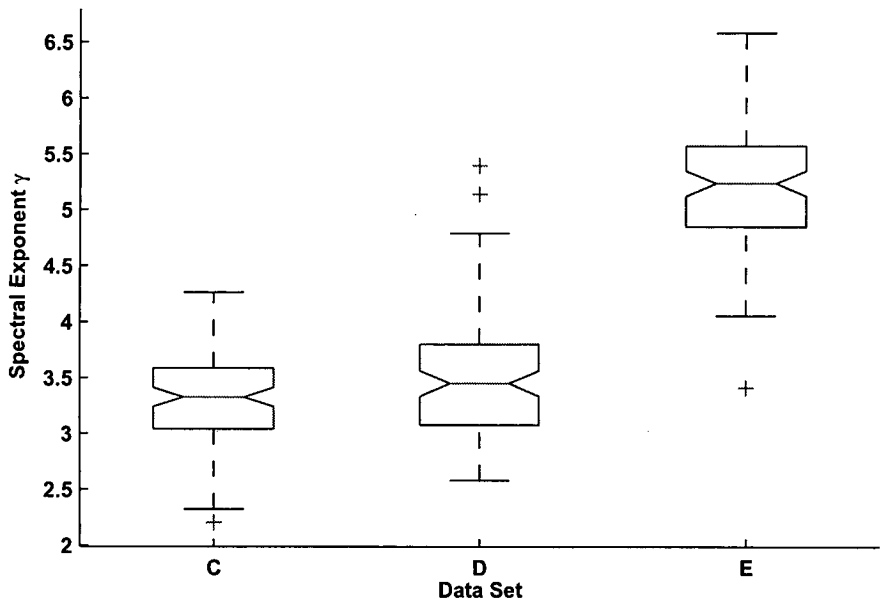


Figure 2: Comparison of the spectral exponents of ECoG of the data sets $C$, $D$ and $E$.

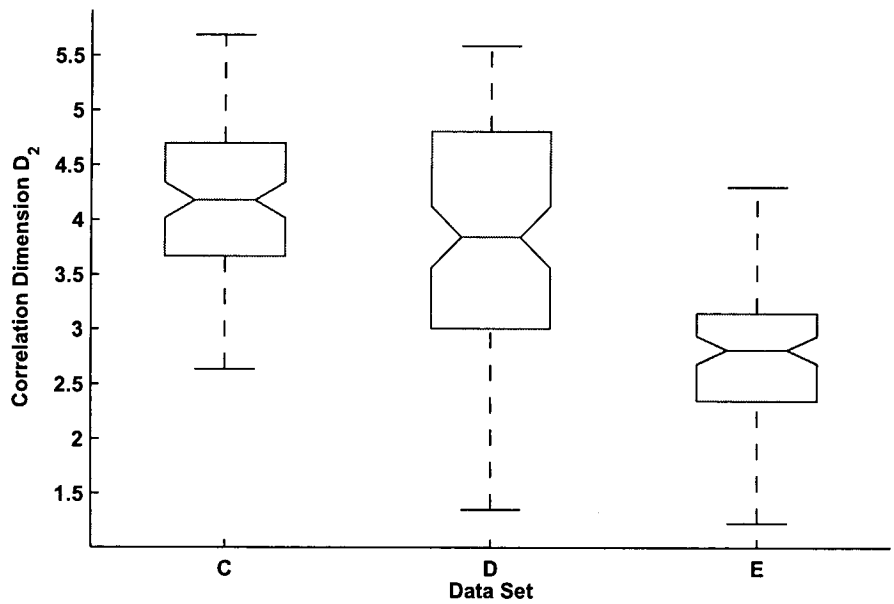


Figure 3: Comparison of the correlation dimensions of ECoG of the data sets $C$, $D$ and $E$.

2009 International Symposium on Intelligent Signal Processing and Communication Systems (ISPACS 2009) December 7-9, 2009

MP1-C-3

# Wavelet-Based Fractal Analysis of the Epileptic EEG Signal

Suparerk Janjarasjitt* and Kenneth A. Loparo†
* Department of Electrical and Electronic Engineering, Ubon Ratchathani University, Thailand
Department of Electrical Engineering and Computer Science, Case Western Reserve University, USA
E-mail: ensupajt@ubu.ac.th, suparerk.janjarasjitt@case.edu Tel: +66-4535-3332
† Department of Electrical Engineering and Computer Science, Case Western Reserve University, USA
E-mail: kenneth.loparo@case.edu Tel: +1-216-368-4115

***Abstract*—The wavelet transform is a natural tool for characterizing self-similar signals. In this work, the spectral exponent $\gamma$ derived from the wavelet-based representation for $1/f$ processes is used to investigate the self-similarity of electrocorticography (intracranial EEG) signals from an epilepsy patient. An increase in $\gamma$ leads to sample signals with smoother temporal patterns. Our computational results show that during an epileptic seizure $\gamma$ is significantly higher than that associated with other states of the brain, implying that wavelet-based fractal analysis is potentially a useful computational tool for epileptic seizure detection.**

## I. Introduction

Epilepsy is a common brain disorder in which clusters of neurons signal abnormally [1]. More than 50 million individuals worldwide, about 1% of the world's population are affected by epilepsy [2]. In epilepsy, the normal pattern of neuronal activity is disturbed, causing strange sensations, emotions, and behavior, or sometimes convulsions, muscle spasms, and loss of consciousness [1]. There are many possible causes for seizures ranging from illness to brain damage to abnormal brain development [1], and epileptic seizures are manifestations of epilepsy [3]. The electroencephalogram (EEG) is a signal that quantifies the electrical activity of the brain, is used to assess and detect brain abnormalities, and is crucial for the diagnosis of epilepsy [1].

Recently, concepts and computational tools derived from the contemporary study of complex systems including nonlinear dynamics and fractals have gained increasing interest for applications in biology and medicine because physiological signals and systems can exhibit an extraordinary range of patterns and behaviors [4]. The correlation integral and dimension are common nonlinear dynamical analysis techniques that have been applied to EEG signal analysis [5] to study various aspects including sleep [6], [7], neurodevelopment [8], and epilepsy [2], [9].

The mathematical concept of a fractal is commonly associated with irregular objects that exhibit a geometric property called self-similarity [4], [10]. Fractal forms are composed of subunits resembling the structure of the macroscopic object [4] which in nature can emerge from statistical scaling behavior in the underlying physical phenomena [11]. $1/f$ processes are an important class of statistical self-similar random processes [11]. In [12], [13], a wavelet-based representation for $1/f$ processes was developed where the spectral exponent ($\gamma$), estimated from the slope of the log-variance of the wavelet coefficients versus the scale, specifies the distribution of power from low to high frequencies. In previous studies, fractal analysis using the wavelet transform was used to examine epileptiform activity in rats [14] while in [15] the power spectrum was used to calculate the fractal exponent.

In this work, self-similarity characteristics of ECoG (electrocorticography) data from an epilepsy patient is examined using the wavelet-based representation for $1/f$ processes [12], [13]. From the computational results, the spectral exponent $\gamma$ corresponding to various states of the brain, e.g., seizure onset, interictal, pre-ictal, and post-ictal, are distinguishable. Further, the spectral exponent during an epileptic seizure event is significantly higher than that associated with other states of the brain. Therefore, this suggests that the spectral exponent obtained from wavelet-based fractal analysis may be useful in the detection of epileptic seizure events.

## II. Background

### A. Discrete Wavelet Transform

The discrete wavelet transform (DWT) is a representation of a signal $x(t) \in L_2$ using a countably-infinite orthonormal wavelet basis [16]. The synthesis and analysis representations of the discrete wavelet transform of the signal $x(t)$ can be expressed as, respectively, [16]

$$x(t) = \sum_m \sum_n d_{m,n} \psi_{m,n}(t) \tag{1}$$

and

$$d_{m,n} = \int_{-\infty}^{\infty} x(t) \psi_{m,n}(t) dt \tag{2}$$

where $\psi(t)$ is the mother wavelet and $\{d_{m,n}\}$ are the wavelet coefficients. A family of wavelets $\{\psi_{m,n}(t)\}$ is obtained as normalized dilations and translations of the mother wavelet $\psi(t)$ [17], [18]:

$$\psi_{m,n}(t) = 2^{-m/2} \psi\left(2^{-m} t - n\right) \tag{3}$$

where $m$ and $n$ are the dilation and translation indices, respectively. The mother wavelet $\psi(t)$ is localized in both time and frequency [19].

978-1-4244-5016-9/09/$25.00 ©2009 IEEE

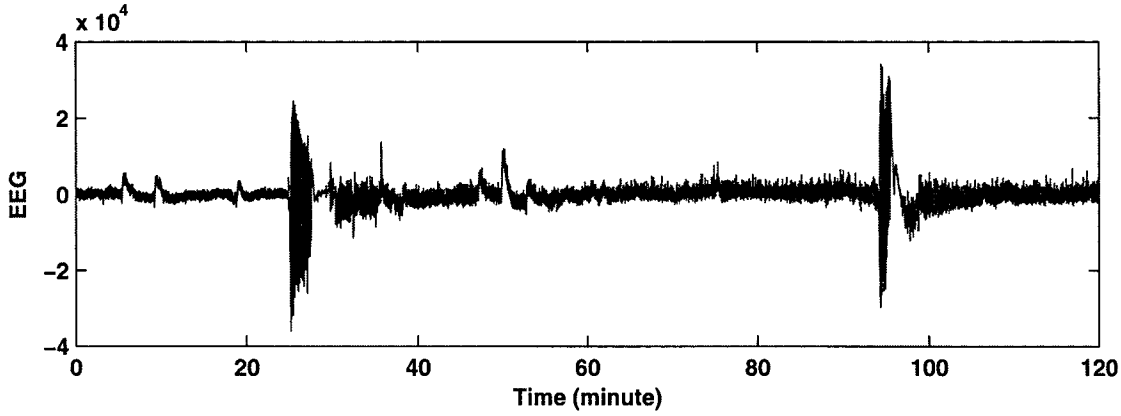


Fig. 1. The intracranial EEG of the epilepsy patient.

For large scale $2^m$, the wavelet $\psi_{m,n}$ is a stretched version of the mother wavelet corresponding to low frequency content, while for small scale $2^m$, the wavelet $\psi_{m,n}$ is a contracted version of the mother wavelet corresponding to high frequency content. From a signal processing point of view, the orthonormal wavelet transform can be interpreted as a generalized octave-band filter bank [13], [20] because the mother wavelet $\psi(t)$ is typically an impulse response of a bandpass filter. The orthonormal wavelet transform can also be interpreted in the context of multiresolution analysis (MRA) [18].

### B. $1/f$ Processes

In general, $1/f$ processes are represented using a frequency domain characterization. The dynamics of $1/f$ processes exhibit power-law behavior [21] and can be characterized in the form of [13]

$$S(\omega) \sim \frac{\sigma_x^2}{|\omega|^\gamma} \tag{4}$$

over several decades of frequency $\omega$, where $S(\omega)$ is the Fourier transform of the signal $x(t)$ and $\gamma$ is a spectral exponent. An increase in the spectral exponent $\gamma$ specifying a distribution of spectral content from low to high frequencies leads to sample functions with smoother temporal patterns [13], [11].

### C. Wavelet-Based Representation for $1/f$ Processes

The wavelet-based representation for $1/f$ processes developed in [12] is presented in the following theorem.

*Theorem 1:* [13] Consider any orthonormal wavelet basis with $R$th-order regularity for some $R \geq 1$. Then the random process constructed via the expansion

$$x(t) = \sum_m \sum_n d_{m,n} \psi_{m,n}(t) \tag{5}$$

where the $d_{m,n}$ are a collection of mutually uncorrelated, zero-mean random variables with variances

$$\text{var}\,(d_{m,n}) = \sigma^2 2^{\gamma m} \tag{6}$$

for some parameter $0 < \gamma < 2R$, has a time-averaged spectrum

$$S_x(\omega) = \sigma^2 \sum_m 2^{\gamma m} |\Psi\,(2^m \omega)|^2 \tag{7}$$

that is nearly $1/f$, i.e.,

$$\frac{\sigma_L^2}{|\omega|^\gamma} \leq S_x(\omega) \leq \frac{\sigma_U^2}{|\omega|^\gamma} \tag{8}$$

for some $0 < \sigma_L^2 \leq \sigma_U^2 < \infty$, and has octave-spaced ripple, i.e., for any integer $k$

$$|\omega|^\gamma S_x(\omega) = |2^k \omega|^\gamma S_x\left(2^k \omega\right). \tag{9}$$

Here, $\Psi(\omega)$ denotes the Fourier transform of the mother wavelet $\psi(t)$.

From Theorem 1, the spectral exponent $\gamma$ of a $1/f$ process can be determined from the linear relationship between $\log_2 \text{var}\,(d_{m,n})$ and the level $m$, and is given by

$$\gamma = \frac{\Delta \log_2 \text{var}\,(d_{m,n})}{\Delta m}. \tag{10}$$

## III. Analytic Framework

### A. Data and Subject

We analyze data from long-term ECoG recordings of an epilepsy patient at University Hospitals of Cleveland, Case Medical Center in Cleveland, Ohio, USA before surgery. With the consent of the patient, ECoG data were recorded for few days using a Nihon-Kohden EEG system (band-pass (0.10-300 Hz) filter, 1000Hz sampling rate).

A single channel of a 2-hour record acquired from within the focal region of the seizures is examined. The ECoG signal is illustrated in Fig. 1 where 2 epileptic seizure events between 24m 47s and 27m 36s and between 93m 57s and 95m 45s, are observed. Note: The first seizure occurred several hours after the preceeding epileptic seizure event.

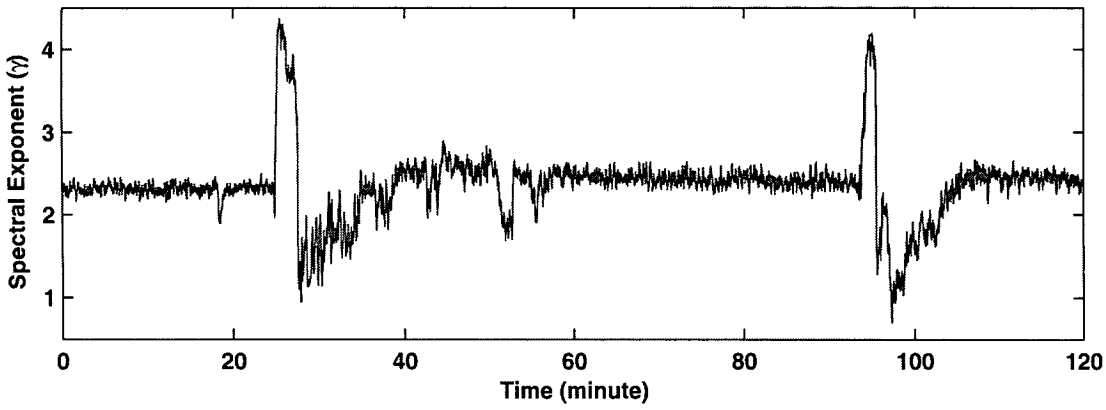


Fig. 2. The spectral exponent $\gamma$ of the intracranial EEG of the epilepsy patient.

### *B. The Wavelet-Based Fractal Analysis*

In the computational experiment, the ECoG signal is partitioned into epochs of 8000 samples (8 seconds). The 5th order Coiflet orthonormal wavelet bases is used with the number of vanishing moments for $\psi$ and $\phi$ equal to 10 and 9, respectively. The ECoG epochs are decomposed into 6 levels and wavelet coefficients of levels $m = 1, 2, 3, 4, 5$ are used to estimate the spectral exponent $\gamma$ using a linear least-squares regression technique.

## IV. Results

The spectral exponent of the ECoG signal is illustrated in Fig. 2 where it is observed that $\gamma$ has distinguishable characteristics corresponding to different states of the brain. In particular, we observe that during an epileptic seizure event $\gamma$ is significantly higher than that associated with other states of the brain. Further, $\gamma$ dramatically increases during seizure onset, suddenly decreases right after the epileptic seizure, and then gradually increases returning to baseline as the influence of the epileptic seizure diminishes. In addition, the ECoG signal around the first and second epileptic seizure events (plotted in gray) is compared to the corresponding spectral exponent $\gamma$ (plotted in black) in Fig. 3(a) and Fig. 3(b), respectively.

From the computational result shown in Fig. 2, it is evident that both the proposed technique can be used to detect a seizure event using a simple method such as thresholding. However, the threshold value is likely patient specific and would need to be adjusted based on recorded data. For the current patient, if $\gamma = 3$ is set as the threshold, the first and the second seizures are then detected between 25m 9s and 27m 38s, and between 94m 1s and 95m 37s, respectively.

## V. Conclusions

Self-similarity characteristics of the ECoG signal from an epilepsy patient are examined using wavelet-based fractal analysis. From the computational results it is observed that during an epileptic seizure the spectral exponent of the ECoG data exhibits a significantly value than associated with other states of the brain.

Because of the limited space, only data from a single patient recording with two epileptic seizure events are presented. The computational experiments were however performed on a larger number of patients with similar results and conclusions: ECoG signals during epileptic seizures have smoother temporal patterns and less complex temporal characteristics. This is consistent with other findings in the literature, e.g. [9], that suggests that complexity of the intracranial EEG decreases during epileptic seizure events.

We hypotesize that the the spectral exponent $\gamma$ of the ECoG signal can be used to identify and classify various states of the brain. Future work will further investigate the application of wavelet-based fractal analysis as a computational tool for epileptic seizure detection.

## Acknowledgments

Dr. Janjarasjitt is supported by a TRF-CHE Research Grant for New Scholar, jointly funded by the Thailand Research Fund (TRF) and the Commission on Higher Education (CHE), the Ministry of Education, Thailand, under Contract No. MRG5280189. The authors thank Mary Ann Werz, M.D. for her assistance in acquiring and visually analyzing the patient data used in this study.

## References

[1] Seizure and Epilepsy: Hope through Research National Institute of Neurological Disorders and Stroke (NINDS), Bethesda, MD, 2004 [Online]. Available: http://www.ninds.nih.gov/disorders/epilepsy/detail_epilepsy.htm

[2] B. Litt and J. Echauz, "Prediction of epileptic seizures," *Lancet Neurology*, vol. 1, pp. 22-30, 2002.

[3] A. Subasi, "Epileptic seizure detection using dynamic wavelet network," *Expert Systems with Applications*, vol. 29, pp. 343-355, 2005.

[4] A. L. Goldberger, "Complex systems," *Proc. Am. Thorac. Soc.*, vol. 3, pp. 467-472, 2006.

[5] W. S. Pritchard and D. W. Duke, "Measuring chaos in the brain: a tutorial review of EEG dimension estimation," *Brain Cogn.*, vol. 27, pp. 353-397, 1995.

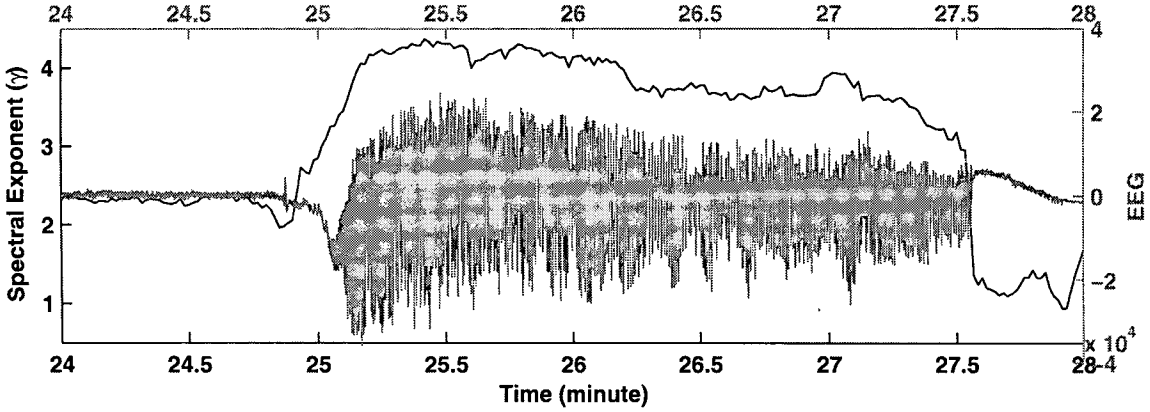


(a) The first epileptic seizure

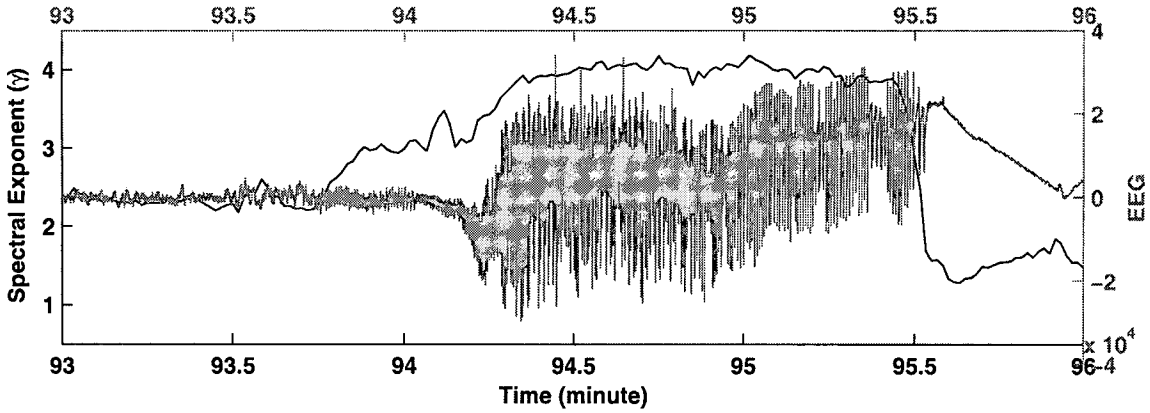


(b) The second epileptic seizure

Fig. 3. The segments of the intracranial EEG compared to the corresponding spectral exponent $\gamma$.

[6] R. Ferri, L. Parrino, A. Smerieri, M. G. Terzano, M. Elia, S. A. Musumeci, S. Pettinato, and C. J. Stam, "Non-linear EEG measures during sleep: effects of the different sleep stages and cyclic alternating pattern," *Int. J. Psychophysiol.*, vol. 43, pp. 273-286, 2002.

[7] S. Janjarasjitt, M. S. Scher, and K. A. Loparo, "Nonlinear dynamical analysis of the neonatal EEG time series: the relationship between sleep state and complexity," *Clin. Neurophysiol.*, vol. 119, pp. 1812-1823, 2008.

[8] S. Janjarasjitt, M. S. Scher, and K. A. Loparo, "Nonlinear dynamical analysis of the neonatal EEG time series: the relationship between neurodevelopment and complexity," *Clin. Neurophysiol.*, vol. 119, pp. 822-836, 2008.

[9] K. Lehnertz and C. E. Elger, "Spatio-temporal dynamics of the primary epileptogenic area in temporal lobe epilepsy characterized by neuronal complexity loss," *Electroenceph. and Clin. Neurophyiol.*, vol. 95, pp. 108-117, 1995.

[10] B. B. Mandelbrot, *The Fractal Geometry of Nature.* WH Freeman: San Francisco, 1982.

[11] G. W. Wornell, *Signal Processing with Fractals: A Wavelet-Based Approach.* Prentice Hall: New Jersey, 1995.

[12] G. W. Wornell, "A Karhunen-Loève-like expansion for $1/f$ processes via wavelets," *IEEE Trans. Inform. Theory*, vol. 36, pp. 859-861, 1990.

[13] G. W. Wornell, "Wavelet-based representations for the $1/f$ family of fractal processes," *Proceedings of the IEEE*, vol. 81, pp. 1428-1450, 1993.

[14] X Li, J. Polygiannakis, P. Kapiris, A. Peratzakis, K. Eftaxias, and X. Yao, "Fractal spectral analysis of pre-epileptic seizures in terms of criticality," *J. Neural Eng.*, vol. 2, pp. 11-16, 2005.

[15] E. Pereda, A. Gamundi, R. Rial, J. Gonzalez, "Non-linear behaviour of human EEG: fractal exponent versus correlation dimension in awake and sleep stages," *Neuroscience Letters*, vol. 250, pp. 91-94, 1998.

[16] S. Mallat, *A Wavelet Tour of Signal Processing.* Academic Press: San Diego, 1998.

[17] I. Daubechies, "Orthonormal bases of compactly supported wavelets," *Commun. Pure Appl. Math.*, vol. XLI, pp. 909-996, 1988.

[18] S. G. Mallat, "Atheory for multiresolution signal decomposition: the wavelet representation," *IEEE Trans. Pattern Analysis and Machine Intelligence*, vol. 11. pp. 674-693, 1989.

[19] A. Cohen and J. Kovacevic, "Wavelets: the mathematical background," *Proceedings of the IEEE*, vol. 84, pp. 514-522, 1996.

[20] G. W. Wornell and A. V. Oppenheim, "Estimation of fractal signals from noisy measurements using wavelets," *IEEE Trans. Signal Processing*, vol. 40, pp. 611-623, 1992.

[21] P. A. Watters, "Fractal structure in the electroencephalogram," *Complexity Internation*, vol. 5, 1998. Available:http://www.complexity.org.au/ci/vol05/watters/watters.html"

# Wavelet-Based Fractal Analysis of Multi-Channel Epileptic ECoG

Suparerk Janjarasjitt
Department of Electrical and Electronic Engineering
Ubon Ratchathani University
Ubon Ratchathani, Thailand
Department of Electrical Engineering
and Computer Science
Case Western Reserve University
Cleveland, Ohio, USA
Email: ensupajt@ubu.ac.th
Telephone: +66-4535-3332

Kenneth A. Loparo
Department of Electrical Engineering
and Computer Science
Case Western Reserve University
Cleveland Ohio, USA
Email: kenneth.loparo@case.edu
Telephone: +1-216-368-4115

*Abstract*—**In this work, the spectral exponent $\gamma$ derived from the wavelet-based representation for $1/f$ processes is used to analyze multi-channel electrocorticogram (ECoG) data obtained from a subject with temporal lobe epilepsy. The computational results show that the spectral exponents of different channels of the ECoG data exhibit different characteristics of spectral exponent $\gamma$. Also during an epileptic seizure the spectral exponent $\gamma$ of the ECoG signals is significantly higher than that associated with other states of the brain. An increase in the spectral exponent can however be observed in only channels that exhibit the ictal behavior, suggesting that regions of the brain that are involved in ictal activity can be localized.**

*Index Terms*—**Electrocorticogram, epilepsy, seizure, fractals, wavelet transform.**

## I. Introduction

Epilepsy is a common brain disorder in which clusters of neurons signal abnormally [1]. More than 50 million individuals worldwide, about 1% of the world's population are affected by epilepsy [2], where normal patterns of neuronal activity are disturbed causing strange sensations, emotions, and behavior, or sometimes convulsions, muscle spasms, and loss of consciousness [1]. There are many possible causes for seizures ranging from illness to brain damage to abnormal brain development [1], and epileptic seizures are manifestations of epilepsy [3]. Electrocorticography measures electrical activity from the surface of the brain (cortex) and is used to assess and detect brain abnormalities, and is crucial for the diagnosis of severe epilepsy in patients [1].

Recently, concepts and computational tools derived from the contemporary study of complex systems including nonlinear dynamics and fractals have gained increasing interest for applications in biology and medicine because physiological signals and systems can exhibit an extraordinary range of patterns and behaviors [4]. The correlation integral and dimension are common nonlinear dynamical analysis techniques that have been applied to both EEG [5] and ECoG signals to study various aspects including sleep [6], [7], neurodevelopment [8], and epilepsy [2], [9], [10].

The mathematical concept of a fractal is commonly associated with irregular objects that exhibit a geometric property called self-similarity [4], [11]. Fractal forms are composed of subunits resembling the structure of the macroscopic object [4] which in nature can emerge from statistical scaling behavior in the underlying physical phenomena [12]. $1/f$ processes are an important class of statistical self-similar random processes [12]. In [13], [14], a wavelet-based representation for $1/f$ processes was developed where the spectral exponent ($\gamma$), estimated from the slope of the log-variance of the wavelet coefficients versus the scale, specifies the distribution of power from low to high frequencies. In previous studies, fractal analysis using the wavelet transform was used to examine epileptiform activity in rats [15] while in [16] the power spectrum was used to calculate the fractal exponent.

In this work, the characteristics of multi-channel ECoG data obtained from a subject with temporal lobe epilepsy are examined using the wavelet-based representation for $1/f$ processes [13], [14]. In the previous study using the same computational approach reported in [10], it was found that the spectral exponent $\gamma$ of a single-channel ECoG signal during an epileptic seizure is significantly higher than that associated with other states of the brain. An increase in the spectral exponent $\gamma$ leads to sample functions with smoother temporal patterns. From computational results, significant differences in the spectral exponent are observed during an epileptic seizure. Furthermore, it is observed that the spectral exponents $\gamma$ of multi-channel ECoG data are different and vary according to both regions of the brain and states of the brain. This therefore suggests that the spectral exponent $\gamma$ may be a useful quantitative measure for detecting and spatially localizing epileptic seizure events.

This work is supported by a TRF-CHE Research Grant for New Scholar, jointly funded by the Thailand Research Fund (TRF) and the Commission on Higher Education (CHE), the Ministry of Education, Thailand, under Contract No. MRG5280189.

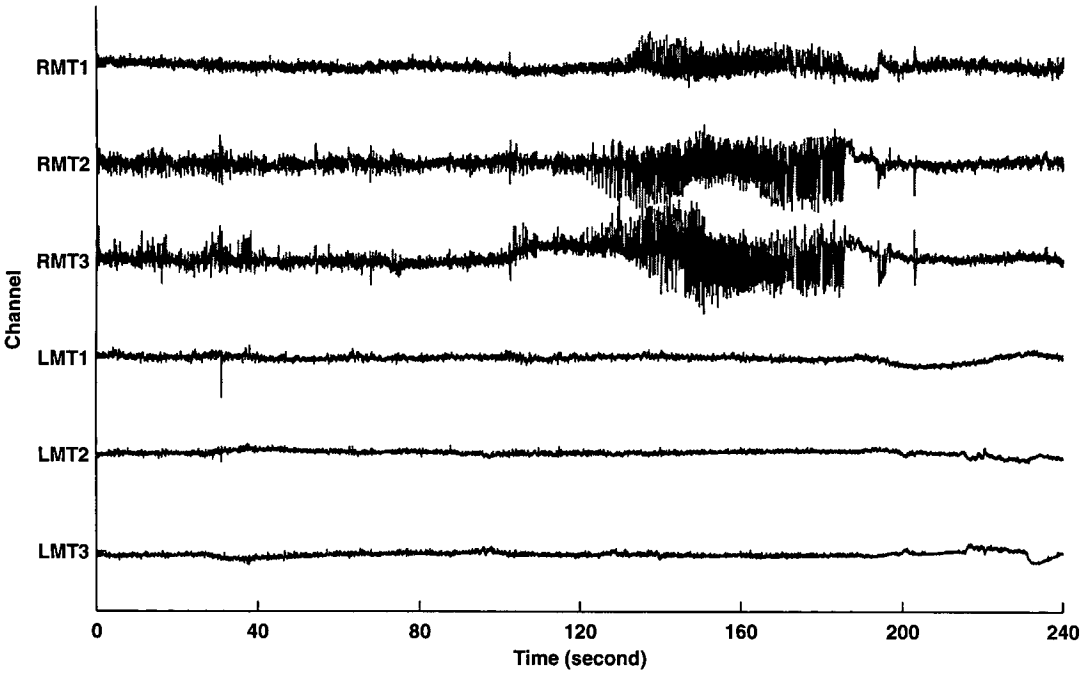


Fig. 1. Multi-channel ECoG data of the subject with temporal lobe epilepsy.

## II. Background

### A. Discrete Wavelet Transform

The discrete wavelet transform (DWT) is a representation of a signal $x(t) \in L_2$ using a countably-infinite orthonormal wavelet basis [17]. The synthesis and analysis representations of the discrete wavelet transform of the signal $x(t)$ can be expressed as, respectively, [17]

$$x(t) = \sum_m \sum_n d_{m,n} \psi_{m,n}(t) \tag{1}$$

and

$$d_{m,n} = \int_{-\infty}^{\infty} x(t) \psi_{m,n}(t) dt \tag{2}$$

where $\psi(t)$ is the mother wavelet and $\{d_{m,n}\}$ are the wavelet coefficients. A family of wavelets $\{\psi_{m,n}(t)\}$ is obtained as normalized dilations and translations of the mother wavelet $\psi(t)$ [18], [19]:

$$\psi_{m,n}(t) = 2^{-m/2} \psi\left(2^{-m} t - n\right) \tag{3}$$

where $m$ and $n$ are the dilation and translation indices, respectively. The mother wavelet $\psi(t)$ is localized in both time and frequency [20].

For large scale $2^m$, the wavelet $\psi_{m,n}$ is a stretched version of the mother wavelet corresponding to low frequency content, while for small scale $2^m$, the wavelet $\psi_{m,n}$ is a contracted version of the mother wavelet corresponding to high frequency content. From a signal processing point of view, the orthonormal wavelet transform can be interpreted as a generalized octave-band filter bank [14], [21] because the mother wavelet $\psi(t)$ is typically an impulse response of a bandpass filter. The orthonormal wavelet transform can also be interpreted in the context of multiresolution analysis (MRA) [19].

### B. $1/f$ Processes

In general, $1/f$ processes are represented using a frequency domain characterization. The dynamics of $1/f$ processes exhibit power-law behavior [22] and can be characterized in the form of [14]

$$S(\omega) \sim \frac{\sigma_x^2}{|\omega|^\gamma} \tag{4}$$

over several decades of frequency $\omega$, where $S(\omega)$ is the Fourier transform of the signal $x(t)$ and $\gamma$ is a spectral exponent. An increase in the spectral exponent $\gamma$ specifying a distribution of spectral content from low to high frequencies leads to sample functions with smoother temporal patterns [12], [14].

### C. Wavelet-Based Representation for $1/f$ Processes

The wavelet-based representation for $1/f$ processes developed in [13] is presented in the following theorem.

*Theorem 1:* [14] Consider any orthonormal wavelet basis with $R$th-order regularity for some $R \geq 1$. Then the random process constructed via the expansion

$$x(t) = \sum_m \sum_n d_{m,n} \psi_{m,n}(t) \tag{5}$$

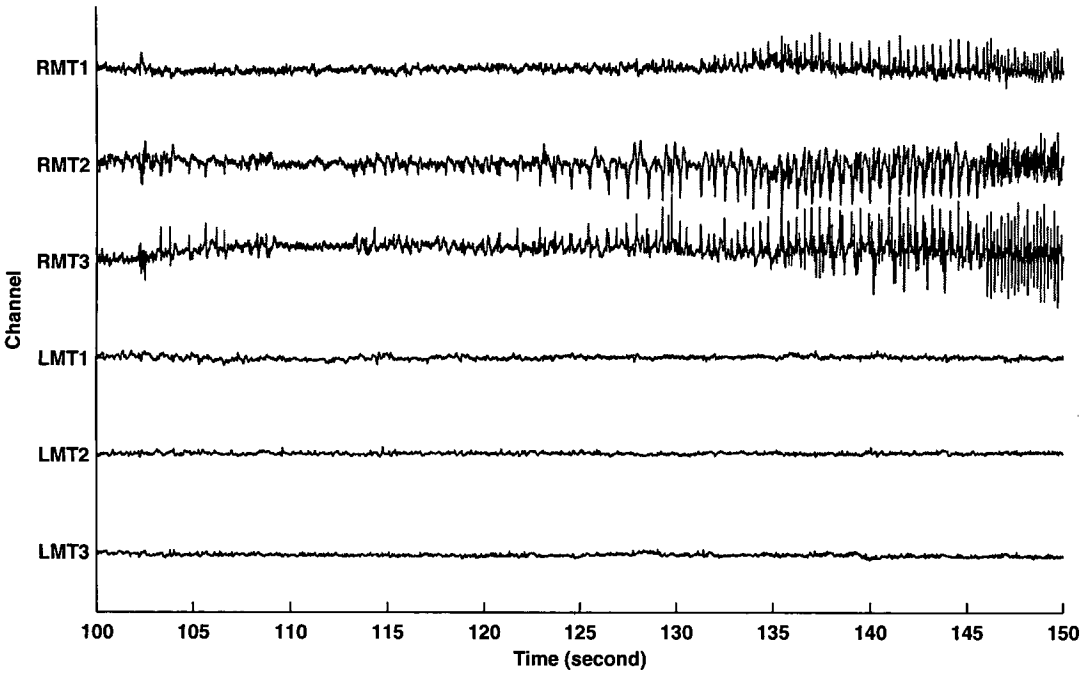


Fig. 2. Multi-channel ECoG data of the subject with temporal lobe epilepsy at the seizure onset.

where the $d_{m,n}$ are a collection of mutually uncorrelated, zero-mean random variables with variances

$$\text{var}\,(d_{m,n}) = \sigma^2 2^{\gamma m} \tag{6}$$

for some parameter $0 < \gamma < 2R$, has a time-averaged spectrum

$$S_x(\omega) = \sigma^2 \sum_m 2^{\gamma m} |\Psi\,(2^m \omega)|^2 \tag{7}$$

that is nearly $1/f$, i.e.,

$$\frac{\sigma_L^2}{|\omega|^\gamma} \leq S_x(\omega) \leq \frac{\sigma_U^2}{|\omega|^\gamma} \tag{8}$$

for some $0 < \sigma_L^2 \leq \sigma_U^2 < \infty$, and has octave-spaced ripple, i.e., for any integer $k$

$$|\omega|^\gamma S_x(\omega) = |2^k \omega|^\gamma S_x\left(2^k \omega\right). \tag{9}$$

Here, $\Psi(\omega)$ denotes the Fourier transform of the mother wavelet $\psi(t)$.

From Theorem 1, the spectral exponent $\gamma$ of a $1/f$ process can be determined from the linear relationship between $\log_2 \text{var}\,(d_{m,n})$ and the level $m$, and is given by

$$\gamma = \frac{\Delta \log_2 \text{var}\,(d_{m,n})}{\Delta m}. \tag{10}$$

## III. Methods

### A. Data and Subject

A 4-minute section of long-term ECoG data of an epilepsy patient studied at University Hospitals of Cleveland, Case Medical Center in Cleveland, Ohio, USA is examined. With the consent of the patient, the long-term ECoG data were recorded for a few days using a Nihon-Kohden EEG system (band-pass (0.10–300 Hz) filter, 1,000 Hz sampling rate) prior to surgery. The patient was diagnosed with right mesial temporal lobe epilepsy.

The section of long-term ECoG data examined in this study consists of six channels of differential ECoG signals and contains an epileptic seizure event. The first three channels of differential ECoG signals, referred to as RMT1, RMT2 and RMT3, were obtained from the right mesial temporal lobe region, while the other three channels of differential ECoG signals, referred to as LMT1, LMT2 and LMT3, were obtained from left mesial temporal lobe region.

The section of long-term ECoG data is shown in Fig. 1. The epileptic seizure occurs between 1m 50s and 3m 6s in this section. Fig. 2 shows the multi-channel ECoG data around the seizure onset. From Fig. 1 and Fig. 2, it can be observed that there are only changes in the ECoG signals during the epileptic seizure event for the channels RMT1, RMT2 and RMT3 which were obtained from the right mesial temporal lobe region.

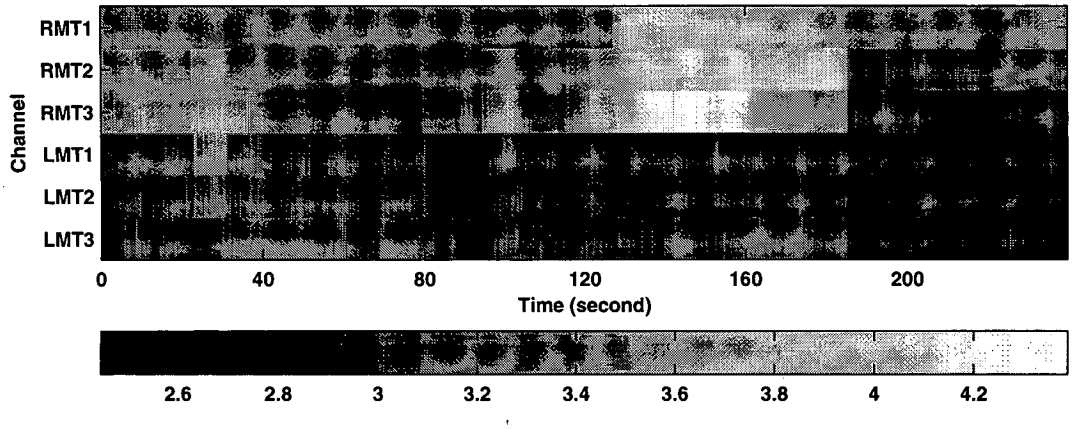


Fig. 3. The spectral exponents of multi-channel ECoG data.

### B. Analytic Framework

In the computational experiment, the ECoG signals are partitioned into epochs of 8,000 samples (8 seconds) with a sliding window of 100 samples (0.1 second). The epochs of the ECoG signals are decomposed into 6 levels using the 5th order Coiflet wavelets which provide the highest number of vanishing moments for both phi and psi for a given support. Wavelet coefficients of all levels, i.e., $m = 1, 2, \ldots, 6$, are used to estimate the spectral exponent $\gamma$ using a linear least-squares regression technique.

## IV. Results

The spectral exponents of the multi-channel ECoG data for channels RMT1, RMT2, RMT3, LMT1, LMT2 and LMT3 are displayed as a color-map plot shown in Fig. 3. From the computational results, it is observed that different channels of the ECoG data exhibit different characteristics of the spectral exponent $\gamma$. Furthermore, the spectral exponent $\gamma$ has distinguishable characteristics corresponding to different states of the brain. In particular, during an epileptic seizure the spectral exponent $\gamma$ tends to be higher than that associated with other states of the brain, and we observe that the spectral exponent $\gamma$ increases at seizure onset. This characteristics however can be observed only for channels RMT1, RMT2 and RMT3.

Fig. 4 compares the spectral exponents $\gamma$ of the ECoG signals of channels RMT3 and LMT2. Obviously, the spectral exponents of the ECoG signals of channels RMT3 and LMT2 are remarkably different. The spectral exponent $\gamma$ for channel RMT3 significantly increases during an epileptic seizure while the spectral exponent $\gamma$ for channel LMT2 remains steady at the baseline. In addition, the ECoG signal for channel RMT3 around the epileptic seizure (plotted in gray) is compared to the corresponding spectral exponent $\gamma$ (plotted in black) in Fig. 5.

## V. Conclusions

The wavelet-based fractal analysis [10] is used to examine self-similarity characteristics of the multi-channel ECoG data obtained from a subject with temporal lobe epilepsy. From the computational results, it is observed that the characteristics of the spectral exponents $\gamma$ of the ECoG signals are different during non-seizure and seizure periods and vary according to regions of the brain (e.g., between regions that are involve with seizure activity and region that are not involved with seizure activity).

During the epileptic seizure the spectral exponent $\gamma$ of the ECoG signals exhibit a significantly higher value than that associated with non-seizure states of the brain. This implies that ECoG signals during an epileptic seizure event have smoother temporal patterns (less complex temporal characteristics). This is consistent with other findings using different measures in the literature, e.g. [9], that suggests that the complexity of EEG signal decreases during an epileptic seizure event.

The signifcant change of the spectral exponent $\gamma$ during the epileptic seizure can be observed only in the channels RMT1, RMT2 and RMT3 which were obtained from right mesial temporal lobe region. The spectral exponent $\gamma$ of the ECoG signals of the channels LMT1, LMT2 and LMT3 which were obtained from the left mesial temporal lobe region does not considerably change during the epileptic seizure compared to the interictal period. This conclusion is supported by the diagnosis result of the clinical study that reported that the subject has right mesial temporal lobe epilepsy.

The computational results therefore show that the epileptic seizure can be spatially and temporally localized from the spectral exponent. Further, the spectral exponent $\gamma$ that characterize the smoothness of temporal patterns may be a useful computational measure for quantifying the state of the brain during ictal and interictal periods and for determining the regions of the brain that are involved with epileptic seizure activity.

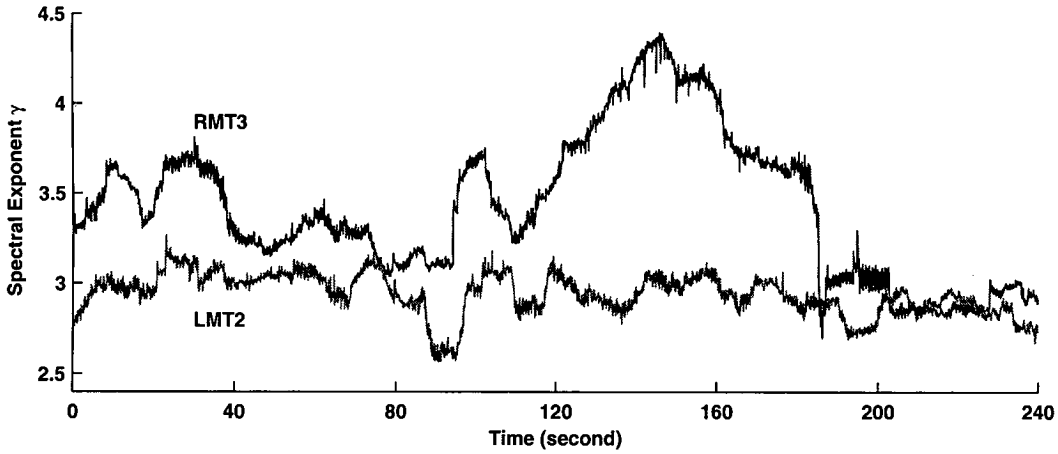


Fig. 4. Comparison of the spectral exponents of the ECoG signals of channels RMT3 and LMT2.

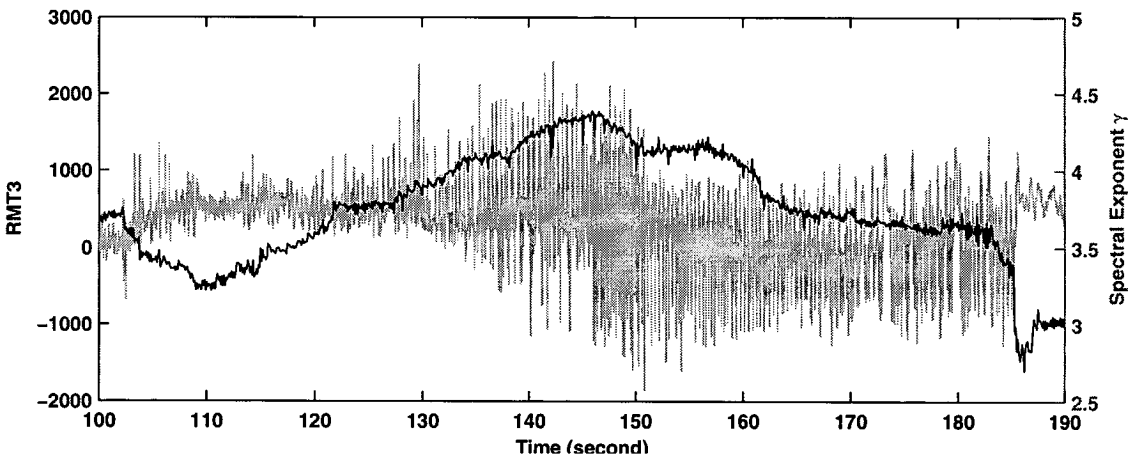


Fig. 5. The ECoG signal of channel RMT3 compared to the corresponding spectral exponent $\gamma$ around the epileptic seizure.

## REFERENCES


[1] Seizure and Epilepsy: Hope through Research National Institute of Neurological Disorders and Stroke (NINDS), Bethesda, MD, 2004 [Online]. Available: http://www.ninds.nih.gov/disorders/epilepsy/detail_epilepsy.htm

[2] B. Litt and J. Echauz, "Prediction of epileptic seizures," *Lancet Neurology*, vol. 1, pp. 22-30, 2002.

[3] A. Subasi, "Epileptic seizure detection using dynamic wavelet network," *Expert Systems with Applications*, vol. 29, pp. 343-355, 2005.

[4] A. L. Goldberger, "Complex systems," *Proc. Am. Thorac. Soc.*, vol. 3, pp. 467-472, 2006.

[5] W. S. Pritchard and D. W. Duke, "Measuring chaos in the brain: a tutorial review of EEG dimension estimation," *Brain Cogn.*, vol. 27, pp. 353-397, 1995.

[6] R. Ferri, L. Parrino, A. Smerieri, M. G. Terzano, M. Elia, S. A. Musumeci, S. Pettinato, and C. J. Stam, "Non-linear EEG measures during sleep: effects of the different sleep stages and cyclic alternating pattern," *Int. J. Psychophysiol.*, vol. 43, pp. 273-286, 2002.

[7] S. Janjarasjitt, M. S. Scher, and K. A. Loparo, "Nonlinear dynamical analysis of the neonatal EEG time series: the relationship between sleep state and complexity," *Clin. Neurophysiol.*, vol. 119, pp. 1812-1823, 2008.

[8] S. Janjarasjitt, M. S. Scher, and K. A. Loparo, "Nonlinear dynamical analysis of the neonatal EEG time series: the relationship between neurodevelopment and complexity," *Clin. Neurophysiol.*, vol. 119, pp. 822-836, 2008.

[9] K. Lehnertz and C. E. Elger, "Spatio-temporal dynamics of the primary epileptogenic area in temporal lobe epilepsy characterized by neuronal complexity loss," *Electroenceph. and Clin. Neurophyiol.*, vol. 95, pp. 108-117, 1995.

[10] S. Janjarasjitt and K. A. Loparo, "Wavelet-based fractal analysis of the epileptic EEG signal," in *Proc. ISPACS*, 2009, pp. 127–130.

[11] B. B. Mandelbrot, *The Fractal Geometry of Nature*. WH Freeman: San Francisco, 1982.

[12] G. W. Wornell, *Signal Processing with Fractals: A Wavelet-Based Approach*. Prentice Hall: New Jersey, 1995.

[13] G. W. Wornell, "A Karhunen-Loève-like expansion for $1/f$ processes via wavelets," *IEEE Trans. Inform. Theory*, vol. 36, pp. 859-861, 1990.

[14] G. W. Wornell, "Wavelet-based representations for the $1/f$ family of fractal processes," *Proceedings of the IEEE*, vol. 81, pp. 1428-1450, 1993.

[15] X Li, J. Polygiannakis, P. Kapiris, A. Peratzakis, K. Eftaxias, and X. Yao, "Fractal spectral analysis of pre-epileptic seizures in terms of criticality," *J. Neural Eng.*, vol. 2, pp. 11-16, 2005.

[16] E. Pereda, A. Gamundi, R. Rial, J. Gonzalez, "Non-linear behaviour of human EEG: fractal exponent versus correlation dimension in awake and sleep stages," *Neuroscience Letters*, vol. 250, pp. 91-94, 1998.

[17] S. Mallat, *A Wavelet Tour of Signal Processing*. Academic Press: San Diego, 1998.

[18] I. Daubechies, "Orthonormal bases of compactly supported wavelets," *Commun. Pure Appl. Math.*, vol. XLI, pp. 909-996, 1988.
[19] S. G. Mallat, "A theory for multiresolution signal decomposition: the wavelet representation," *IEEE Trans. Pattern Analysis and Machine Intelligence*, vol. 11. pp. 674-693, 1989.
[20] A. Cohen and J. Kovacevic, "Wavelets: the mathematical background," *Proceedings of the IEEE*, vol. 84, pp. 514-522, 1996.
[21] G. W. Wornell and A. V. Oppenheim, "Estimation of fractal signals from noisy measurements using wavelets," *IEEE Trans. Signal Processing*, vol. 40, pp. 611-623, 1992.
[22] P. A. Watters, "Fractal structure in the electroencephalogram," *Complexity Internation*, vol. 5, 1998. Available:http://www.complexity.org.au/ci/vol05/watters/watters.html"